EFFECTS OF VASOFLUX ON SURVIVAL IN A MURINE MODEL OF SEPSIS

EFFECTS OF VASOFLUX ON DNA-HISTONE COMPLEXES IN VITRO AND ON ORGAN FUNCTION AND SURVIVAL OUTCOME IN A MURINE MODEL OF SEPSIS

BY NEHA SHARMA, BSc

A Thesis Submitted to the School of Graduate Studies in Partial Fulfillment of the Requirements for the Degree Master of Science

McMaster University MASTER OF SCIENCE (2018) Hamilton, Ontario (Medical Sciences)

TITLE: Effects of Vasoflux on DNA-Histone Complexes in Vitro and on Organ Function and Survival Outcome in a Murine Model of Sepsis

AUTHOR: Neha Sharma, BSc (McMaster University)

SUPERVISOR: Patricia C. Liaw

NUMBER OF PAGES: xvii, 147

LAY ABSTRACT

Sepsis is a life threatening condition caused by the body's extreme response to microbial infection of the blood, whereby neutrophils release traps composed of cell-free DNA (cfDNA), histones, and antimicrobial proteins. In addition to fighting off infections, these traps also exert harmful effects like triggering clotting and killing host cells. Currently, no specific anti-septic drugs exist. Studies have shown that DNase1 (a recombinant protein that digests double stranded cfDNA) or a modified form of heparin (neutralizes histones) improves survival in septic mice. Our goal was to explore the protective effects of Vasoflux, (a non-anticoagulant heparin) and DNase1 in a mouse model of sepsis. We hypothesize that the combined therapy of DNase1 and Vasoflux will improve survival. We found that Vasoflux has minimal blood thinning activity and can prevent histones from killing cells. However, Vasoflux administered into septic mice worsened organ damage and decreased survival. We hypothesize that this damage may be due to Vasoflux's ability to displace histones from histone-DNA complexes, thereby releasing free DNA, which promotes excessive blood clotting in sepsis.

ABSTRACT

Sepsis is life-threatening organ dysfunction produced by a dysregulated host response to infection in which neutrophils release neutrophil extracellular traps (NETs). NETs consist of DNA, histones, and antimicrobial peptides which kill pathogens. However, DNA and histones also exert damage by activating the intrinsic pathway of coagulation and inducing endothelial cell death, respectively. AADH, a 15kDa non-anticoagulant unfractionated heparin (UFH), prevents histone-mediated cytotoxicity in vitro and improves survival in septic mice. We explored the effectiveness of Vasoflux, a 5.5kDa low-molecular-weight-heparin as an anti-sepsis treatment as compared to enoxaparin and UFH. Vasoflux has reduced anticoagulant functions and hence reduces the risk of bleeding as compared to enoxaparin or UFH. We showed that UFH, enoxaparin, or Vasoflux at concentrations of up to 13.3μM, 40μM, or 40μM, neutralize histone-mediated cytotoxicity. These results suggest that these glycosaminoglycans (GAGs) are able to neutralize histone-mediated cytotoxicity independent of the AT-binding pentasaccharide. To quantitate the binding affinity between GAGs and histones, surface plasmon resonance was conducted. UFH is a more potent inhibitor of histone-mediated cytotoxicity compared to Vasoflux as UFH has a 10-fold greater binding affinity to histones compared to Vasoflux. To translate our *in vitro* findings to *in vivo*, Vasoflux, enoxaparin, and UFH were administered in a murine model of sepsis. Vasoflux at 8mg/kg - 50mg/kg reduced survival and exhibited damage in the lung, liver, and kidney in septic mice compared to 10 mg/kg of UFH or 8mg/kg of enoxaparin. This may be due to Vasoflux and UFH disrupting the DNA-histone complex, thereby releasing free procoagulant DNA. This is evident by our gel electrophoresis experiments, where addition of 1μM Vasoflux or 3.3μM UFH to DNA-histone complexes lead to histone dissociation from DNA. UFH bound to histones may be able to inhibit DNA-mediated thrombin generation, as it retains its anticoagulant properties,

demonstrated by UFH-histone complexes attenuating DNA and TF-mediated thrombin generation. In contrast, Vasoflux may not neutralize the procoagulant DNA leading to a hypercoagulable state in the mice. Our study may have important clinical implications as there is an ongoing trial, HALO, which will administer intravenous UFH to patients suspected to have septic shock to reduce mortality. Based on our results, future clinical trials should consider the antithrombin-dependent anticoagulant activity of UFH being used as a sepsis treatment.

ACKNOWLEDGEMENTS

This thesis would not have been possible without the continued support, motivation, and guidance of several individuals who contributed and extended their valuable assistance in the completion of this study.

First and foremost, I would like to express my deepest gratitude to my supervisor, Dr. Patricia Liaw for her wisdom, expertise, and patience. I feel I have grown significantly as a scientist, as a writer, and as a person with her guidance, constructive criticism, and encouragement. I would not have had the ability to succeed in this program without her confidence in me. I will be forever grateful for her ongoing support, time, and mentorship throughout my graduate studies.

I would also like to thank each and every member of my supervisory committee, Dr. Alison Fox-Robichaud, Dr. Peter Gross, and Dr. Jeffrey Weitz, for their valuable feedback and insights, which helped to guide and improve this study.

There are many individuals at TaARI to whom I owe my gratitude for their moral support, technical assistance, expertise and help with the studies. Of special mention are Dr. Dhruva Dwivedi, Dr. Ji Zhou, Peter Grin, and Andrew Kwong, who consistently provided moral support through the ups and downs of this project. I want to extend a special thanks to Dhruva and Andrew, who have always been ready and willing to help with anything. Thank you from the bottom of my heart for being my earth angels. I would like to express my sincere gratitude to Andrew, our boy genius, who has been my rock during the most difficult times, my partner in crime for our overnight studies, and always being there for me. I will always be grateful for your continued support.

I would also like to thank the members of TaARI for their expertise and technical support. I would like to acknowledge Dr. Jim Fredenburgh and Rida Malik for always willing to drop what they were doing to help me conduct experiments. Thank you to Dr. Peng Liao for always making sure we have enough isoflurane to do our animal studies.

I would like to thank my fellow TaARI labmates, both past and present. I greatly appreciate both the camaraderie and support they have provided me and will miss working in such a high-spirted environment. Thank you all for being my confidence booster; teasing can definitely make you stronger! The lunchroom conversations, card games, and epic pranks will forever remain some of my favorite memories of graduate school.

I would also like to thank my parents, Meena and Inderjit, for their continued support and encouragement throughout my graduate studies. Thank you to my brother, Hitesh, who has never failed to make me laugh and restore my spirits whenever I was feeling down. Thank you all for being the everlasting support system that is always there for me.

TABLE OF CONTENTS

LIST OF FIGURES

LIST OF TABLES

LIST OF ABBREVIATIONS

APTT – Activated Partial Thromboplastin Time
AADH – Antithrombin affinity-depleted heparin
ANOVA – Analysis of variance
APC – Activated protein C
AT – Antithrombin III
BSA – Bovine serum albumin
cfDNA – Cell-free DNA
CAT – Calibrated automated thrombin generation
cfDNA – Cell free Deoxyribonucleic acid
CLP – Cecal ligation and puncture
DAMP – Damage-associated molecular pattern
DIC – Disseminated intravascular coagulopathy
DNase – Deoxyribonuclease
EPCR – endothelial protein C receptor
GRK2 (G-protein coupled receptor kinases 2)
GPCR (G protein-coupled receptor family)
H&E – Hematoxylin and eosin
HEK293 – Human embryonic kidney-293
iNOS- Inducible nitric oxide synthase
I.P – Intraperitoneal
IVC – Inferior vena cava
LMWH – Low-molecular-weight heparin
MPO – Myeloperoxidase
NE – Neutrophil elastase
NET – Neutrophil extracellular trap
PAD4 – Peptidyl arginine deiminase 4
PAI – plasminogen activator inhibitor
PAMP – Pathogen-associated molecular pattern
PARs – Protease-activated receptors
PBS – Phosphate buffered saline
PC – Protein C
PMA – Phorbol 12-myristate 13-acetate
PPP – Platelet-poor plasma
PRR – Pattern recognition receptor
PS – Protein S
PTAH – Phosphotungstic-acid and hematoxylin
ROS – Reactive oxygen species
TAFI – Thrombin activatable fibrinolysis inhibitor
TF – Tissue Factor
TLR – Toll-like receptor
TFPI – Tissue factor pathway inhibitor
TM – Thrombomodulin

TNF – Tumor necrosis factor
tPA – Tissue-type plasminogen activator
uPA – Urokinase-type plasminogen activator
VWF – Von Willebrand Factor

DECLARATION OF ACADEMIC ACHIEVEMENT

Neha Sharma contributed to the conception and design of the studies, performed all experiments, analysed and interpreted the data, and performed the statistical analyses.
Dr. Patricia C. Liaw contributed to the conception and design of the studies, obtained funding to support the studies, and critically reviewed the obtained results.

1.0 Introduction to Sepsis

1.0.1 Sepsis as a health problem

Sepsis is a life-threatening organ dysfunction due to a dysregulated host response to infection (Singer et al., 2016). Septic shock is defined as sepsis with the presence of refractory hypotension despite fluid resuscitation, a condition associated with a greater risk of mortality (Singer et al., 2016). Current treatments for sepsis involve cardiorespiratory resuscitation to improve cardiovascular parameters, such as intravenous fluids and vasopressors, in combination with oxygen therapy and mechanical ventilation (Singer et al., 2016). Furthermore, the use of early and appropriate antibiotic therapy is recommended to target the infection (Mossie, 2013). Despite these potential interventions, sepsis remains a major healthcare issue that affects millions of people worldwide each year (Matzner et al., 1985). In Canada, sepsis affects approximately 90,000 people annually, with mortality rates ranging from 30% to 50% (Husak et al., 2010; Martin et al., 2009; Statistics Canada., 2016). Importantly, there are currently no FDA approved drugs for sepsis despite significant scientific advances over the past 30 years, suggesting that some fundamental knowledge is still lacking in our understanding of sepsis pathophysiology (Rossaint et al., 2015).

1.0.2 Link between infection, inflammation, and coagulation

In sepsis, the initial infection is detected by the immune system, resulting in an inflammatory response (Rittirsch et al., 2008). The initial infection is rarely the cause of mortality; rather, death is caused by the body's maladaptive response to infection (Stearns-Kurosawa et al., 2011). Pattern recognition receptors (PRRs) on host immune cells such as

monocytes, neutrophils, platelets, and endothelial cells bind pathogen-associated molecular patterns (PAMPs) such as lipopolysaccharide (LPS) (Rittirsch et al., 2008; Takeuchi et al., 2010). PRPs are also able to recognize damage-associated molecular patterns (DAMPs), which are endogenous molecules released from damaged cells, such as histones and cell free DNA (cfDNA) (Rittirsch et al., 2008; Takeuchi et al., 2010). Both events lead to the production of pro-inflammatory cytokines and chemokines that promote leukocyte extravasation to tissues and pathogen elimination (Rittirsch et al., 2008). These proinflammatory mediators upregulate tissue factor (TF) on monocytes and macrophages, thereby triggering the extrinsic pathway of coagulation (Rittirsch et al., 2008). The compensatory anti-inflammatory response is crucial to dampen the pro-inflammatory response and minimize tissue damage (van der Poll et al., 2008). However, these changes are immunosuppressive and enhance susceptibility to secondary infections (van der Poll et al., 2008). Coagulopathy is common in sepsis and can result in disseminated intravascular coagulation (DIC), a condition characterized by microvascular thrombosis and hemorrhage due to the consumption of platelets and clotting proteins (Levi et al., 2010; Semeraro et al., 2010).

1.1 The Coagulation Cascade

1.1.1 The Coagulation Cascade

The coagulation cascade is composed of a series of sequentially activated enzymes, which ultimately leads to the cleavage of prothrombin to thrombin (Versteeg et al., 2013). Thrombin then converts soluble fibrinogen to an insoluble fibrin clot (Versteeg et al.,

2013). This process is divided into the extrinsic, intrinsic, and common pathways (Figure 1.1) (Owens et al., 2010; Versteeg et al., 2013).

1.1.2 The Extrinsic Pathway

The extrinsic pathway is initiated by the formation of the Tissue Factor (TF) and coagulation factor (F) VII (FVII) complex (Monroe et al., 2006). TF, also known as thromboplastin, is a 47 kDa glycosylated, integral-membrane protein that is expressed by extravascular cells such as fibroblasts and vascular smooth muscle cells (Drake et al., 1989; Wilcox et al., 1989). Upon vascular damage, subendothelial TF is exposed to the blood and binds coagulation factor FVII. TF acts as a cofactor by promoting proteolysis and activation of FVII to activated FVII (FVIIa) (Yau et al., 2015). The TF/FVIIa complex proteolytically cleaves and activates the zymogens FIX and FX in the presence of Ca^{2+} and phosphatidylserine (PS) (Monroe et al., 2006). FXa binds to its cofactor FVa to form the prothrombinase complex on platelet surfaces, which generates a small amount of thrombin (Neuenschwander et al., 1993). This minute amount of thrombin amplifies the coagulation cascade by activating the cofactors FVIII and FV as well as FXI. Thrombin can also activate platelets via cleavage of protease-activated-receptor (PAR-1) (Neuenschwander et al., 1993; Versteeg et al., 2013). Furthermore, the exposure of PS on the platelet surface provides an anionic membrane for the assembly of coagulation complexes (Ahmad et al., 1992). This anionic membrane allows for the assembly of the intrinsic tenase complex (which consists of FVIIIa and FIXa) and the prothrombinase complex (which consists of FVa and FXa) that results in the generation of FXa and thrombin, respectively (Hoffman et al., 2001).

1.1.3 The Intrinsic Pathway

The intrinsic pathway, also known as the contact pathway, is initiated by the exposure of blood to negatively charged surfaces (Colman & Schmaier, 1997). Examples of non-physiological activators include kaolin, glass, and silica and physiological activators include collagen, polyphosphates (polyP), and nucleic acids (Colman & Schmaier, 1997). In plasma, 75% of prekallikrein (PK) circulates non-covalently bound to high molecular weight kininogen (HK) and this nonenzymatic cofactor is responsible for localizing kallikrein to negatively charged surfaces (Colman & Schmaier, 1997). Binding of FXII to a negatively charged surface induces a conformational change that results in its autoactivation (Colman & Schmaier, 1997; Yang et al., 2014). FXIIa catalyzes the activation of plasma PK to kallikrein that further converts additional FXII to FXIIa (Yang et al., 2014). FXIIa in complex with cofactor HK, catalyzes the activation of FXI, resulting in further activation of the downstream coagulation factors FIX, and FX (Wu, 2015).

1.1.4 The Common Pathway

Both the extrinsic and intrinsic pathways converge upon the generation of FXa forming the common pathway of the coagulation cascade (Smith et al., 2015). FXa associates with cofactor FVa on an anionic phospholipid surface to form the prothrombinase complex (Monroe et al., 2006). This complex catalyzes the conversion of prothrombin into thrombin (Smith et al., 2015). This “burst” of thrombin is required for cleavage of soluble fibrinogen to an insoluble fibrin clot (Wolberg & Campbell, 2008). Finally, thrombin also activates FXIII to FXIIIa, which crosslinks adjacent fibrin polymers to stabilize the platelet plug (Ariëns et al., 2002).

1.1.5 Fibrinolysis

Fibrinolysis is a highly regulated enzymatic process that prevents excessive clot formation and enables the removal of thrombi (Cesarman-Maus et al., 2005). Plasminogen is converted to plasmin by a single cleavage at Arg^{560}-Val^{561} by tissue plasminogen activator (tPA) or urokinase plasminogen activator (uPA) (Naldini et al., 1992). Both of these plasminogen activators have short half-lives in circulation (4-8 minutes) as a result of inhibitors such as plasminogen activator inhibitors-1 (PAI-1) and alpha-2 plasmin inhibitor (α_2PI) (Bu et al., 1994; Schneider et al., 2004). In the presence of fibrin, the catalytic activity of tPA is increased by approximately 500-fold and fibrin-bound tPA efficiently converts plasminogen into plasmin (Hoylaerts et al., 1982). Once formed, plasmin cleaves the Lys-Arg sites on fibrin, thereby exposing carboxy-terminal lysine residues that have the capacity to enhance the rate of plasmin generation and ultimately the production of fibrin degradation products (FDPs) (Broze & Higuchi, 1996; Cesarman-Maus et al., 2005). The kringle domains of both tPA and plasminogen contain lysine binding sites that mediate binding of tPA/plasminogen to fibrin leading to further fibrin degradation (Cesarman-Maus et al., 2005). Plasminogen activation can be blocked by thrombin activated fibrinolysis inhibitor (TAFI), a carboxypeptidase that removes C-terminal lysine and arginine residues on fibrin and by α_2PI. This impairs the binding of tPA and plasminogen, thereby slowing plasmin generation and stabilizing the fibrin clot (Bajzar, 2000; Cesarman-Maus et al., 2005).

1.1.6 Inhibitors of Coagulation

Naturally occurring anticoagulants in the body exert a regulatory role over the coagulation cascade to prevent unnecessary occlusion of the blood vessel (Sira et al., 2016). The coagulation cascade is negatively regulated by a number of natural anticoagulant mechanisms, including tissue factor pathway inhibitor (TFPI), antithrombin (AT), and the protein C (PC) pathway (Kubier et al., 2012).

Tissue factor pathway inhibitor (TFPI) is a Kunitz-type protease inhibitor that is produced by platelets and endothelial cells. It circulates in plasma at a concentration of 1.6 nM (Dahm et al., 2003; Maroney et al., 2008). It has a molecular weight of 43 kDa and a half-life of 60-120 minutes (Broze & Girard, 2012; Lwaleed & Bass, 2006). TFPI consists of 3 Kunitz-type domains, which bind and inhibit a target protease (Girard et al., 1989). The Kunitz domain 1 (K1) inhibits the TF/FVIIa complex when FXa is present and the K2 domain binds and inhibits FXa (Girard et al., 1989). Furthermore, TFPI inhibits the initiation of thrombin generation by blocking the prothrombinase complex (Wood et al., 2013).

Antithrombin (AT) is a serine protease inhibitor (serpin) that is produced by the liver and circulates in plasma at a concentration of 2.5 μM (Heit, 2013). It has a molecular weight of 58 kDa and a half-life of 3 days (Heit, 2013; Roemisch et al., 2002). It targets multiple coagulation factors including FXa, FIXa, FXIa, FXIIa, FVIIa, and thrombin (Hirsh et al., 2001). In the presence of glycosaminoglycans (GAGs) such as heparin or heparan sulfate, AT activity is increased more than 1000-fold (Tollefsen et al., 1983). Heparin binds to AT via a high-affinity pentasaccharide sequence that induces a conformational change

in AT and accelerates the rate of inactivation of FXa (Hirsh et al., 2001; Jordan et al., 1980). To inhibit thrombin, the heparin chain must contain ≥ 18 saccharides to allow the simultaneously binding of heparin to AT (Hirsh et al., 2001; Hirsh et al., 2001; Jordan et al., 1980).

The protein C anticoagulant pathway involves thrombomodulin (TM), the endothelial cell protein C receptor (EPCR), protein C (PC), and protein S (Esmon, 2003). Protein C circulates in plasma at a concentration of 70 nM, has a molecular weight of 62 kDa, and a half-life of 10 hours in circulation (Gruber et al., 1992; Kisiel, 1979; Okajima et al., 1990). Upon thrombin generation, thrombin complexes with TM expressed on the endothelial cell surface (Fukudome et al., 1994, 1995). EPCR augments the activation of PC to APC by 20-fold by presenting PC to the thrombin-TM complex (Fukudome et al., 1994, 1995). APC, in complex with its cofactor protein S, inactivates FVa and FVIIIa, thereby decreasing thrombin generation (Rosing et al., 1995).

1.1.7 Impairment of Physiological Mechanisms

Normally, a delicate balance is maintained between clot formation and clot lysis to prevent hemorrhage and disseminated thrombosis (Palta et al., 2014). During sepsis, this homeostatic state is disrupted by inflammation and several anticoagulant pathways are impaired, resulting in a shift toward a procoagulant state (Semeraro et al., 2010). Lower circulating concentrations of TFPI are found in septic patients and their depletion is associated with poor prognosis (Levi, 2008). Antithrombin levels are decreased in sepsis due to consumption from ongoing coagulation, impaired synthesis, and degradation by neutrophil proteases (Levi, 2008; Seitz et al., 1989) Furthermore, inflammatory stimuli

result in down-regulation of GAGs on the endothelial surface resulting in reduced AT function in sepsis (Levi, 2008; Opal et al., 2002) APC levels are also decreased as a result of down-regulation of TM at the endothelial surface due to exposure to inflammatory cytokines (Levi, 2008; Nawroth et al., 1986). Inflammation also results in shedding of EPCR via tumor necrosis factor-α converting enzyme/ADAM17 (TACE) (Qu et al., 2007). Abnormalities in fibrinolysis observed in sepsis include increases in plasminogen activator inhibitor-1 (PAI-1) (Semeraro et al., 2010). Administration of LPS to humans and nonhuman primates resulted in endotoxemia that was associated with a transient increase in activation of fibrinolysis, followed by a rise in PAI-1 levels, leading to a hypofibrinolytic state (de Boer et al., 1993; Suffredini et al., 1989).

The most severe form of pathologic coagulation is known as disseminated intravascular coagulation (DIC) (Levi et al., 1999). It is characterized by systemic microvascular fibrin deposition that ultimately results in the thrombotic occlusion of small vessels with associated tissue ischemia and organ failure (Levi et al., 2003). The entire continuum of disease in sepsis results from complex pathogenesis that heavily involves monocytes, platelets, and neutrophils (Dewitte et al., 2017; Stearns-Kurosawa et al., 2011; von Hundelshausen et al., 2007).

Figure 1.1: The coagulation cascade. The coagulation cascade is composed of the sequential conversion of zymogens to proteolytic enzymes and is divided into the intrinsic, extrinsic, and common pathways (Versteeg et al., 2013). The extrinsic pathway is initiated by vascular injury exposing TF, which binds to FVII and promotes proteolysis and activates FVII to activated FVII (FVIIa) (Neuenschwander et al., 1993; Yau et al., 2015). The TF/FVIIa complex cleaves FIX to FIXa, and FX to FXa (Monroe et al., 2006). FXa associates with FVa to form the prothrombinase complex on a negatively charged surface in the presence of calcium ions, which converts prothrombin to thrombin (Neuenschwander et al., 1993; Yau et al., 2015). This minute amount of thrombin initiates a positive feedback loop on itself through activation of FV and FVIII, which then converts soluble fibrinogen to insoluble fibrin (Neuenschwander et al., 1993). The intrinsic pathway is initiated by the exposure of blood to negatively charged activators, such as DNA or polyp (Colman & Schmaier, 1997). FXII binds to negatively charged surfaces, which causes a conformational change that activates FXII (Colman & Schmaier, 1997; Yang et al., 2014). FXIIa catalyzes the activation of prekallikrein to kallikrein and factor XII to XIIa (Yang et al., 2014). FXIIa with high molecular weight kininogen, activates factor IX and factor X (Wu, 2015). The common pathway is the convergence of the extrinsic and intrinsic pathways (Monroe et al., 2006). Thrombin converts soluble fibrinogen to insoluble fibrin that is further stabilized by cross-linking mediated by factor XIIIa. The fibrin clot is degraded by the activation of plasminogen into plasmin by tissue-type plasminogen activator (tPA) and urokinase-type plasminogen activator (uPA) (Smith et al., 2015). Modified source (Liu et al., 2014).

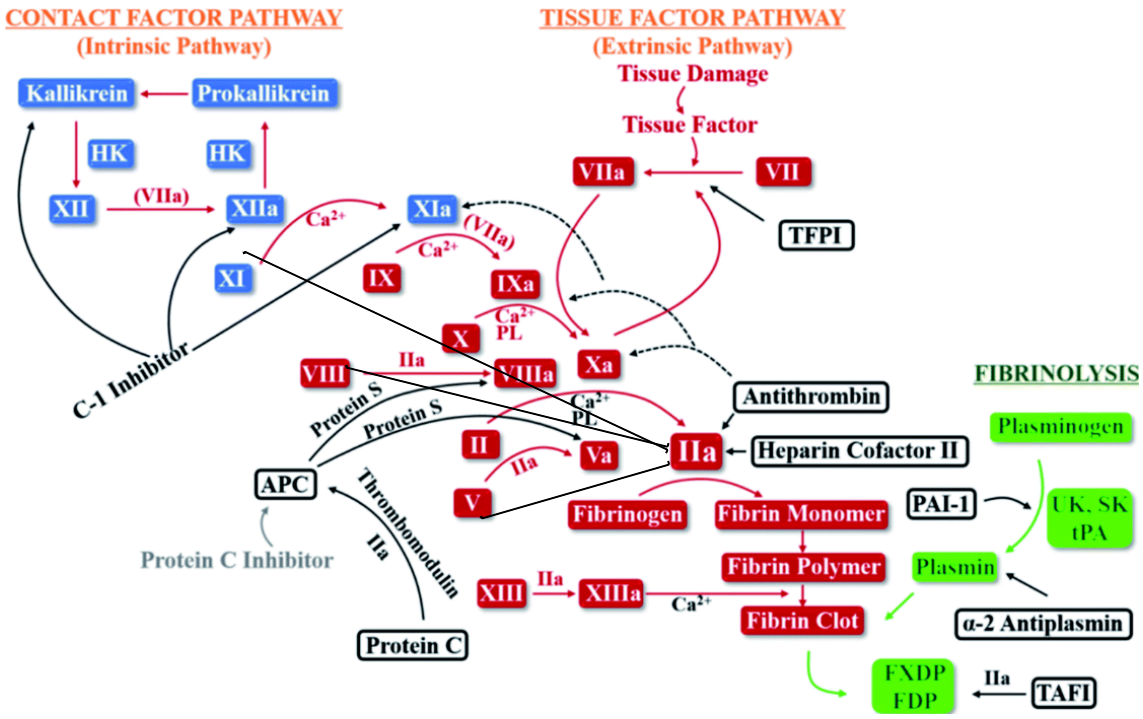
CONTACT FACTOR PATHWAY
(Intrinsic Pathway)
TISSUE FACTOR PATHWAY
(Extrinsic Pathway)
Tissue Damage
Tissue Factor
Kallikrein
Prokallikrein
HK
HK
XII
(VIIa)
XIIa
XI
XIa
(VIIa)
VIIa
VII
TFPI
IX
IXa
X
Xa
VIII
IIa
VIIIa
Antithrombin
Protein S
Protein S
II
IIa
Va
IIa
Heparin Cofactor II
V
APC
Protein C Inhibitor
Thrombomodulin
IIa
Protein C
Fibrinogen
Fibrin Monomer
Fibrin Polymer
Fibrin Clot
XIII
IIa
XIIIa
C-1 Inhibitor
FIBRINOLYSIS
Plasminogen
PAI-1
U K, SK
tPA
Plasmin
α-2 Antiplasmin
FXDP
FDP
IIa
TAFI

1.2 The Monocyte

1.2.1 Monocyte structure and function

Monocytes are circulating mononuclear phagocytes originating from bone marrow hematopoietic stem cells that terminally differentiate into macrophages upon entry into tissue (Cavaillon et al., 2005). During infection, monocytes mediate host antimicrobial defense and produce inflammatory mediators upon activation by microbial stimuli (Cavaillon & Adib-Conquy, 2005).

1.2.2 Role of monocyte in sepsis pathophysiology

Monocytes and macrophages are the initiators of the early immune response following infection (Egorina et al., 2011). During infection, danger-associated molecular patterns (DAMPs), molecules released from cells undergoing necrosis, are recognized by toll-like receptors (TLRs) on immune cells such as monocytes and macrophages (Semeraro et al., 2010). In response to inflammatory stimuli, macrophages release cytokines such as tissue necrosis factor (TNF-α), IL-1, IL-6, reactive oxygen species, and nitric oxide (Duque & Descoteaux, 2014; Beutler, 1999).

Monocytes also contribute to the procoagulant state in sepsis by expressing TF in response to LPS and inflammatory cytokines. The majority of cell surface TF exists in a cryptic or non-functional form and only TF that has been decrypted exerts a procoagulant effect (Rao et al., 2012). Studies have showed that TF can be de-encrypted *in vitro* in several ways such as exposure to calcium ionophore, repeated freeze-thaw cycles and pathological stimuli including LPS, cytokines, and thrombin (Le et al., 1992; Maynard et al., 1975; Wolberg et al., 1999). The primary model by which cryptic TF is decrypted is

the membrane phospholipid asymmetry (Shaw et al., 2007). During pathological conditions, inhibition of ATP-dependent transmembrane lipid transporter proteins, leads to loss of lipid asymmetry and results in increased exposure of negatively charged phosphatidylserine (Comfurius et al., 1990). It has been shown that TF procoagulant activity requires association with phospholipids and the presence of phospholipids greatly increase clotting times (Comfurius et al., 1990; Nemerson, 1968). Furthermore, the release of small membrane vesicles (MVs), from activated monocytes into the circulation facilitates platelet-MV interactions and platelet activation (Kleinjan et al., 2012; Rauch et al., 2000).

1.3 The Platelet

1.3.1 Platelet structure and function

Platelets, characterized by cytoplasmic granules that contain growth factors, pro- and anti-inflammatory cytokines, and adhesion molecules, play a role in primary hemostasis (Triplett, 2000). Upon disruption of the vessel wall, collagen in the basement membrane is exposed, initiating platelet activation, adhesion, and aggregation at the site of vascular injury to form a platelet plug (Hou et al., 2015). This contributes to vessel integrity and prevents hemorrhage (Hou et al., 2015). While these anucelate megakaryocyte fragments participate in defense against infection, they also contribute to sepsis complications such as hyperinflammation, DIC, and multiple organ failure (Wang et al., 2014). Activated platelets play a role in the development of forming microthrombi in capillaries and further contribute to the development of DIC (Semeraro et al., 2010).

1.3.2 Role of platelet in sepsis pathophysiology

The interaction of platelets with other cells contributes to the complications of sepsis (Gawaz et al., 1997). During sepsis, there is an increase in platelet-neutrophil complexes (Gawaz et al., 1997). Platelets express a ligand for Triggering Receptor Expressed on Myeloid Cells (TREM-1) (Haselmayer et al., 2007). Upon stimulation by LPS, TREM-like transcript TLT-1, a receptor expressed only on platelets and megakaryocytes, is upregulated in patients with sepsis, allowing for platelet neutrophil interaction (Semple et al., 2011; Washington et al., 2009). This results in an increase of cytokines and ROS that aids in elimination of pathogens, but may also cause harm to host cells (Semple et al., 2011). Specifically, platelet-neutrophil complexes contribute to multiple organ failure by contributing to immune cell recruitment and hyperinflammation, which develop microthrombi in capillaries (Figure 1.2) (McDonald et al., 2012).

A study conducted by Clark et al., demonstrated that activation of platelet TLR4 (in the presence of *E. coli*) induces platelets to activate adherent neutrophils, which are recruited to the microvasculature by the detection of LPS (Clark et al., 2007). This results in the release of neutrophil extracellular traps (NETs) which, in addition to participating in bacterial trapping, also provide a scaffold for thrombus formation and further contribute to DIC and vascular damage (Clark et al., 2007).

Figure 1.2: Inflammatory function of platelets in sepsis. Activated platelets play a role in primary hemostasis in the formation of the initial platelet plug (Stalker et al., 2013). In sepsis, there is an increase in platelet-neutrophil complexes (Russwurm et al., 2002). Endothelial cells, activated by platelet derived CD40L and platelet derived IL1β positive microparticles, express adhesion molecules (such as P-selectin von Willebrand factor (vWF)) and TF (Badimon et al., 2016; Gawaz et al., 1997). Platelets bound to the endothelium support adhesion of neutrophils (Buse, 2006; Gawaz et al., 1997). Platelets express a ligand for Triggering Receptor Expressed on Myeloid Cells (TREM-1), which results in an increase in proinflammatory mediators (Washington et al., 2009). Platelet-neutrophil complexes contribute to multiple organ failure by recruiting immune cells and by producing microthrombi in capillaries (McDonald et al., 2012). Source (de Stoppelaar et al., 2014).

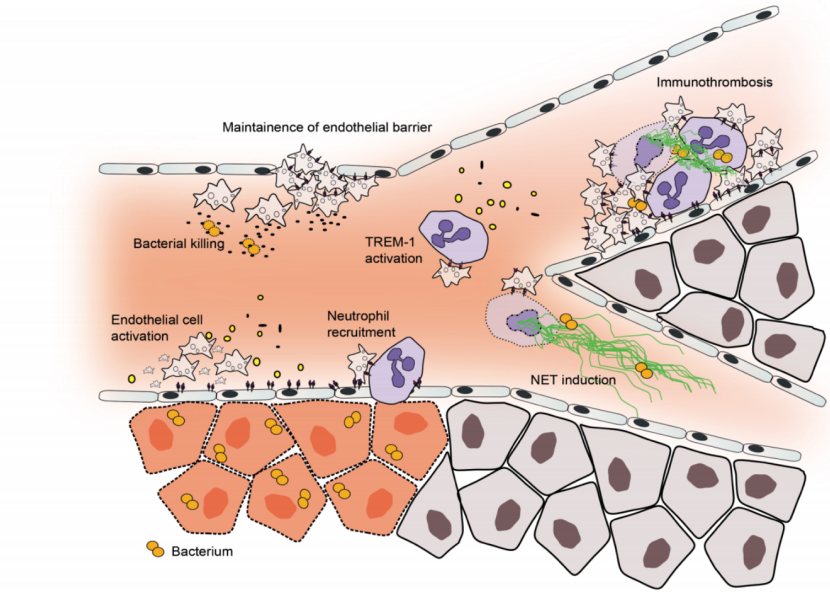

1.4 The Neutrophil

1.4.1 Neutrophil structure and function

Neutrophils, characterized as leukocytes with multi-lobed nuclei and enzyme-containing granules, are the most abundant immune cells (Summers et al., 2010). These are the first cells to be recruited to the site of infection in response to a variety of cytokines, bacterial products, and other inflammatory mediators, where they induce killing of pathogens via phagocytosis, degranulation, or the release of neutrophil extracellular traps (NETs) (Kaplan et al., 2012). The molecular mechanisms of NET release are described in section 1.4.2.

The control of infection is dependent on efficient migration of neutrophils to the site of infection (Sônego et al., 2014). Neutrophils expressing CXCR2, a chemokine receptor, migrate to the site of infection in response to chemoattractants, where they release NETs and produce reactive oxygen species (ROS) and NO (nitric oxide) (Rios-Santos et al., 2007). These intermediates kill and prevent the dissemination of microbes. During sepsis, neutrophils lose their ability to migrate to the site of infection because a variety of mechanisms contribute to internalization of CXCR2 (chemokine receptor) (Rios-Santos et al., 2007). Excessive stimulation of TLRs to bacteria pathogen-associated molecular markers (PAMPs) produces TNF-α and iNOS (nitric oxide synthase) that upregulate GRK2 (G-protein coupled receptor kinases 2) (Alves-Filho et al., 2009). As a GPCR (G protein-coupled receptor family) kinase, GRK2 phosphorylates CXCR2 to cause its endocytosis and results in CXCR2 desensitization (Alves-Filho et al., 2009). This limits neutrophil

migration to the site of infection and neutrophils fail to restrict bacterial growth (Figure 1.3) (Liu et al., 2014).

Figure 1.3: Neutrophil migration in a local infection and in sepsis. In a localized infection, neutrophils expressing CXCR2 are recruited to the site of infection in response to chemoattractants (Rios-Santos et al., 2007). Here, they release NETs and ROS to kill the invading pathogens. In contrast, there is impaired neutrophil migration to the site of infection in sepsis due to the desensitization of CXCR2 by various mechanisms (Rios-Santos et al., 2007). For instance, activation of TLRs, via bacterial components, promotes the activation of TNF-α and NOS, which upregulate GRK2, and leads to the down-regulation of CXCR2 (Rios-Santos et al., 2007). This causes neutrophil migration to fail and the growth of bacteria is not controlled (Rios-Santos et al., 2007). This leads to organ damage with capillary occlusion and hypoperfusion (Sônego et al., 2016). Source (Sônego et al., 2016).

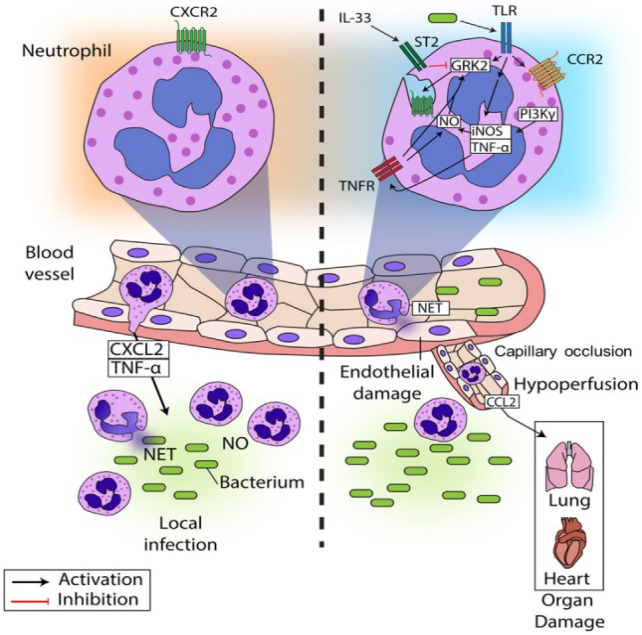

1.4.2 NETosis: A novel form of cell death

In 2004, a novel form of regulated cell death termed NETosis was discovered in which NETs, composed of cfDNA, histones, and anti-microbial peptides, are released by activated neutrophils. Induced by various exogenous and endogenous stimuli such as bacterial LPS, cytokines, immune complexes, and activated platelets, NETosis involves the degradation of cytosolic membranes, the decondensation of chromatin, and NET release (Figure 1.4) (Brinkmann et al., 2004). Binding of stimuli to neutrophil receptors increases cytoplasmic Ca^{2+} concentrations, which triggers activation of peptidyl arginine deiminase 4 (PAD4) (Kovach et al., 2012). This enzyme converts arginine resides to citrulline on histones via a deamination process, thereby reducing the positive charge of histones and as a result weakens the histone-DNA binding (Kovach et al., 2012). Reactive oxygen species (ROS) stimulate myeloperoxidase (MPO) to further activate neutrophil elastase (NE) from azurophilic granules (Papayannopoulos, 2017). NE then translocates to the nucleus to promote chromatin decondensation by cleaving linker histone H1 (Papayannopoulos, 2017). ROS is also involved in the disintegration of the nuclear envelope and granular membranes, allowing chromatin to mix with neutrophil granular enzymes (Yang et al., 2016). Finally, the rupture of the plasma membrane leads to the release of NETs into the extracellular space (Yang et al., 2016). The chromatin fibers, which form the structural backbone of NETS, not only trap pathogens to limit dissemination, but also facilitate a high local concentration of antimicrobial factors (Kaplan et al., 2012). Addition of deoxyribonuclease 1 (DNase 1) degrades NETs in vitro, thereby eliminating their antimicrobial activity (Brinkmann et al., 2004). Furthermore, neutrophils from PAD4-

deficient mice lack the ability to generate NETs and as a result are more prone to bacterial infection (Li et al., 2010).

Figure 1.4: Inducers and molecular mediators of NETosis. NETosis is triggered by a variety of stimuli such as microorganisms, damage-associated molecular patterns, and immune complexes. The induction of ROS via the extracellular signal-regulated kinase (ERK) signalling leads to the release of MPO and NE. NE and PAD4 promote chromatin decondensation through independent mechanisms and are critical intracellular effectors of NETosis (Papayannopoulos, 2017). Similarly, stimulation of neutrophils with phorbol 12-myristate 13-acetate (PMA) results in activation of PKC and triggers the generation of ROS (Urban et al., 2009). Source (Papayannopoulos, 2017).

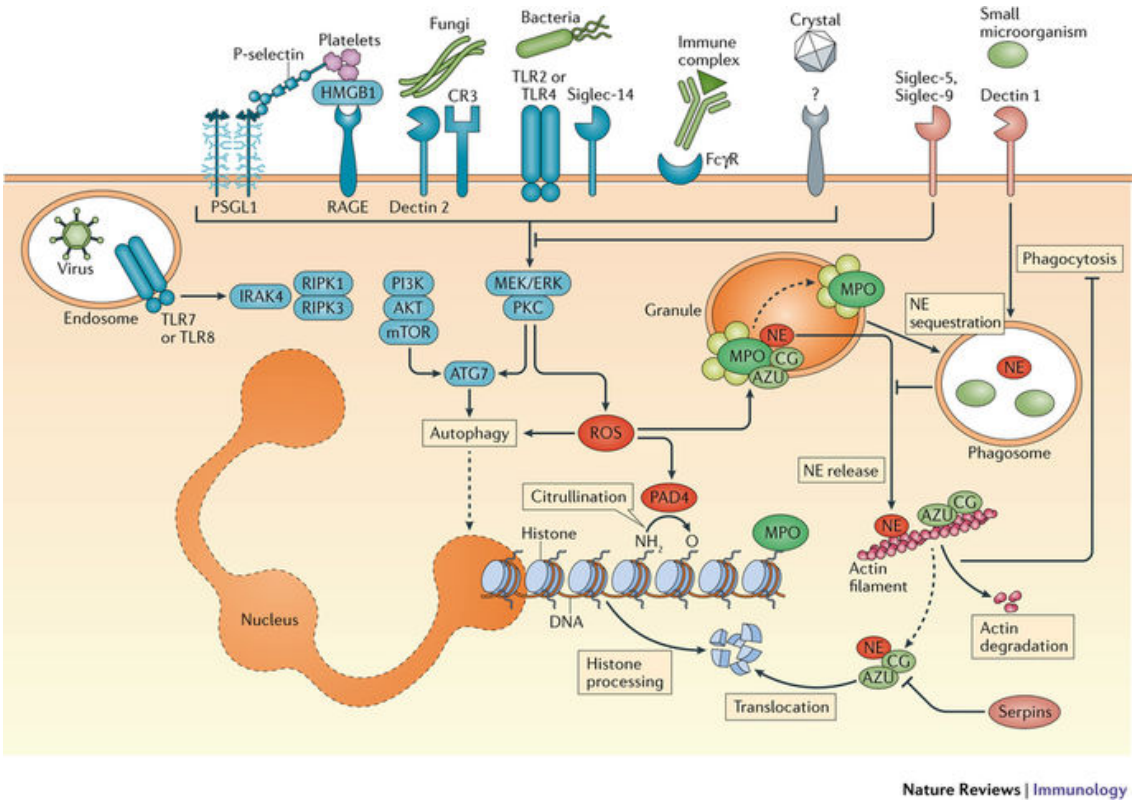

Nature Reviews | Immunology

1.4.3 Role of NET components in sepsis pathophysiology

'Immunothrombosis,' a term coined by Engelmann and Massberg, is defined as an innate immune response involving the activation of the coagulation system to assist with the destruction of pathogens (Engelmann et al., 2013). NETs are an important feature of immunothrombosis, as the DNA component of NETs can activate the intrinsic pathway via binding to factor XII (Engelmann et al., 2003; von Brühl et al., 2012). Although NETs play an important role in innate immunity, the cfDNA and histone components of NETs can also exert collateral damage to the host (Yipp et al., 2013). cfDNA promotes blood coagulation through the intrinsic pathway (a schematic diagram of blood coagulation is shown in Fig. 1.1) (Komissarov et al., 2011). A study by Gould and colleagues, demonstrated that the addition of FXII and FXI to FXII- or FXI- deficient plasma, restored the procoagulant activity of DNA (Gould et al., 2014). Furthermore, another study by Gould et al. showed that high levels of cfDNA in septic samples were correlated with clots being resistant to lysis (Gould et al., 2015). This may be due to the ability of cfDNA to bind both fibrin and plasmin to form a non-productive ternary complex, which results in delayed fibrinolysis (Gould et al., 2015). Treatment of septic plasma samples with 20 μg/ml of DNase1 partially restored fibrinolytic activity, suggesting that cfDNA impairs fibrinolysis (Gould et al., 2015). A study conducted by Dwivedi et al., showed that cfDNA is a prognostic biomarker with a high discriminative power in predicting mortality in patients with severe sepsis in the intensive care units (Dwivedi et al., 2012).

Histones, another major component of NETS, are highly basic proteins rich in arginine and lysine and are highly conserved amongst species (Szerlong et al., 2015; Xu et

al., 2011; Xu et al., 2009). In the nucleus, an octamer consisting of two dimers of histone H2A and H2B and a tetramer of histone H3 and H4 forms a core around 147 base pairs of double-stranded DNA (Andrews et al., 2011; Szerlong et al., 2015). This complex is referred to as a nucleosome (Andrews et al., 2011). These core particles are connected by linker histone H1 that connects two nucleosomes and facilitates the folding of nucleosomes into higher order chromatin structures (Szerlong et al., 2015).

Histones activate platelets, modulate coagulation, inhibit fibrinolysis, and exert cytotoxic effects through several mechanisms. Both histones H3 and H4 stimulate platelet activation through TLR2 and TLR4 (Davis et al., 2016; Semeraro et al., 2011). Histones promote thrombin generation in a platelet-dependent manner through interaction with platelet toll-like receptor (TLR) 2 and TLR4 (Gould et al., 2014; Semeraro et al., 2011; Xu et al., 2011). Furthermore, histone H4 induces erythrocytes to display phosphatidylserine (PS) on their surface, which promotes coagulation and increases fibrin formation (F. Semeraro et al., 2014). In the presence of TLR2 and TLR4 neutralizing antibodies, thrombin generation in histone-treated CTI-inhibited platelet-rich plasma (PRP) was impaired (Semeraro et al., 2011). In addition, histones impair endogenous anticoagulant pathways by inhibiting thrombomodulin-dependent protein C activation, and by interfering with antithrombin-mediated neutralization of thrombin (Ammollo et al., 2011; Varjú et al., 2015). Binding of histones to fibrin increases the thickness of clot fibers and impairs fibrinolysis (Longstaff et al., 2013). Furthermore, histone H4 is cytotoxic towards endothelial and epithelial cells and administering histone antibodies protected mice from LPS-mediated death (Silk et al., 2017). Thus, even though cfDNA and histones are vital in

host defense, they also exert procoagulant, proinflammatory, and antifibrinolytic effects in sepsis.

1.4.4 Inhibitors of NET components

CFDNA circulates at low levels (2 μg/ml) in healthy individuals, with elevated levels observed in an array of diseases, including sepsis (Gould et al., 2014). Given the fact that cfDNA is both procoagulant and antifibrinolytic, eliminating the pathological role of DNA may be a novel therapeutic strategy for sepsis. DNase1, a Ca^{2+}/Mg^{2+}-dependent endonuclease, targets and destroys NETs in a concentration-dependent manner by degrading DNA (Meng et al., 2012; Prince et al., 1998). Mannherz et al., demonstrated that murine and human serum contains two nucleases, DNase1 (major serum nuclease) and DNase1-like 3 (DNase1l3), that both function in DNA degradation (Napirei et al., 2009). Wild-type *Dnase1*$^{-/-}$, *Dnase1l3*$^{-/-}$, and *Dnase1*$^{-/-}$*Dnase1l3*$^{-/-}$ mice with chronic neutrophilia exhibited intravascular clots consisting of DNA, neutrophil granule-derived MPO, antimicrobial peptides, and citrullinated histones (Jiménez-Alcázar et al., 2017). Hepatic expression of Dnase1 or Dnase1l3 in *Dnase1*$^{-/-}$ *Dnase1l3*$^{-/-}$ mice prevented the formation of NETs and reduced injury in septicemia (Jiménez-Alcázar et al., 2017). In a model of Methicillin-resistant Staphylococcus aureus (MRSA), injection of DNase1 into mice removed cfDNA. However, 70% of histones remained bound to the vessel wall and contributed to liver injury (Kolaczkowska et al., 2015). In mice subjected to a cecal ligation and puncture (CLP) model of polymicrobial sepsis, late DNase 1 administration led to decreased levels of cfDNA and IL-6, increased levels of IL-10 and reduced organ damage and spreading of bacteria (Mai et al., 2015). Taken together, these studies suggest that

targeting cfDNA may provide a protective role in experimental sepsis.

Histones, another major component of NETs, can also be targeted and neutralized. A study by Xu et al. demonstrated that an intravenous injection of 75 mg/kg of histones resulted in death of all mice in one hour, whereas the addition of anti-histone antibodies protected mice from LPS, TNF-α, and cecal ligation and puncture (CLP) models of sepsis (Abrams et al., 2013). Histones can also be cleaved by APC) which eliminates their cytotoxic effects. In mice, co-infusion of APC with histones prevented histone-mediated mortality (Xu et al., 2009).

Given the relationship between coagulation and inflammation in sepsis, the use of anticoagulant agents to attenuate both coagulation and inflammation has been investigated (Zarychanski et al., 2015). For example, the PROWESS study demonstrated that intravenous infusion of recombinant human APC (drotrecogin alfa) significantly reduced mortality in patients with severe sepsis (Bernard et al., 2001). However, drotrecogin alfa was removed from the market after PROWESS-SHOCK trial demonstrated no survival benefit in patients with high-risk septic shock (Ranieri et al., 2012). The infection etiologies, co-interventions, and geographic enrollments were significantly different between the two trials, making them incomparable and may explain the mortality differences (Kalil et al., 2013).

1.5 Heparins

1.5.1 Unfractionated heparin (UFH)

Another anticoagulant that is currently being explored as a therapeutic agent in patients with sepsis is heparin (Zarychanski et al., 2015). Heparin, an anticoagulant

extracted from porcine intestinal mucosa, produces its major anticoagulant effect by inactivating thrombin and factor Xa via an AT- dependent mechanism (as described in section 1.1.6) (Hirsh, Anand, et al., 2001). In addition to the anticoagulant effects of heparin, this sulfated polysaccharide also possesses various biological properties such as immunomodulatory and anti-inflammatory effects (Ludwig, 2009). In mice, pretreatment of an intravenous injection of UFH in LPS-induced endotoxemic rats attenuated inflammation and coagulation and prevented lethality (Li et al., 2013).

In addition to UFH's anticoagulant activity, it is also a potent modulator of inflammation. UFH inhibits the expression and function of adhesion molecules, such as P-selectin and L-selectin (Wang et al., 2002). The sulfate groups at C6 on the glucosamine residues may occupy the same site in the selectins and hence facilitate the interaction between UFH and P- and L-selectins (Wang et al., 2002). This interferes with the adhesion between neutrophils and endothelium, a vital event preceding neutrophil trans-endothelial migration into the tissue (Derhaschnig et al., 2003; Nelson et al., 1993). Furthermore, UFH affects pro-inflammatory mediators, such as nuclear factor-κβ and cytokines, and attenuates endothelial dysfunction by enhancing nitric oxide (Baldus et al., 2006).

UFH has pharmacokinetic, biophysical, and biological limitations. The pharmacokinetic limitations of UFH arise because of its nonspecific binding to proteins and cells (Hirsh, Anand, et al., 2001). UFH has a natural tendency to bind to positively charged proteins and surfaces, resulting in a variable anticoagulant response (Hirsh, Anand, et al., 2001). Furthermore, UFH binds to platelets, resulting in activation and release of platelet factor 4 (PF4) (Walenga et al., 2004). UFH complexes with PF4 and leads to the

generation of antibodies that cause heparin-induced thrombocytopenia (HIT) (Walenga et al., 2004). Biophysical limitations include the inability of the heparin-AT complex to catalyze the inactivation of factor Xa in the prothrombinase complex or thrombin bound to fibrin or to subendothelial surfaces (Hirsh, 1998).

1.5.2 Low-molecular-weight heparin (LMWH)

Low-molecular-weight heparins (LMWHs) are derived from UFH via chemical or enzymatic depolymerization to produce fragments with a mean molecular weight of 4000 to 5000 Da (Hirsh, Anand, et al., 2001). Similar to UFH, LMWHs exert their anticoagulant effect by interacting and activating AT via an unique pentasaccharide sequence found on less than one third LMWH molecules (Hirsh, 1998). Approximately 25% to 50% of LMWHs molecules have a chain length of $\geq$ 18 saccharides, which allows for the formation of the LMWH-AT-thrombin ternary complex which inactivates thrombin (Hirsh, Anand, et al., 2001). The remaining percent of LMWH molecules contain less than 18 saccharide units and inhibit only factor Xa (Hirsh, Anand, et al., 2001).

LMWHs overcome some of the limitations of UFH (Hirsh, Anand, et al., 2001). For example, LMWHs exhibit reduced nonspecific binding to plasma proteins and cells, they produce a more predictable dose-response relationship, and have a longer plasma half-life (Hawkins, 2004; Hirsh, Anand, et al., 2001). Due to the shorter length of LMWHs, they have a reduced binding affinity for PF4 tetramer and hence are less likely to cause HIT compared with UFH (Hirsh, 1998; Walenga et al., 2004).

1.5.3 The interaction between heparin, DNases, and NET components

Mannherz et al., demonstrated that murine and human serum contain two nucleases with different properties toward DNA substrates, DNase1 and DNase1-like 3 (DNase1l3). Heparin has been shown to displace histones from chromatin and to enhance chromatin degradation by serum DNase1 (Napirei et al., 2009). This effect is likely due to the displacement of the histones from chromatin by heparin, thereby releasing histone-free DNA, which is more efficiently cleaved by DNase1 (Napirei et al., 2009). In contrast, DNase1l3 degrades intact chromatin with a greater efficiency than histone-free chromatin due to preferential cleavage at internucleosomal sites (Napirei et al., 2009). In contrast, DNase1 is negatively charged at physiological pH values and is not inhibited by heparin. Collectively, these findings support a key role for a combination therapy of GAG and DNase 1 in neutralizing histones and degrading cfDNA, respectively.

1.5.4 The use of heparin in sepsis

Numerous clinical trials have been conducted to explore the use of heparin as a therapeutic agent in patients with sepsis. The KyberSept trial demonstrated that high dose antithrombin therapy administered 6 hours after onset had no effect on 28-day mortality on patients with sepsis (Warren et al., 2001). Furthermore, high-dose antithrombin was associated with a higher risk of hemorrhage when administered with heparin (Warren et al., 2001). A retrospective study showed that intravenous heparin (administered to patients within 48 hours after arrival to ICU) was associated with reduced 28-day mortality suggesting that early heparin therapy may be an effective treatment for severe sepsis (Zarychanski et al., 2008). However, a subsequent double blind study called HETRASE

found no significant benefit after heparin treatment (Jaimes et al., 2009). A potential confounder across these clinical trials may be the underlying target population, which are heterogeneous in illness severity (Jaimes et al., 2009). It is possible that heparin may be beneficial in a subgroup of septic patients (Li & Ma, 2017).

An ongoing clinical study, Heparin AnticoaguLation to Improve Outcomes in Septic Shock (HALO), aims to investigate the effect of UFH in reducing inflammation and coagulation in patients diagnosed with septic shock (Houston et al., 2015). In a pilot study, which compared administration of intravenous doses of 18 IU/kg/hr of UFH with dalteparin (5000IU daily), UFH treatment reduced thrombin generation, shortened clot lysis time and increased levels of endogenous protein C (Houston et al., 2015). Given the biological implications of these findings, HALO has proceeded into a phase 2 clinical trial to evaluate the effects of UFH on mortality and morbidity in patients with suspected septic shock ("Heparin Anticoagulation in Septic Shock - Full Text View - ClinicalTrials.gov," 2018.).

A study by Wildhagen et al., demonstrated that a 15 kDa non-anticoagulant heparin, AADH, purified from clinical grade unfractionated heparin (UFH), binds to histones and prevents histone-mediated cytotoxicity in vitro (Wildhagen et al., 2014). The non-anticoagulant heparin was produced by fractionation of UFH via affinity chromatography using an antithrombin column, and retained 0.2% to 0.5% of the anticoagulant activity of UFH (Wildhagen et al., 2014). Intraperitoneal (I.P) injection of 570 μg of AADH at either 4 hours post-CLP or at a prophylactic regimen (12 hours pre-CLP, directly after CLP, and 12 hours post-CLP) reduced 72-hour mortality without increasing the risk of bleeding

(Wildhagen et al., 2014).

1.5.5 Vasoflux

An alternative strategy to decrease the anticoagulant potential of UFH is via chemical modification (Weitz et al., 1999). Vasoflux, developed by Weitz and colleagues, is a low-molecular-weight heparin (LMWH) that has been subjected to periodate oxidation to reduce antithrombin affinity (Weitz et al., 1999). Vasoflux was originally developed as a novel anticoagulant, which can catalyze the inactivation of fibrin- bound thrombin by heparin cofactor II (HCII) (Fig. 1.5) (Peters et al., 2001; Weitz et al., 1999). Vasoflux has minimal effects on the thrombin clotting time and has no effect on the prothrombin time (Weitz et al., 1999). Interestingly, Vasoflux prolongs the activated partial thromboplastin time (aPTT), suggesting that it inhibits the intrinsic pathway of coagulation (Weitz et al., 1999). Vasoflux at concentrations of 30 μg/ml (5.5 μM) and 60 μg/ml (11 μM) inhibits factor Xa generation in the absence of antithrombin and HCII (Weitz et al., 1999). The interaction between Vasoflux and factor IXa may weaken or damage the catalytic site of the enzyme and hence inhibit the activation of factor X by the FIXa/FVIIIa complex (Weitz et al., 1999).

Compared to UFH and LMWH, Vasoflux can inactivate fibrin-bound thrombin and inhibit factor Xa generation (Weitz et al., 1999). In animal models, addition of Vasoflux at concentrations of 15mg/kg to streptokinase, reduced clot weight with no adverse effects on bleeding (Weitz et al., 1999). Vasoflux binds clot-bound thrombin, a characteristic that differentiates it from the limited ability of UFH in this regard (Peters et al., 2001; Weitz et al., 1999). In a phase 1 study, an intravenous dose of 16 mg/kg of Vasoflux was well

tolerated and safe in 40 human volunteers (Peters et al., 2001). A phase-2 dose finding study was conducted to investigate whether Vasoflux improves the results of thrombolysis with streptokinase (SK) for acute myocardial infarction (Peters et al., 2001). Patients were either administered intravenous UFH at 70 units/kg bolus followed by 14 units/kg or intravenous Vasoflux 1, 4, 8, or 16 mg/kg as a bolus followed by 1, 4, 8, or 16 mg/kg/hour in combination with streptokinase and aspirin (Peters et al., 2001). There was no statistically significant differences for mortality and nonfatal reinfarction between the treatment groups (Peters et al., 2001). At doses that lead to increases in bleeding complications, no superior efficacy between Vasoflux or UFH was observed (Peters et al., 2001). The excessive bleeding may have been a result of excessive factor inhibition by Vasoflux or due to the combination therapy with streptokinase or aspirin (Peters et al., 2001). Thus, the addition of Vasoflux to SK and aspirin did not improve patency rated compared to UFH in combination with SK and aspirin (Peters et al., 2001). However, Vasoflux may be a promising new therapy for sepsis since it has the potential to neutralize histones as well as to inhibit the contact pathway of coagulation without increasing the risk of bleeding as compared to UFH (Figure 1.6).

Figure 1.5: Comparison of sites of Vasoflux action with those of heparin, LMWH, and direct thrombin inhibitors. Vasoflux inhibits factor IXa-mediated activation of factor X independently of AT and HCII and catalyzes inactivation of fibrin-bound thrombin by HCII (Weitz et al., 1999). Heparin and LMWH inactivate factor Xa and thrombin (Weitz et al., 1999). Direct thrombin inhibitors inactivate fibrin-bound thrombin and thrombin (Weitz et al., 1999).

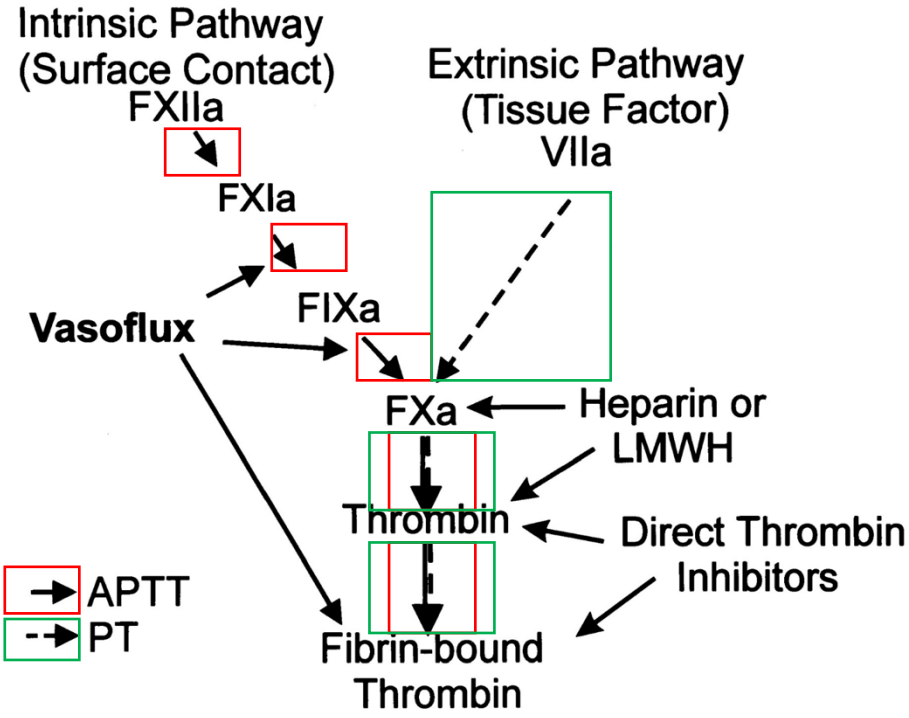

1.6 Hypotheses and Specific Aims

1.6.1 Hypotheses

1. Vasoflux will exert a protective effect in a cecal ligation and puncture (CLP) murine model of sepsis.
2. The combination of Vasoflux and DNase 1 will have a greater protective effect in a CLP murine model of sepsis compared to monotherapy.

1.6.2 Specific Aims

1. To compare the effects of UFH, enoxaparin and Vasoflux on the intrinsic and extrinsic pathways of the coagulation cascade.
2. To assess whether UFH, enoxaparin and Vasoflux prevent histone-mediated cytotoxicity.
3. To determine the binding affinity between a) Vasoflux and histones H2A, H3, and H4 and b) UFH and histones H2A, H3, and H4.
4. To evaluate if Vasoflux alone, or in combination with DNase1 will lead to reduced mortality rates, lower scores of surrogate markers of death, and reduced organ damage in septic mice compared to saline-treated mice.

Figure 1.6: Proposed Mechanism of Vasoflux and DNase1 in Sepsis. Activated neutrophils release NETs which are scaffolds of DNA, histones, antimicrobial peptides, and neutrophil enzymes (such as MPO, NE). The double stranded DNA component of NETs may be digested by DNases, thereby releasing histones into the circulation. Due to the negative charge on heparan sulfate, which is expressed on the surface of endothelial cells, it may also displace histones from the DNA-histone complexes in NETs. Vasoflux, a negatively charged non-anticoagulant, neutralizes the harmful effects of histones.

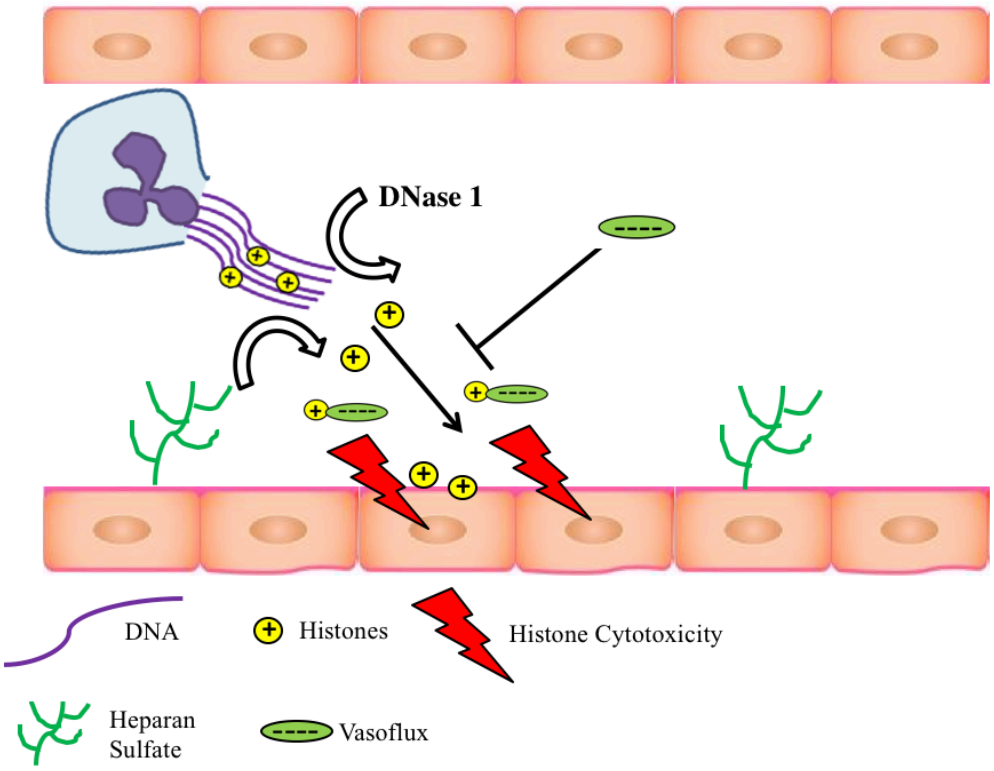

2.0 Materials and Methods

2.0.1 Materials

Vasoflux was prepared by depolymerizing UFH to a LMWH and reducing its affinity for AT via sodium periodate oxidation (Weitz et al., 1999). It was kindly provided by Dr. Jeff Weitz (TaARI, Canada). Heparin was purchased from Leo Pharma (Thornhill, ON, Canada). Enoxaparin was purchased from Hamilton General Hospital Pharmacy (Hamilton, ON, Canada). Recombiplastin was purchased from Instrumental Laboratory (Bedford, MA, USA). Technothrombin TGA thrombin generation assay and Technothrombin TGA software were purchased from Technoclone (Vienna, Austria, Europe). APTT-SP HemoSil reagent was purchased from Instrumentation Laboratory (Bedford, MA, USA). Tissue plasminogen activator (tPA) was purchased from Aviva Systems Bio (San Diego, Ca). Unfractionated bovine histones were purchased from Worthington Biochemical Corporation (Lakewood, NJ, USA). Trypan blue was purchased from Gibco from Life Technologies (NY, USA). Penicillin-streptomycin was from Invitrogen (Carlsbad, CA, USA). Fetal bovine serum (FBS) was purchased from Sigma (St. Louis, MO, USA). FBS Dulbecco's Modified Eagle Medium (DMEM) was purchased from Life Technologies (Burlington, ON, CA). Human histones H1, H2A, H2B, H3 and H4 were purchased from New England Biolabs (Massachusetts, USA). Polyclonal rabbit anti-human fibrin antibody, monoclonal goat anti-fibrin antibody, and alkaline phosphatase goat anti-rabbit secondary antibody were purchased from Dako (Burlington, ON). Vector Red was purchased from Vector Laboratories, Burlington, ON. Phosphate-buffered saline was purchased from Sigma-Aldrich (St. Louis, MO, USA). Histological photomicrographs

were collected using an Olympus BX41 fluorescent microscope and an Olympus DP72 camera (Olympus Corporation).

2.0.2 Preparation of Platelet-Poor Plasma (PPP)

To prepare platelet-poor plasma (PPP), blood was obtained from healthy human blood via venipuncture into 3.2% trisodium citrate. Next, whole blood was centrifuged at 1500 × g for 10 minutes at room temperature. The plasma layer was collected, pooled, and stored in aliquots at -80°C.

2.0.3 Thrombin Generation Assay (TGA)

Thrombin generation assays (TGAs) were performed as per the manufacturer's instruction. PPP (40 μl) was loaded into a 96-well black costar plate and coagulation was initiated by the addition of either Recombiplastin (1:500 dilution) or 20 μg/ml of DNA (obtained from buffy coats of healthy donors) to activate the extrinsic or intrinsic pathway, respectively. Where specified, UFH, enoxaparin, Vasoflux or UFH-histone complexes was added to the samples. UFH-histone complexes were prepared by incubating 6.7 μM of UFH and increasing concentrations of a mixture of unfractionated bovine histones for 1 hour at 37°C. To generate thrombin, 25 μl of technothrombin containing 30 mM of $CaCl_2$ and 2 mM of fluorogenic thrombin substrate, Z-Gly-Arg-AMC were added, and monitored using the Technothrombin TGA thrombin generation assay. Absorbance was monitored at 450 nm for 90 minutes at 37°C in a SpectraMax plate reader (Molecular Devices, Sunnyvale CA, USA). The concentration of thrombin (nM) produced was calculated using the thrombin calibration curve. Thrombin generation profiles were analyzed using Technothrombin TGA software.

2.0.4 Activated Partial Thromboplastin Time (aPTT)

Increasing concentrations of Vasoflux, diluted in a total volume of 40 µl of PPP, were added to wells containing 40 µl of APTT-SP HemoSil reagent. The plate was incubated at 37°C for 5 minutes, after which 40 µl of 30 mM $CaCl_2$ was added. Absorbance was monitored at 340 nm for 1 hour at 37°C in a SpectraMax plate reader (Molecular Devices, Sunnyvale CA, USA).

2.0.5 Prothrombin Time (PT)

Increasing concentrations of Vasoflux, diluted in a total volume of 40 µl of PPP, was added to a 96 well plate. The plate was incubated at 37°C for 5 minutes, after which 40 µl of RecombiPlasTin 2G Hemosil reagent containing 7.5 mM $CaCl_2$ was added. Absorbance was monitored at 340 nm for 1 hour at 37°C in a SpectraMax plate reader (Molecular Devices, Sunnyvale CA, USA).

2.0.6 Investigating the pharmacokinetics of intravenously administered Vasoflux after every 30 minutes in C57Bl/6J mice

To investigate the pharmacokinetics of Vasoflux, healthy C57Bl/6J mice were intravenously injected with 10 mg/kg of Vasoflux and after 30 minutes blood was collected via IVC (as described in section 2.0.11). The blood was spun at 5000xg for 20 minutes and platelet-poor plasma was stored in aliquots at -80°C. APTT assays were conducted on the PPP to quantitate the amount of Vasoflux as described in section 2.0.4.

2.0.7 Cytotoxicity Assay

Human embryonic kidney (HEK 293) cells were cultured in DMEM supplemented with 5% FBS and 1% Penicillin-Streptomycin (100 U/mL of penicillin and 100 µg/mL of streptomycin). HEK 293 (50,000 cells/well) were seeded in a 24-well tissue culture plate and grown to 50-60% confluency in medium. The following formula was used to determine the concentration of cells/ml to be seeded:

$$\text{Concentration of cells} = \left(\frac{\text{Number of cells counted}}{4}\right) \times 10{,}000$$

After an overnight incubation, cells were treated with 50 μg/ml of unfractionated bovine histone alone or in combination with Vasoflux, enoxaparin, or UFH at concentrations of 1 μg/ml, 10 μg/ml, 50 μg/ml, 100 μg/ml and 200 μg/ml for 24 hours. The negative control consisted of only the cell solution and media. Cell viability was assessed using a trypan blue assay.

2.0.8 Surface Plasmon Resonance (SPR)

Binding interactions were studied by surface plasmon resonance (SPR) using a Biacore T200 (GE Healthcare, Piscataway, NJ) and were performed with the guidance of Dr. Jim Fredenburgh. Human histones H2A, H3, and H4, diluted to 10 µg/ml in 10 mM sodium acetate, pH 4.5, were covalently linked to individual flow cells on a CM5 sensor chip using an amine coupling kit (according to Biacore protocol) at a flow rate of 10 μL/min for 600 s, when approximately 4000 response units (RU) were bound. Briefly, an injection of N-3-dimethylaminopropyl-N'-ethylcarbodiimide hydrochloride (EDC) and N-hydroxysuccinimide (NHS) was used to activate the CM5 chip and 1 M ethanolamine was used to block any non-specific binding. To measure the binding of GAGs to histones,

increasing concentrations of up to 50 μg/ml of Vasoflux, UFH, or calf-thymus DNA were injected into the flow cells at a flow rate of 20 μl/min for 180 s and a dissociation time of 300 s with buffer only. All SPR runs for this sensor chip were performed with HBS containing 20 mM Hepes, 150 mM NaCl, 0.01% Tween 20 at pH 7.4. Between runs, flow cells were regenerated with 1M NaCl, 250 mM imidazole, 10mM EDTA at pH 7.4 for 60s.

For each condition, RU values at equilibrium were determined by instrument software by subtracting the RU values obtained in the control flow cell blocked with ethanolamine. Equilibrium values were then plotted against the starting concentrations of UFH or Vasoflux and data were fit to the model below using Biacore T200 to determine the dissociation constant values (K_D):

$$R_{eq} = \frac{CR_{max}}{K_D + C} + RI$$

This model calculates the K_D for a 1:1 interaction from a plot of steady state binding levels (R_{eq}) against analyte concertation (C). R_{max} measures the analyte binding capacity of the surface. The equation includes a term for the bulk refractive index contribution RI, which is assumed to be the same for all samples (GE Healthcare Biacore T200 Getting Started, 2012).

2.0.9 Experimental Sepsis: Cecal Ligation and Puncture (CLP)

C57Bl/6J mice (Helicobacter hepaticus-free) were purchased from Charles River Laboratories (Sherbrooke, Quebec, Canada) and bred at the Thrombosis and Atherosclerosis Research Institute at McMaster University (Hamilton, ON, Canada). Mice were housed in a Helicobacter/Murine Norovirus-negative clean room in individually

ventilated cages (Tecniplast Sealsafe Plus system) under 12 hr dark/light cycles. Air was filtered through HEPA filters using Touch Slimline air handling units, which guarantee 75 air changes per hour in each cage. The mice were provided with enrichment, and sterilized water and food (Harlan Teklad Rodent Diet #2018) ad libitum. Mice received humane care in accordance with Canadian Council on Animal Care (CCAC) guidelines and all studies were approved by the Animal Research Ethics Board at McMaster University.

Healthy 8-12 weeks old male C57BL/J6 mice were randomized to either CLP to induce sepsis or sham surgery as a non-septic control. The CLP model implemented in our 24 hour survival study is adapted from past protocols with minor modification (Rittirsch et al., 2009). To maintain consistent conditions and reduce variability among the groups, surgeries were performed in a clean surgical site in the morning. The preoperative setup consisted of anesthetizing the mice with isoflurane and shaving the lower quadrant of the abdomen. The area was disinfected and sterilized with a proviodine solution followed by wiping with 70% alcohol pads. Under isoflurane, a longitudinal skin midline laparotomy was performed and the cecum was located. In CLP mice, 1 cm of the cecum was ligated and punctured through-and-through using a sterile 18-gauge needle. 0.5 cm of fecal matter was extruded from each puncture hole and returned back to the peritoneal cavity. The abdominal muscle and skin layer were closed with simple running sutures with the first and last suture being a double knot for each layer. In sham mice, the cecum was exteriorized and returned to the peritoneal cavity without ligation or puncture. Buprenorphine (0.1 mg/kg, Temgesic) was administered subcutaneously pre-operatively and every 6 hours post-operatively for pain relief. Ringer's lactate (2 ml) was administered subcutaneously

pre-operatively and every 4 hours post-operatively (Mai et al., 2015). Starting at 12 hours, fluid volume was reduced to 1 ml every 4 hours till 24 hour endpoint. External heat was provided for all mice through heating blankets set at low temperature that were placed below half of each cage.

2.0.10 Experimental Design

A series of studies were conducted to determine the optimal therapeutic regimen of Vasoflux. First, mice were injected intraperitoneally (I.P.) with either enoxaparin or Vasoflux at 8 mg/kg at 4 hours and 12 hours hours-post surgery. This dose was calculated based on equivalence to the previous study conducted by Wildhagen et al, which injected 570 μg of AADH (a non-anticoagulant heparin) into mice (Wildhagen et al., 2014). In a dose finding study, mice were injected I.P. with 10 mg/kg, 30 mg/kg, or 50 mg/kg of Vasoflux every 6 hours until endpoint given that the half-life of LMWH is 4-7 hours. Finally, the effects of a single tail vein intravenous injection of 1 mg/kg or 10 mg/kg of Vasoflux or UFH once at 6 h post-surgery were assessed (Table 1).

Table 1: Outline of a series of studies that were conducted to determine the optimal means of administration of Vasoflux, enoxaparin, and UFH.

Study #	**Treatment groups**	**Molecular Weight (kDa)**	**Mice**	**Dosages**	**Route of adminis-tration**	**Number of Injections**	**Volume for each injection (mL)**	**Time of Administration**
1	Vasoflux	5.5	Sham and CLP	8 mg/kg	I.P.	2	1	4 and 12 hours post-CLP
	Enoxaparin	5.5	Sham and CLP	8 mg/kg	I.P.	2	1	4 and 12 hours post-CLP
	Saline		Sham and CLP		I.P.	2	1	4 and 12 hours post-CLP
2	Vasoflux	5.5	Sham and CLP	10 mg/kg 30 mg/kg 50 mg/kg	I.P.	3	0.5	6, 12, and 18 hours post-CLP
	Saline		Sham and CLP		I.P	3	0.5	6, 12, and 18 hours post-CLP
3	Vasoflux	5.5	Naïve	1 mg/kg 10 mg/kg	I.V.	3	0.1	Time point 0
	UFH	15	Naïve	1 mg/kg (100U/ml) 10 mg/kg (1000U/ml)	I.V.	1	0.1	Time point 0
	Saline				I.V.	1	0.1	Time point 0
4	Vasoflux	5.5	Sham and CLP	1 mg/kg 10 mg/kg	I.V	**1**	0.1	6 hours post-CLP
	UFH	15	Sham and CLP	1 mg/kg (100U/ml) 10 mg/kg (1000U/ml)	I.V	1	0.1	6 hours post-CLP
	Saline		Sham and CLP		I.V	1	0.1	6 hours post-CLP

2.0.11 Post-Operative Monitoring and Endpoint

Mice were continuously monitored every 4 hours until 24 hours post-surgery for surrogate markers of death until experimental or humane endpoint. Body temperature was measured using a rectal probe thermometer. Mice were humanely euthanized via cervical dislocation if their Mouse Grimace Score was greater than 1.75, or if their temperature measured via a rectal probe fell below 23°C (Table 2).

Table 2: Endpoint Analysis and Monitoring form.

Endpoint Monitoring Form for Surrogate Markers

Dr. Patricia Liaw
Principal Investigator

Student(s)

15 03 11
AUP #

X40773
Contact #

Date	
Surgery	
Time point	

If any of the following conditions are met, mice will be humanely euthanized:
- **MGS score >1.75, and if MGS >1.5, measure temperature every 2 hour**
- **Temperature by rectal probe <23 degrees C**
- **Study endpoint has been reached (8 or 24 hours post-surgery)**

Mouse ID												
Blood in stool	Y/N											
Vomiting	Y/N											
Inability to ambulate	Y/N											
Mouse Grimace Scale (below)												
Orbital Tightening												
Nose and Cheek Bulge												
Ear Positing-Erected												
Whisker Change-Erected												
→ **Average of above MGS markers**	0-3											
Hunched posture an little movement	0-3											
Difficulty Breathing	0-3											
Cold, blue extremities	0-3											
Restlessness	0-3											
Responsiveness	0-3											
Vocalizations	0-3											
Temperature-Rectal Probe												

2.0.12 IVC Blood Collection

Under gaseous anesthesia, blood was collected via the inferior vena cava (IVC) into a one-tenth volume of 3.2% sodium citrate, spun at 5000xg for 20 minutes and platelet-poor plasma was stored in aliquots at -80°C.

2.0.13 Organ Histology

Organs were collected in formalin, embedded in paraffin wax, processed, and sectioned at 5μm in thickness. Organ sections were stained with hematoxylin and eosin (H&E) phosphotungstic-acid and hematoxylin (PTAH) for the analysis of overall morphology and scored on a 3-point system. The sections were incubated with polyclonal rabbit anti-human fibrin antibody (1:200 dilution) that detects both fibrin and fibrinogen. The anti-fibrin antibody was detected by incubation with an alkaline phosphatase goat anti-rabbit secondary antibody (1:200 dilution) followed by incubation with Vector Red, a substrate that generates a bright-red product. DAPI (1:5000 dilution) was used to counter stain the samples for nuclei. Samples of stained lung, liver, and kidney sections were visualized by an Olympus BX41 fluorescent microscope and images were collected using an Olympus DP72 camera. Two clinical pathologists, who were blinded to the surgery and treatment allocation, assessed the extent of organ injury. Organ sections were scored by evaluating the level of inflammatory cell infiltration, thrombus formation, and capillary leakage (from 0 representing absence of abnormal organ pathology to up to 3 for severe organ damage).

2.0.14 Gel Electrophoresis

Histone-DNA complexes were prepared by incubating 50 μg/ml of histones and 300 μg/ml of calf-thymus DNA for 1 hour at 37°C. Next, increasing concentrations of Vasoflux and heparin were added to the complexes for 1 hour at 37°C. 4 μl of 6X orange blue loading dye was added to 20 μl of samples and 20μL of the prepared samples were added to 1.5% agarose gels for electrophoresis. After staining with RedSafe, gels were photographed using UV transillumination.

2.0.15 Statistical Analysis

Data are represented as mean ± standard error of the mean (SEM) and were statistically analyzed using one-way ANOVA with Bonferroni post-hoc tests, or Mantel-Cox log-rank test for survival curve analyses. All analyses were performed using GraphPad Prism 5.0 software (La Jolla, CA, USA), and differences between groups were considered significant at $p<0.05$.

3.0 Results

3.0.1 Effect of UFH, enoxaparin, and Vasoflux on thrombin generation in platelet-poor plasma

UFH, enoxaparin, and Vasoflux are GAGs with average molecular weights of 15 kDa, 5.5 kDa, and 5.5 kDa, respectively. UFH catalyzes AT-mediated inactivation of thrombin through simultaneous binding of its pentasaccharide sequence to AT and binding of an additional 13 saccharide units to thrombin (Hirsh, Warkentin, et al., 2001). The pentasaccharide of enoxaparin binds to and induces a conformational change in AT, thus significantly accelerating AT's inactivation of FXa (Hirsh, Warkentin, et al., 2001).Vasoflux is a LMWH depleted of the AT-binding pentasaccharide (Weitz et al., 1999). In this study, we examined the effects of UFH, enoxaparin, and Vasoflux on their ability to attenuate thrombin generation in PPP from healthy volunteers. As seen in Figure 3.1, addition of UFH at .067 μM, or enoxaparin at 0.2 μM to plasma significantly attenuates thrombin generation when coagulation was initiated with either Tissue Factor (TF) (panel A) or DNA (panel B). In contrast, much higher concentrations of Vasoflux ($\geq$ 20 μM) are required to completely inhibit thrombin generation in the presence of TF (panel A) or DNA (panel B).

Figure 3.1: Effects of UFH, enoxaparin, or Vasoflux on thrombin generation in platelet-poor plasma. Thrombin generation was initiated with either TF (panel A) or buffy coat DNA (panel B) in PPP in the presence of UFH, enoxaparin, or Vasoflux. Thrombograms are expressed as mean ± SEM of 3 independent experiments. Enoxaparin, UFH, and Vasoflux are compared to PPP. ** P<0.001, ****P<0.0001.

A)

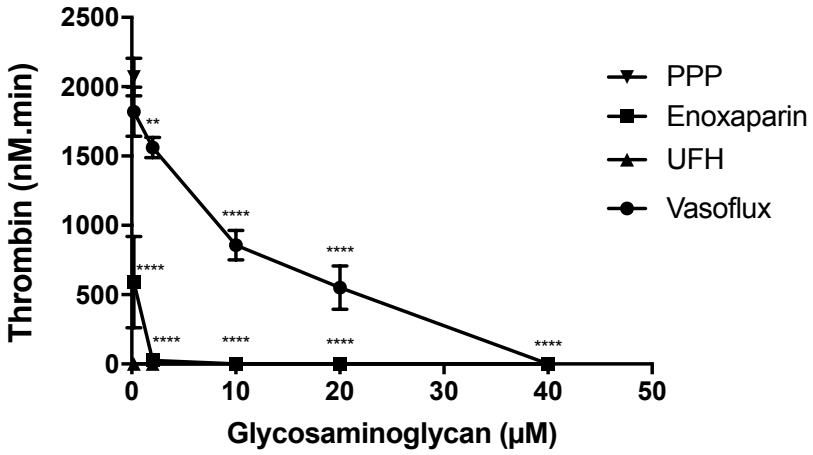

B)

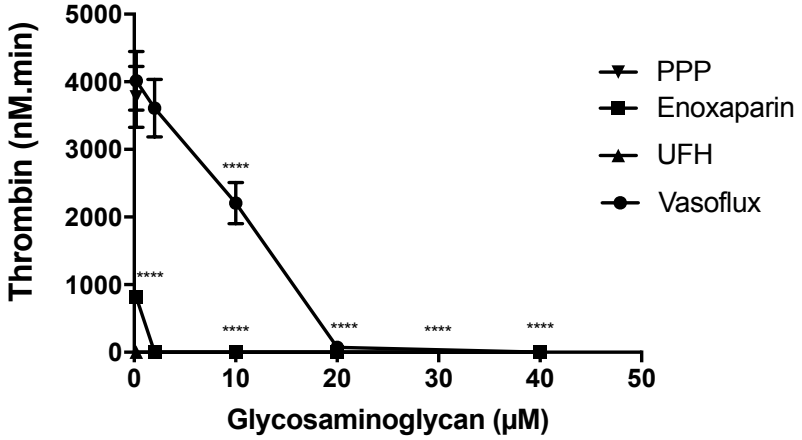

3.0.2 Effect of Vasoflux on activated partial thromboplastin time in murine platelet-poor plasma

To explore the effect of Vasoflux on the intrinsic pathway of coagulation, we conducted an aPTT assay using increasing concentrations of Vasoflux. The aPTT test measures the rate at which coagulation occurs when initiated via the intrinsic pathway. As shown in Figure 3.2, addition of Vasoflux at 20 μM, 40 μM, 181 μM increased clot time ~2-fold, ~4-fold, and ~12-fold, respectively compared to the control group containing PPP, the aPTT reagent, and $CaCl_2$.

Figure 3.2 Effects of Vasoflux on activated partial thromboplastin time in murine platelet-poor plasma. The aPTT was determined in murine PPP in the presence of increasing concentrations of Vasoflux. The relative time to clot is expressed as mean ± SEM of 3 independent experiments.

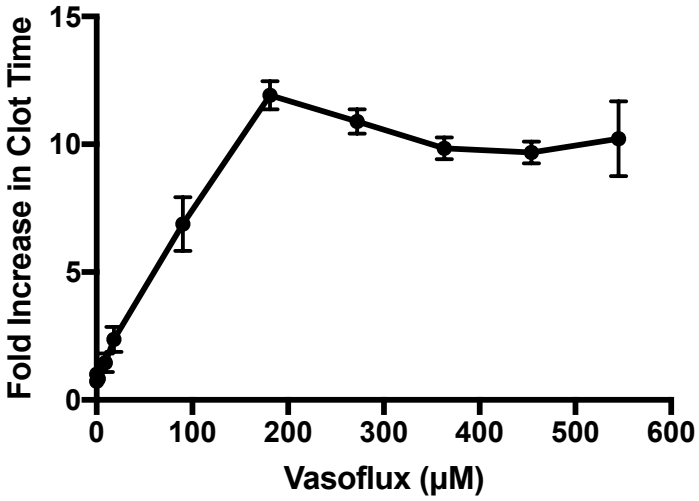

3.0.3 Effect of Vasoflux on prothrombin time in murine platelet-poor plasma

To explore the effect of Vasoflux on the extrinsic pathway of coagulation, we conducted a PT assay using increasing concentrations of Vasoflux. The PT test measures the rate at which coagulation occurs when initiated via the extrinsic pathway. As shown in Figure 3.3, addition of Vasoflux at 18 μM delays the relative clot time approximately 3-fold compared to the control group containing PPP, the PT reagent, and $CaCl_2$.

Figure 3.3 Effects of Vasoflux on prothrombin time in murine platelet-poor plasma. The PT was determined in murine PPP in the presence of increasing concentrations of Vasoflux. The relative time to clot is expressed as mean ± SEM of 2 independent experiments.

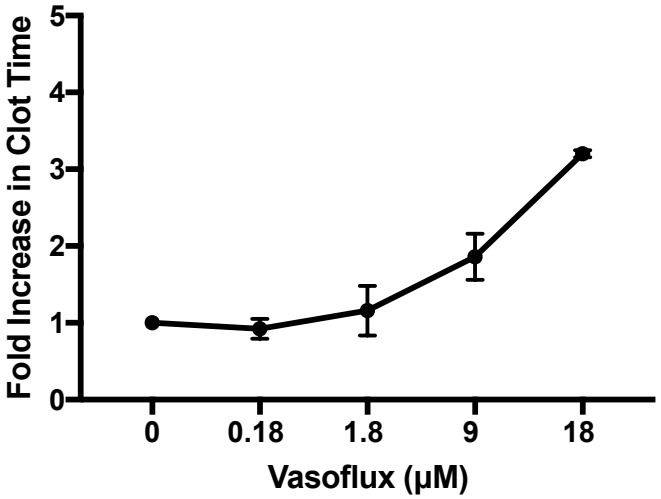

3.0.4 Investigating the pharmacokinetics of intravenously administered Vasoflux after every 30 minutes in murine platelet-poor plasma

To investigate the pharmacokinetics of Vasoflux, healthy mice were intravenously injected with 10 mg/kg of Vasoflux and after 30 minutes blood was collected via IVC (as described in section). APTT assays were conducted on the PPP to quantitate the amount of the Vasoflux in the plasma. As shown in Figure 3.4, at 30 minutes to 2 hours post-injection, the clot time was delayed by 2-fold in mice injected with Vasoflux compared with naïve mice. Interestingly at 2.5 hours post-injection, the clot time was delayed by 15-fold. At 4 hours post-injection, the clot time was delayed by 2-fold and returned back to normal levels at 4 hours. This suggests that injection of 10 mg/kg of Vasoflux into healthy mice does not alter the clotting time with in the first 2.0 hours post-injection. However, we observed a transient anticoagulant effect occurring in the mice at 2.5 hours post-injection.

Figure 3.4: Investigating the pharmacokinetics of intravenously administered Vasoflux after every 30 minutes in healthy C57Bl/6J mice. To investigate the pharmacokinetics of Vasoflux, healthy mice were intravenously injected with 10 mg/kg of Vasoflux and after 30 minutes blood was collected via IVC. APTT assays were conducted on the PPP to quantitate the amount of Vasoflux in the plasma. The relative time to clot is expressed as mean ± SEM of 1 independent experiment (n=2).

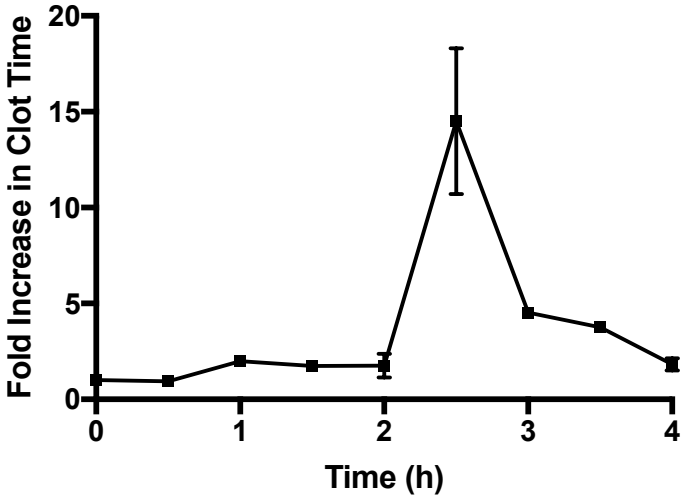

3.0.5 Influence of UFH, enoxaparin, and Vasoflux on neutralizing histone-mediated cytotoxicity

Heparin is known to bind to histones and prevent histone-mediated cytotoxicity in vitro (Wildhagen et al., 2014). To explore the ability of different molecular weight heparins to neutralize histone-mediated cytotoxicity, we conducted a cytotoxicity assay on HEK 293 cells using UFH (15kDa), enoxaparin (5.5 kDa), and Vasoflux (5.5 kDa). HEK 293 cells were used due to their efficient reproduction (Thomas et al., 2005). HEK 293 cells were pre-treated with either 0 μg/ml, 20, μg/ml 40 μg/ml, 80 μg/ml or 200 μg/ml of a mixture of unfractionated bovine histones for 24 hours. Percent cell viability was measured via trypan blue staining. Exposure of cells to elevated concentrations of histones resulted in significantly reduced cell viability compared to untreated cells. To explore the possibility that heparin molecules neutralize the cytotoxic activity of histones, UFH, enoxaparin, or Vasoflux at concentrations of up to 13.3 μM, 40 μM, or 40 μM respectively were incubated with 50 μg/ml of unfractionated histones for 24 hours. As depicted in Figure 3.5, addition of UFH, enoxaparin, or Vasoflux to histones increased the percent of live cells in a dose-dependent manner (panels A, B, and C). These results suggest that the a) ability of GAGs to neutralize histone-mediated cytotoxicity is independent of the AT-binding pentasaccharide and b) based on molarity, UFH is a more potent inhibitor of histone-mediated cytotoxicity compared to Vasoflux or enoxaparin.

Figure 3.5. Effect of histone exposure on cell cytotoxicity in the presence of (A) UFH, (B) enoxaparin, (C) and Vasoflux. HEK 293 cells were treated with either 10 mM H_2O_2 (for 24 hours), 50 μg/ml of histones alone or in combination with heparins for 24 hours. Data are expressed as mean values of 3 independent experiments. * indicates $P < 0.05$ and ** indicates $P < 0.001$.

A)

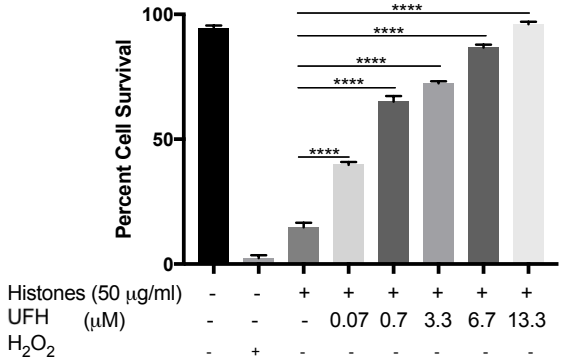

B)

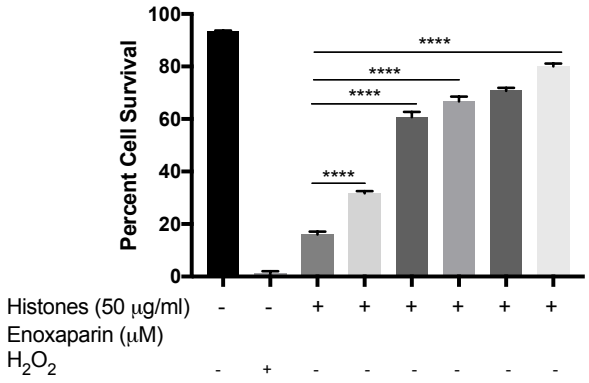

C)

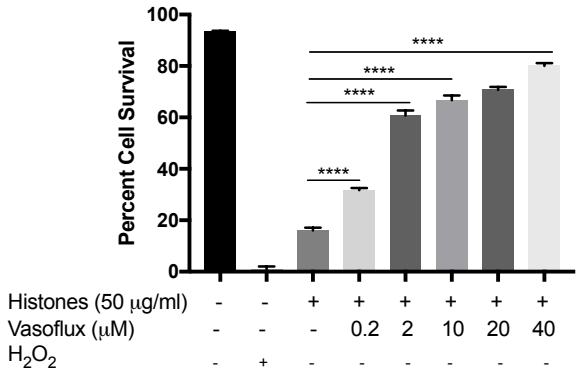

3.0.6 Interaction of Histones H2A, H3, and H4 with DNA, Vasoflux, and UFH

Surface Plasmon Resonance (SPR) was used to quantify the interaction of human histones H2A, H3, and H4 with UFH (Figure 3.6 A-C), Vasoflux (Figure 3.6 D-F), and DNA (Figure 3.6 G-I). As shown in the senosograms, histones exhibit rapid association and slow dissociation with Vasoflux and UFH. UFH and Vasoflux exhibit dose-dependent and saturable binding to the histones. Specifically, UFH binds to histones H2A, H3, and H4 with K_D values of $2.7x10^1 \pm 15$ nM, $1.9\ x10^1 \pm 4.9$ nM, and $1.4\ x10^1 \pm 2.9$ nM, respectively. Vasoflux binds to histones H2A, H3, and H4 with K_D values of $3.6\ x10^2 \pm 149$ nM, $3.8\ x10^2 \pm 110$ nM, and $1.8\ x10^2 \pm 59$ nM, respectively. This suggests that UFH binds to histones H2A, H3, and H4 with ~10-fold higher affinity compared to Vasoflux. DNA exhibits dose dependent binding with H2A, H3 and H4 at concentrations lower than 5 μg/ml, 25 μg/ml, and 25 μg/ml, respectively. However, at higher concentrations, the data was not analyzable as DNA levels did not reach saturation.

Figure 3.6. Binding of UFH, Vasoflux, and DNA to Histones H2A, H3, and H4 as determined by SPR. Human histones H2A (A and D), H3 (B and E), and H4 (C and F) were linked to carboxyl groups on a CM5 sensor chip. UFH (A-C), Vasoflux (D-F), and DNA (G-I) was injected into the flow cells to assess binding, followed by buffer injection to assess dissociation. Binding affinities between UFH and H2A, H3, and H4 are provided in panels J-L. Binding affinities between Vasoflux and H2A, H3, and H4 are provided in panels (M-O). Binding affinities were determined by plotting the maximum response units at equilibrium in the senosograms.

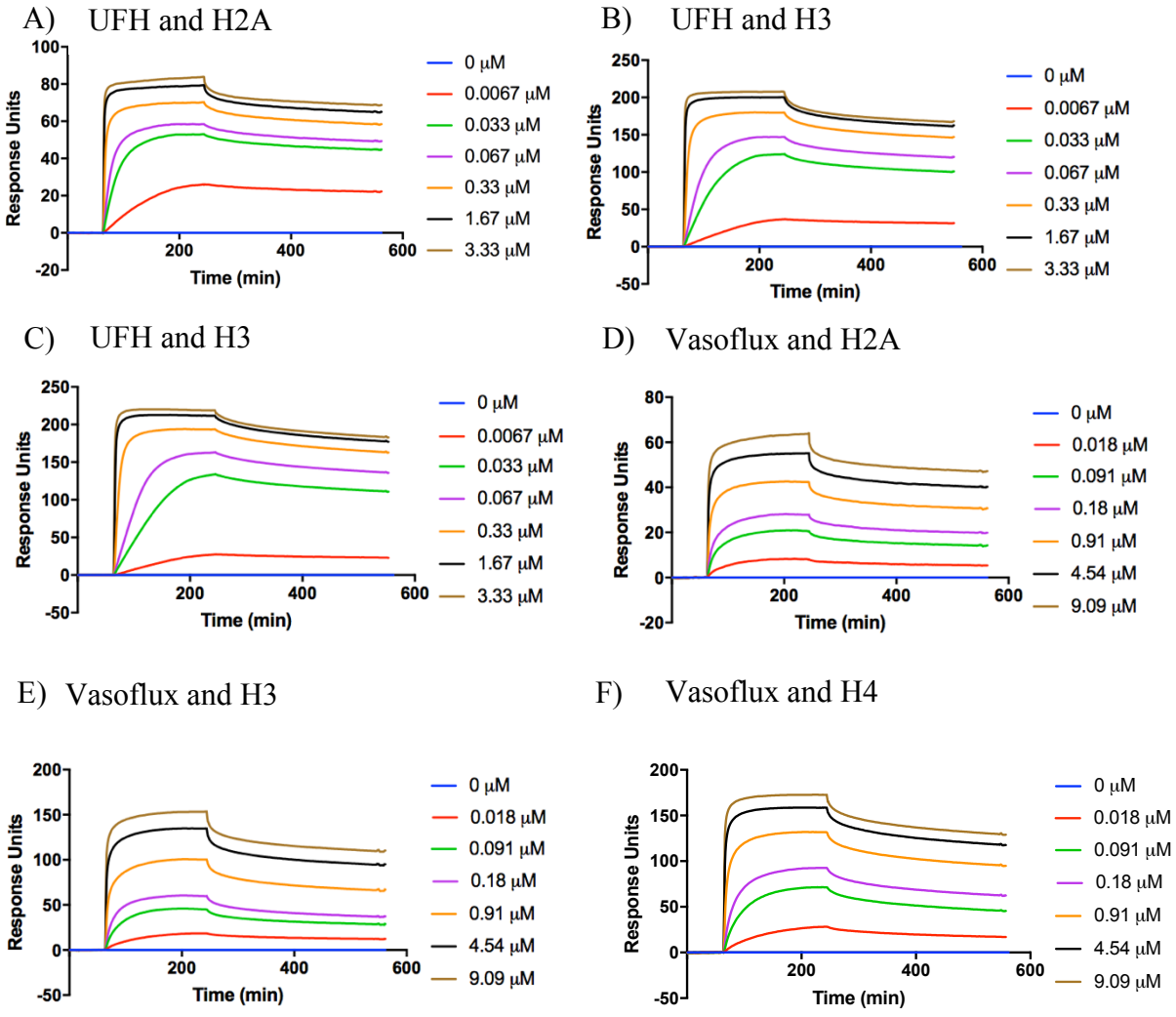

G) DNA and H2A

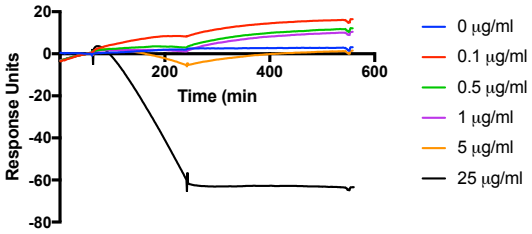

H) DNA and H3

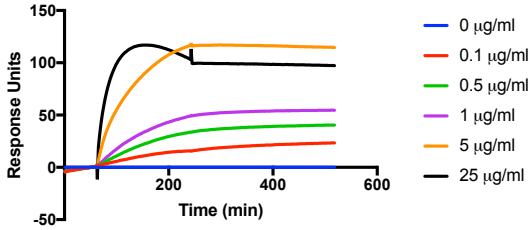

I) DNA and H4

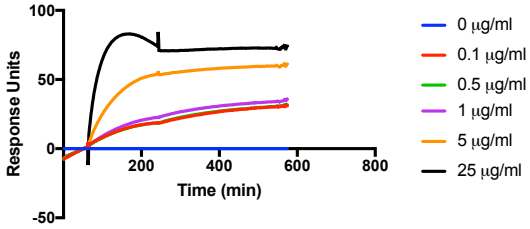

J) UFH and H2A

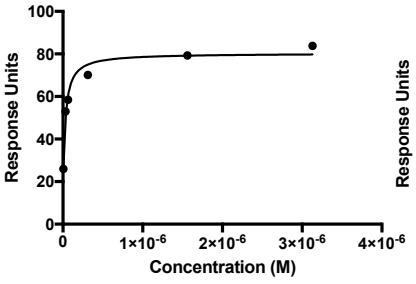

$K_D = 2.7x10^1 \pm 15$ nM

K) UFH and H3

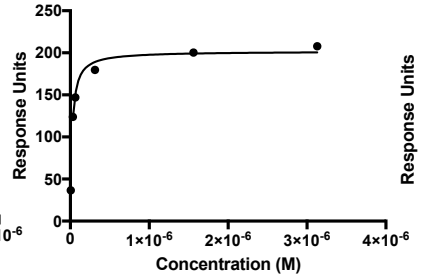

$K_D = 1.9\ x10^1 \pm 4.9$

L) UFH and H4

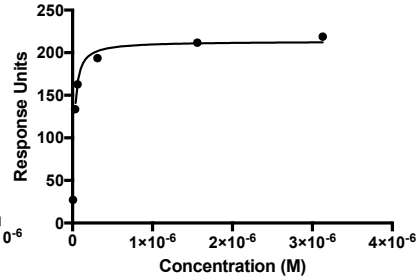

$K_D = 1.4\ x10^1 \pm 2.9$ nM

M) Vasoflux and H2A

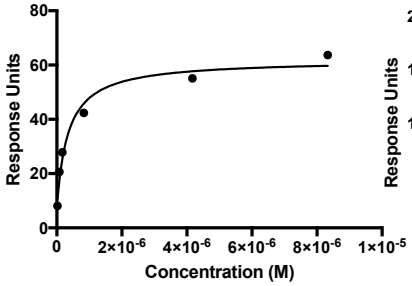

$K_D = 3.6\ x10^2 \pm 149$ nM

N) Vasoflux and H3

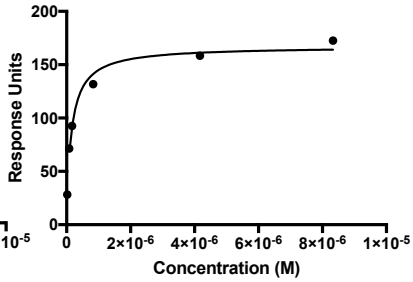

$K_D = 3.8\ x10^2 \pm 110$ nM

O) Vasoflux and H4

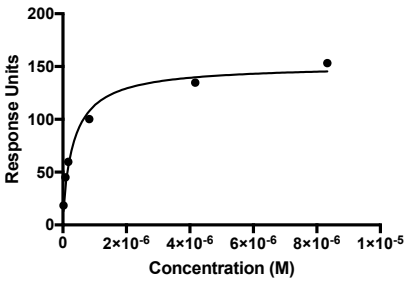

$K_D = 1.8\ x10^2 \pm 50$

3.0.7 Pilot Animal Studies

Our *in vitro* findings support a key role for Vasoflux in binding histones and neutralizing histone-mediated cytotoxicity. Therefore, we explored whether Vasoflux, with a reduced anticoagulant activity, is a more effective sepsis therapy than enoxaparin or UFH. Specifically, we investigated the effects of Vasoflux on organ function and survival in a mouse model of CLP. Before conducting our animal research, the Canadian Council on Animal Care ethic guidelines had to be taken into account, which exclude death as an endpoint and recommend the use of surrogate markers of death to establish humane endpoints of death where possible (Sneddon et al., 2017). In experimental sepsis, researchers have designed different scoring systems as tools to assess the progression of sepsis in mice: the Murine Sepsis Score (MSS); the Mouse Grimace Score; and the Mouse Clinical Assessment Score for Sepsis M-CASS). Despite the development of these validated scoring systems, there is a paucity of animal sepsis research utilizing these tools. Comparisons of these scoring systems have not been performed to inform standardization of surrogate endpoints of death in a clinically relevant CLP model of sepsis. We therefore set out to compare the effectiveness of these scoring systems and body temperature for predicting disease progression as well as death in our murine CLP model of sepsis. The individual components of these scores range from 0-3, where 0 represents characteristics similar to naïve mice. Temperature measurements were taken with a rectal probe, which can be documented as an objective marker in endpoint monitoring.

This research has resulted in a co-first authorship publication titled, “Body temperature and mouse scoring systems as surrogate markers of death in cecal ligation and

puncture sepsis," which has been published in Intensive Care Medicine Experimental (paper attached in Appendix). The authors are as follows: Safiah H. Mai*, Neha Sharma*, Andrew Kwong, Momina Khan, Peter M. Grin, Dhruva J. Dwivedi, Alison E. Fox-Robichaud, and Patricia C. Liaw (* denotes co-first authorship).

3.0.8 Effects of repeated I.P. injections of Vasoflux and Enoxaparin at 4 and 12 hours post-surgery in septic and sham mice

I.P. administration of AADH (a 15 kDa non-anticoagulant UFH) has been shown to neutralize histones in vitro and to improve survival in cecal ligation and puncture (CLP)-induced sepsis (Wildhagen et al., 2014). To explore the protective effects of Vasoflux, enoxaparin, and UFH in a CLP model of sepsis, we conducted a series of 24 h survival studies as outlined previously (Table 1, methods section). In a phase 1 study, Vasoflux was administered intravenously to humans of up to doses of 16 mg/kg, with no bleeding risk and was found to be well tolerated and safe (Peters et al., 2001). Therapeutic doses of enoxaparin range from 1 mg/kg subcutaneous (SC) per 12 hours or 1.5 mg/kg SC per day (Shaikh et al., 2017).

Briefly, 8 mg/kg of Vasoflux or enoxaparin was intraperitoneally injected into healthy C56Bl/6J mice at 4 and 12 h post-surgery. By the 24 hour endpoint, mice administered saline, Vasoflux, or enoxaparin showed 80%, 50% and 75% percent survival, respectively. This differed from the 100% percent survival observed at 24 hours in sham groups treated with saline, Vasoflux, or enoxaparin, suggesting the Vasoflux and enoxaparin do not exert harmful effects in healthy mice subjected to sham surgery (Figure

3.7). There was no significant difference in body temperature between septic mice administered enoxaparin, Vasoflux, or saline (Figure 3.7B and C).

According to the CCAC ethic guidelines, which excludes death as an endpoint and recommends the use of surrogate markers of death to establish humane endpoints of death, mice were continuously monitored every 4 hours for surrogate markers of death until experimental or humane endpoint (please refer to section 2.0.11) (2 mice were not included in the results, as they died and hence were not euthanized). Mice were humanely euthanized via cervical dislocation if their Mouse Grimace Score was greater than 1.75, or if their temperature measured via a rectal probe fell below 23°C. There was no significant difference in either MGS scores or MSS scores between septic treated mice with Vasoflux or enoxaparin treatment compared to saline-treated mice (Figure 3.8). All treatment groups in mice subjected to CLP demonstrated significantly greater MGS and MSS scores than treatment groups in mice subjected to sham surgery (Figure 3.8).

Figure 3.7: Kaplan-Meier survival curves (A) and temperatures for septic and sham mice administered enoxaparin at 8 mg/kg (B) or Vasoflux at 8 mg/kg (C). Mice were injected with 8 mg/kg of Vasoflux or enoxaparin at 4 h and 12h post-CLP. Data are presented as mean ± SEM from 2 independent experiments representing a total number of n=4-5.

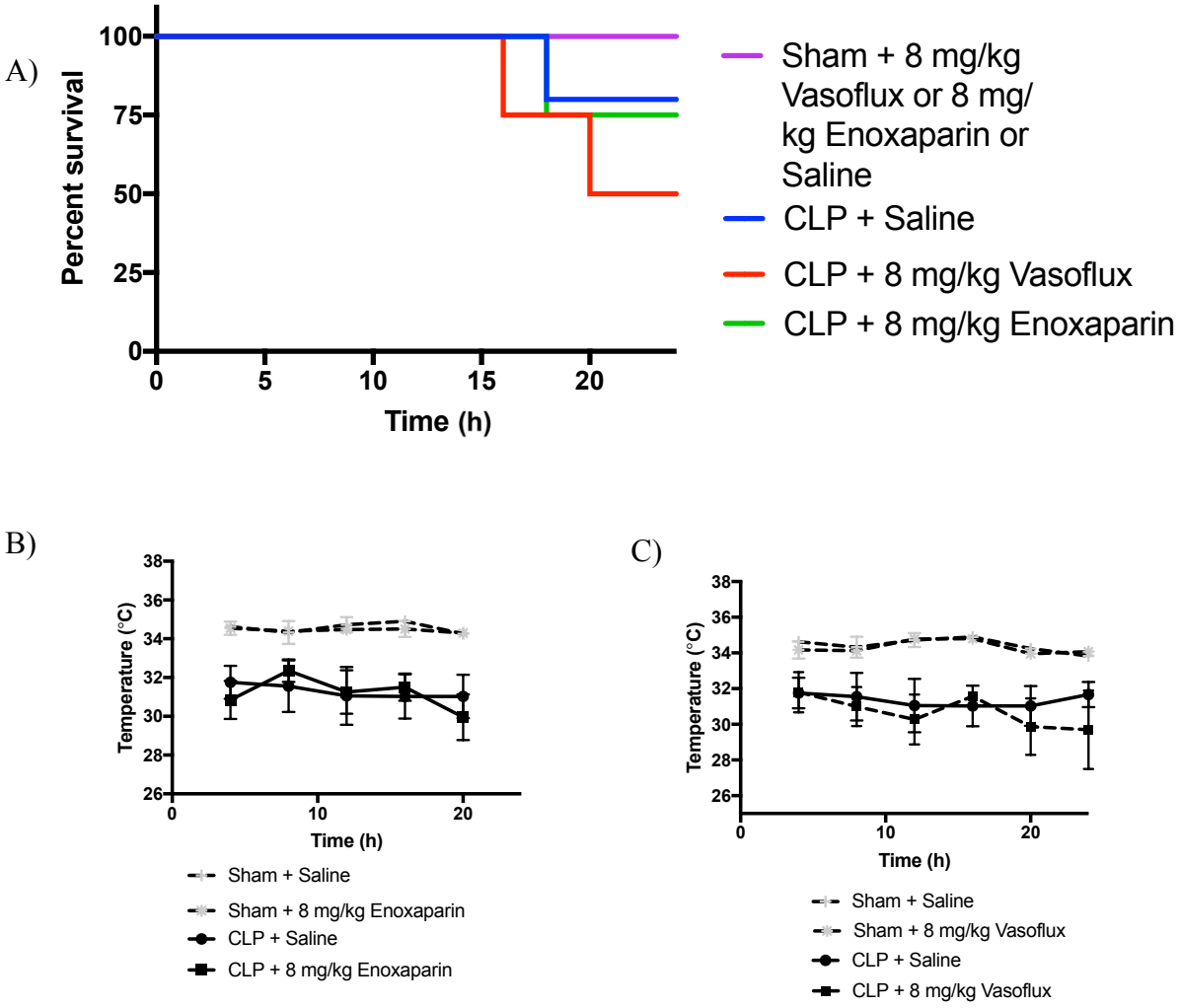

Fig. 3.8: Mouse Grimace Scale (MGS) score over time for septic and sham mice administered Vasoflux (A) and enoxaparin (B). Murine Sepsis Score over time for septic and sham mice administered Vasoflux (C) and enoxaparin (D). Mice were injected with 8 mg/kg of Vasoflux or enoxaparin at 4 h and 12h post-CLP. Data are presented as mean ± SEM from 2 independent experiments representing a total number of n=4.

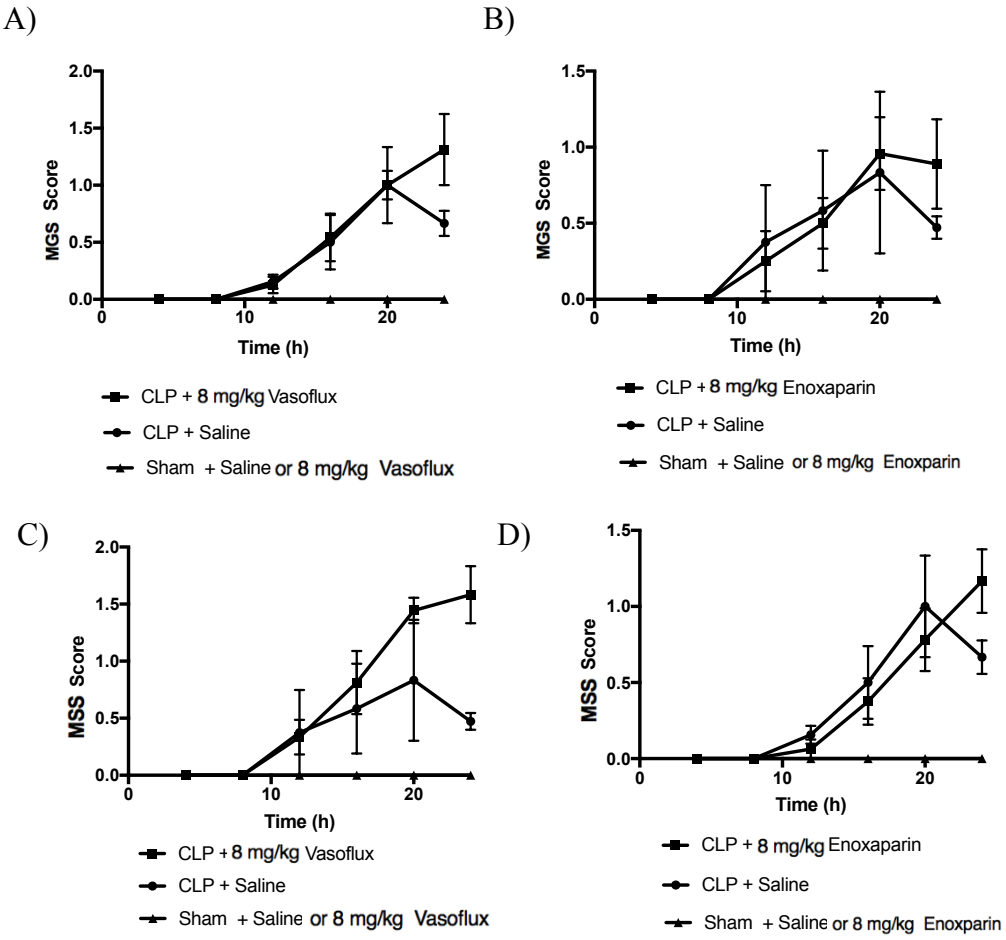

3.0.9 Effects of repeated I.P. injections of Vasoflux at 6, 12, and 18 hours post-surgery in septic and sham mice

As no significant difference was observed in percent survival of septic mice administered either saline or Vasoflux at 8 mg/kg at 4 and 12 hr post-surgery, we next varied the dose and time of administration of Vasoflux. Vasoflux was administered I.P. at doses of 10 mg/kg, 30 mg/kg, or 50 mg/kg to healthy and septic mice. The injections were repeated every 6 hours to account for a half-life of 4 to 7 hours for Vasoflux (Kufel et al., 2017). Briefly, 10 mg/kg, 30 mg/kg or 50 mg/kg of Vasoflux was repeatedly injected into sham and septic C56Bl/6J mice via I.P. at 6, 12, and 18 h post-surgery. There was no significant difference in temperature between septic mice administered Vasoflux or saline (Figure 3.9 B, C, and D). However, the survival rate was much lower in Vasoflux-treated CLP mice. During the 24 h study period, mice administered either 10 mg/kg, 30 mg/kg, or 50 mg/kg of Vasoflux showed 20%, 15%, and 9% percent survival respectively (Figure 3.9 A). This differed significantly from the 70% percent survival observed at 24 hours in mice administered saline and 100% percent survival in sham groups administered with either 10 mg/kg, 30 mg/kg, or 50 mg/kg of Vasoflux or saline. This suggests that Vasoflux at 10 mg/kg to 50 mg/kg is worse than 8 mg/kg (section 3.0.8).

MGS scores were significantly higher from 12 h post-CLP to 18 h post- CLP in mice administered Vasoflux compared to mice administered saline (Figure 3.10). CLP treated mice had significantly higher scores than sham mice. There was no significant difference in MSS scores between mice administered 10 mg/kg or 50 mg/kg of Vasoflux compared to mice administered saline. There was a significant difference in scores at 18 h

post-CLP in mice administered 30 mg/kg Vasoflux compared to mice administered saline (Figure 3.10). This suggests that administration of Vasoflux in septic mice after 12 hours and 16 hours post-surgery demonstrated worsened MGS and MSS, respectively compared to administration of 8 mg/kg of Vasoflux (section 3.0.8) .

Figure 3.9: Kaplan-Meier survival curve (A) and temperature for septic and sham mice administered 10 mg/kg (B), 30 mg/kg (C), or 50 mg/kg (D) of Vasoflux. Mice were injected I.P. with 10 mg/kg (B), 30 mg/kg (C), or 50 mg/kg of Vasoflux (D) at 6, 12, and 18 hours post-CLP or sham surgery. Data are presented as mean ± SEM from 4 independent experiments representing a total number of n=10.

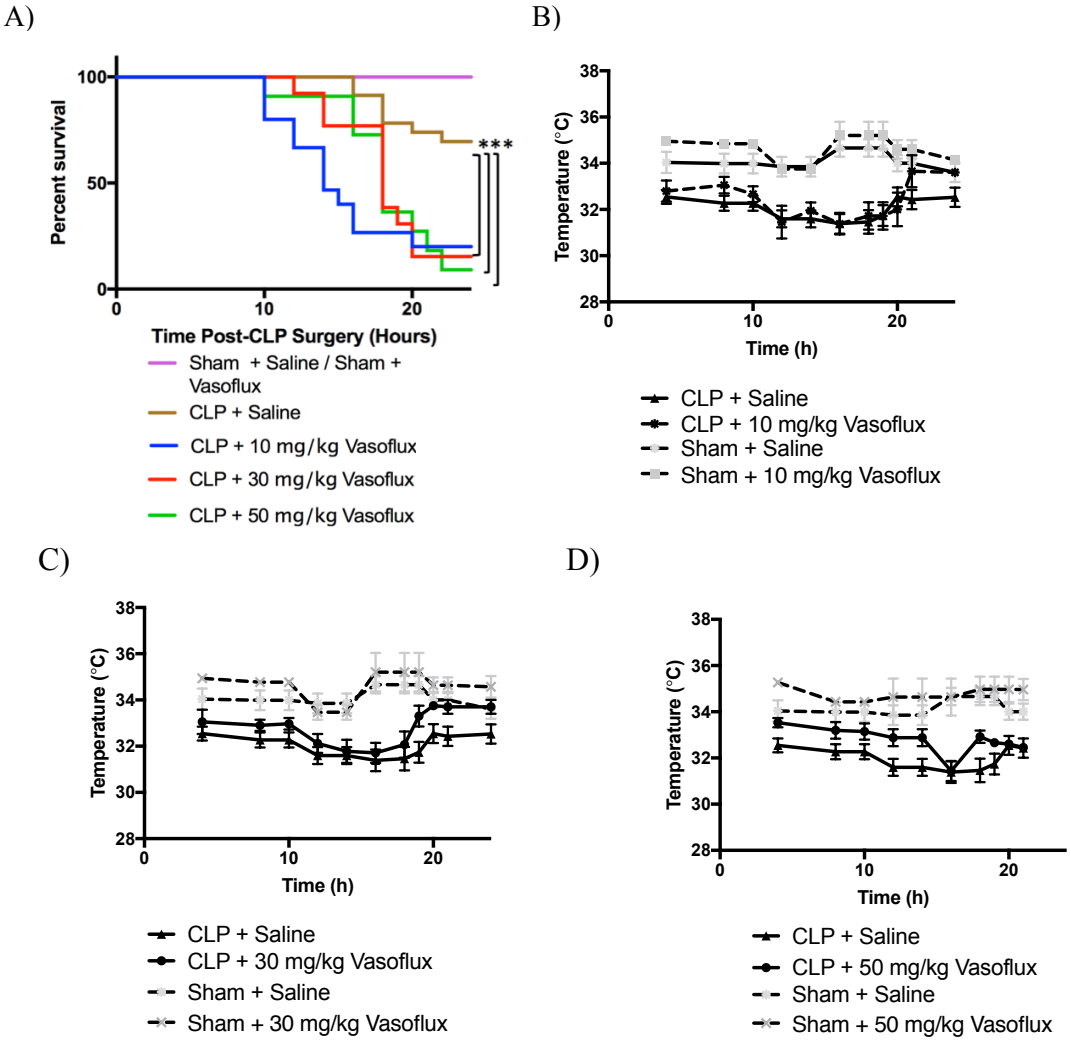

Fig. 3.10. Mouse Grimace Scale (MGS) score over time for septic and sham mice administered Vasoflux at 10 mg/kg (A), 30 mg/kg (B), or 50 mg/kg (C). Murine Sepsis Score (MSS) over time for septic and sham mice administered Vasoflux at 10 mg/kg (D), 30 mg/kg (E), or 50 mg/kg (F). Mice were injected with 10 mg/kg (A), 30 mg/kg (B), or 50 mg/kg of Vasoflux 6, 12, and 18 hours post-CLP or sham surgery. Data are presented as mean ± SEM from 4 independent experiments representing a total number of n=10-13.

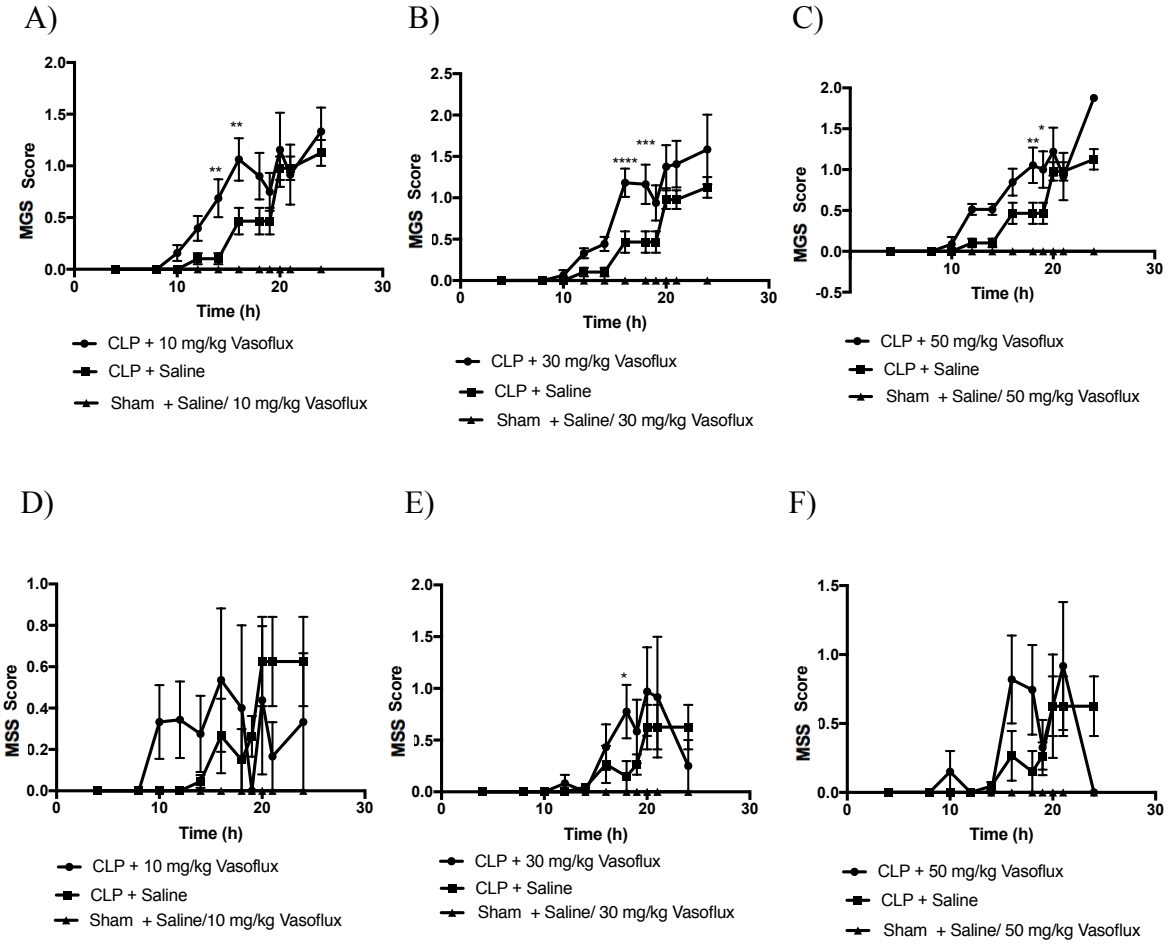

3.0.10 Effect of repeated I.P. injections of Vasoflux at 6, 12, and 18 h post-surgery on organ histology

Organ histology from sham- and CLP-operated mice was examined to confirm the presence of organ damage. Sham mice administered Vasoflux exhibited a significant dose-dependent increase in lung damage compared to sham mice administered saline. Septic mice administered Vasoflux exhibited significant lung, liver, and kidney damage (such as neutrophil accumulation, red blood cell congestion, and thrombi) compared to sham mice injected with Vasoflux. Large thrombi and fibrin meshwork were observed in septic mice administered Vasoflux. A pink material (stained with H&E) was observed around the glomerulus, alveoli, and vessels in the kidney, lung and liver respectively (Figures 3.11-3.12).

The administration of Vasoflux intraperitoneally to CLP mice significantly reduced survival compared to saline-treated mice especially in mice receiving high doses of Vasoflux. We thus changed the route of administration was changed to tail vein, the number of injections was reduced to one injection 6 h post-CLP at two lower doses (1 mg/kg and 10 mg/kg) were explored. The intravenous route of delivery allows for direct infusion of the substance into the blood vessels, by bypassing the need for solute absorption (Lukas et al., 1971). In contrast, the absorption for the material delivered intraperitoneally may undergo hepatic metabolism before reaching the systemic circulation (Abu-Hijleh et al., 1995).

Figure 3.11: Histology scores of sham-operated and CLP-operated mice administered saline or Vasoflux at 10 mg/kg, 30 mg/kg, or 50 mg/kg. Results are presented as mean organ damage scores for lung (A), liver (B), and kidney (C). Three repeated injections of Vasoflux (at 6, 12, and 18 hours post-surgery) were administered into sham and septic mice. Data are presented as mean ± SEM from 4 independent experiments representing a total number of n=10-13. * indicates $P < 0.05$, ** indicates $P < 0.001$, and *** indicates $P<0.0001$.

A)

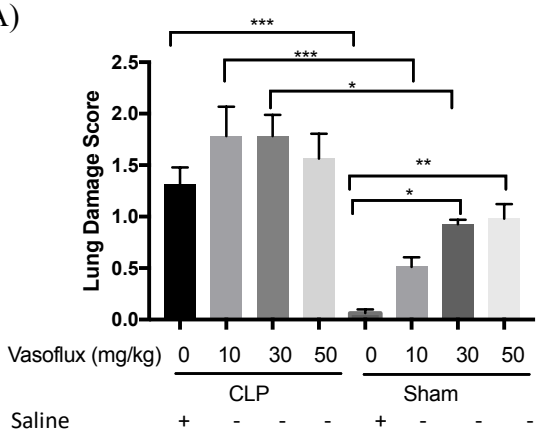

B)

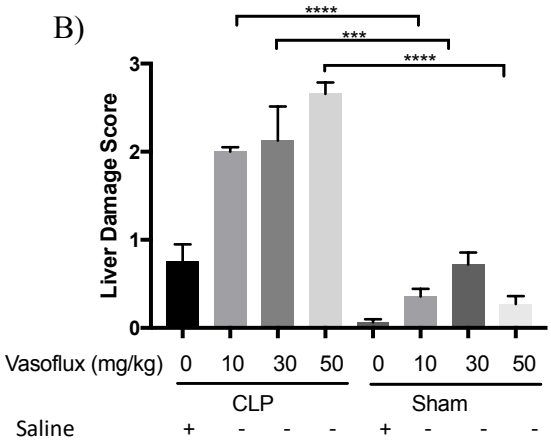

C)

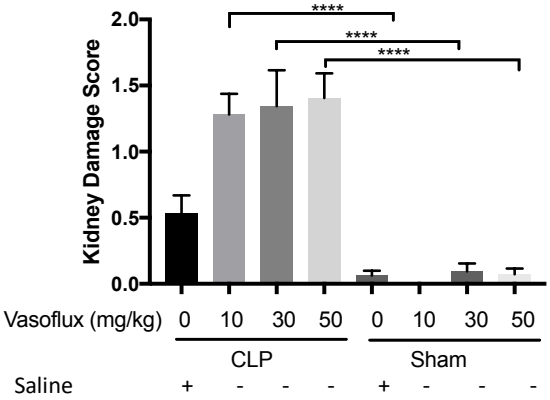

Figure 3.12: Histological photomicrographs of H&E (A) and fibrin (B) and DAPI (C) stained lungs, livers, and kidneys from sham- operated and CLP-operated mice injected I.P. with saline or Vasoflux at 10 mg/kg, 30 mg/kg, or 50 mg/kg. 6, 12, and 18 hours post-surgery, mice were treated with either saline or Vasoflux and at experimental or humane endpoint, organs were harvested in formalin and embedded in paraffin wax. The organs were sectioned 5 μm thick and stained with H&E for overall morphology and phosphotungstic acid for fibrin staining. Photomicrographs of sections were visualized under 20X magnification. The length of the scale bar represents 25 μm.

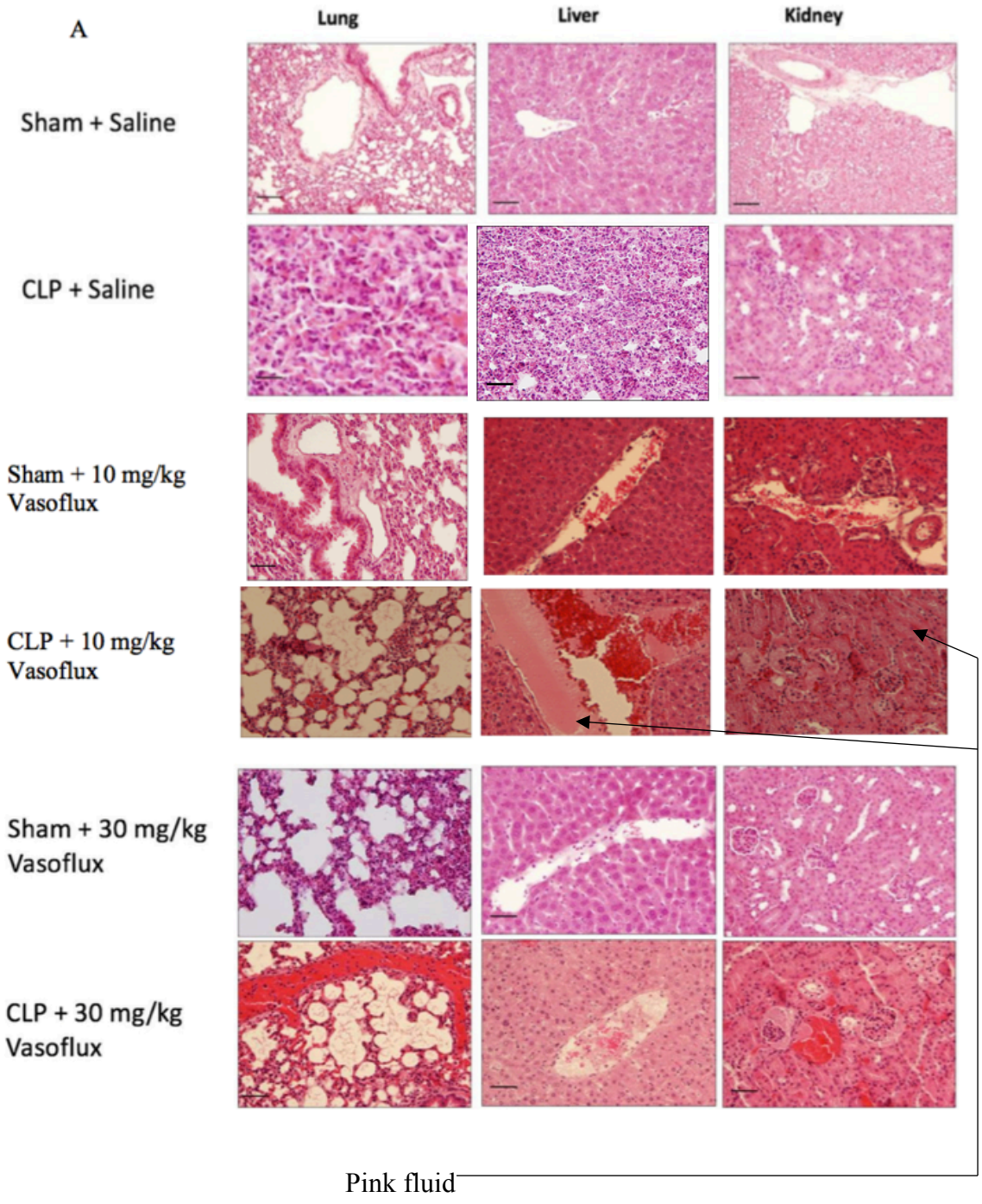
A
Lung
Liver
Kidney
Sham + Saline
CLP + Saline
Sham + 10 mg/kg Vasoflux
CLP + 10 mg/kg Vasoflux
Sham + 30 mg/kg Vasoflux
CLP + 30 mg/kg Vasoflux
Pink fluid

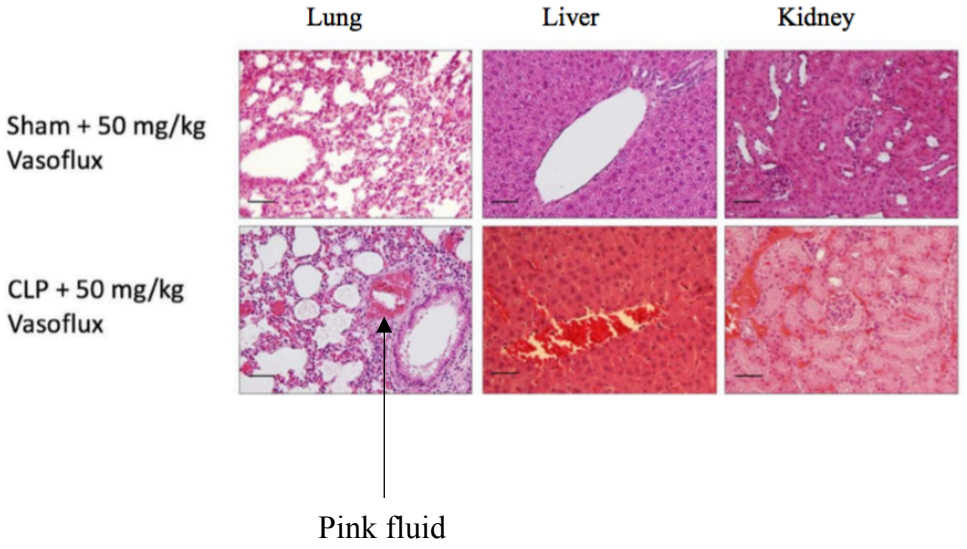
Lung
Liver
Kidney
Sham + 50 mg/kg Vasoflux
CLP + 50 mg/kg Vasoflux
Pink fluid

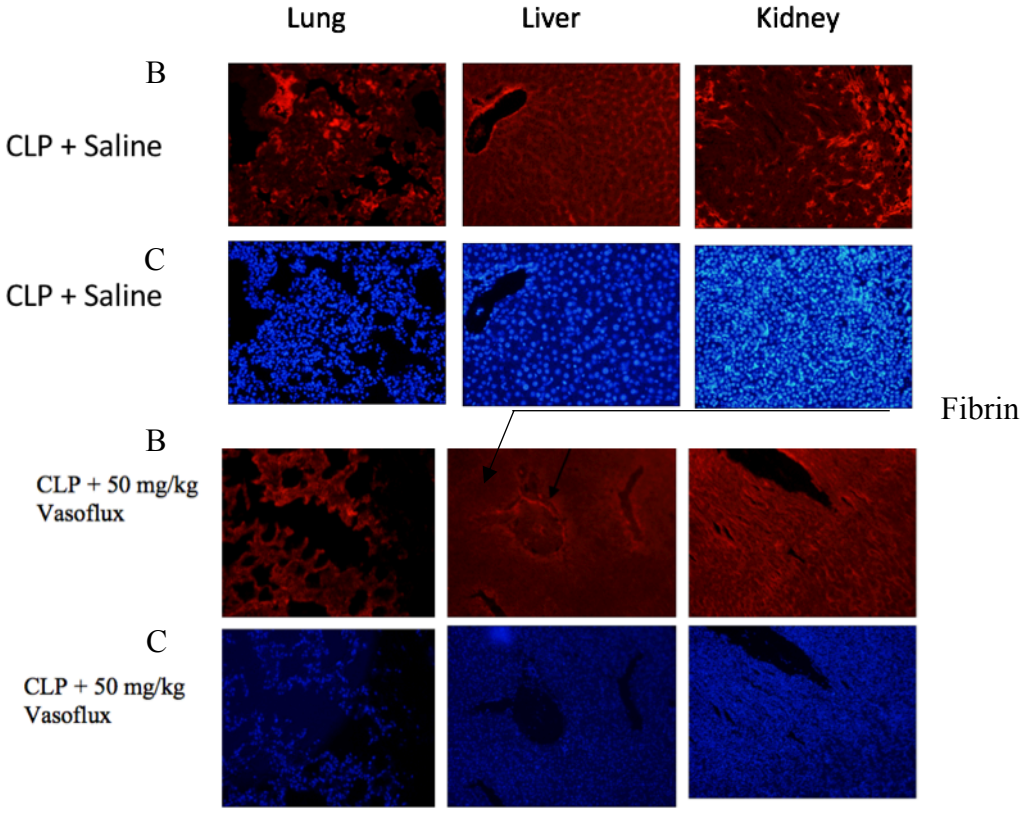
Lung
Liver
Kidney
B
CLP + Saline
C
CLP + Saline
Fibrin
B
CLP + 50 mg/kg Vasoflux
C
CLP + 50 mg/kg Vasoflux

3.0.11 Effect of a tail vein injection of Vasoflux or UFH in healthy mice

Since the starting material for the production of Vasoflux is UFH, the following experiments described below include UFH as a control. To determine the effects of Vasoflux or UFH in naïve healthy C56Bl/6J mice (from Jackson Laboratory), Vasoflux or UFH were administered at doses of 1 mg/kg or 10 mg/kg via a single tail vein injection. During the 24h period, all mice administered either saline, 1 mg/kg or 10 mg/kg of either Vasoflux or UFH showed a 100% survival (data not shown). There was no significant difference in temperature, between mice administered either Vasoflux, UFH, or saline. All MGS and MSS scores for the mice remained at 0 for the duration of the study (data not shown). There was also no differences in plasmas IL-6 levels between healthy mice administered 10 mg/kg of Vasoflux and naïve mice.

Organ histology was examined to determine the effects of Vasoflux or UFH in healthy mice. Healthy mice administered saline, 1 mg/kg or 10 mg/kg of Vasoflux or UFH exhibited no significant lung, liver, and kidney damage compared to the naïve mouse (Figure 3.13-3.14). These results suggest that Vasoflux is not detrimental in naïve C57BL/6J mice.

Figure 3.13: Histology scores of healthy mice injected with saline, Vasoflux, or UFH via tail vein at 1 mg/kg or 10 mg/kg. Results are presented as mean organ damage scores for lung (A), kidney (B), and liver (C). A single tail vein injection of either saline, Vasoflux, or UFH into naïve, healthy mice. Data are presented as mean ± SEM from experiment representing a total number of n=1-3.

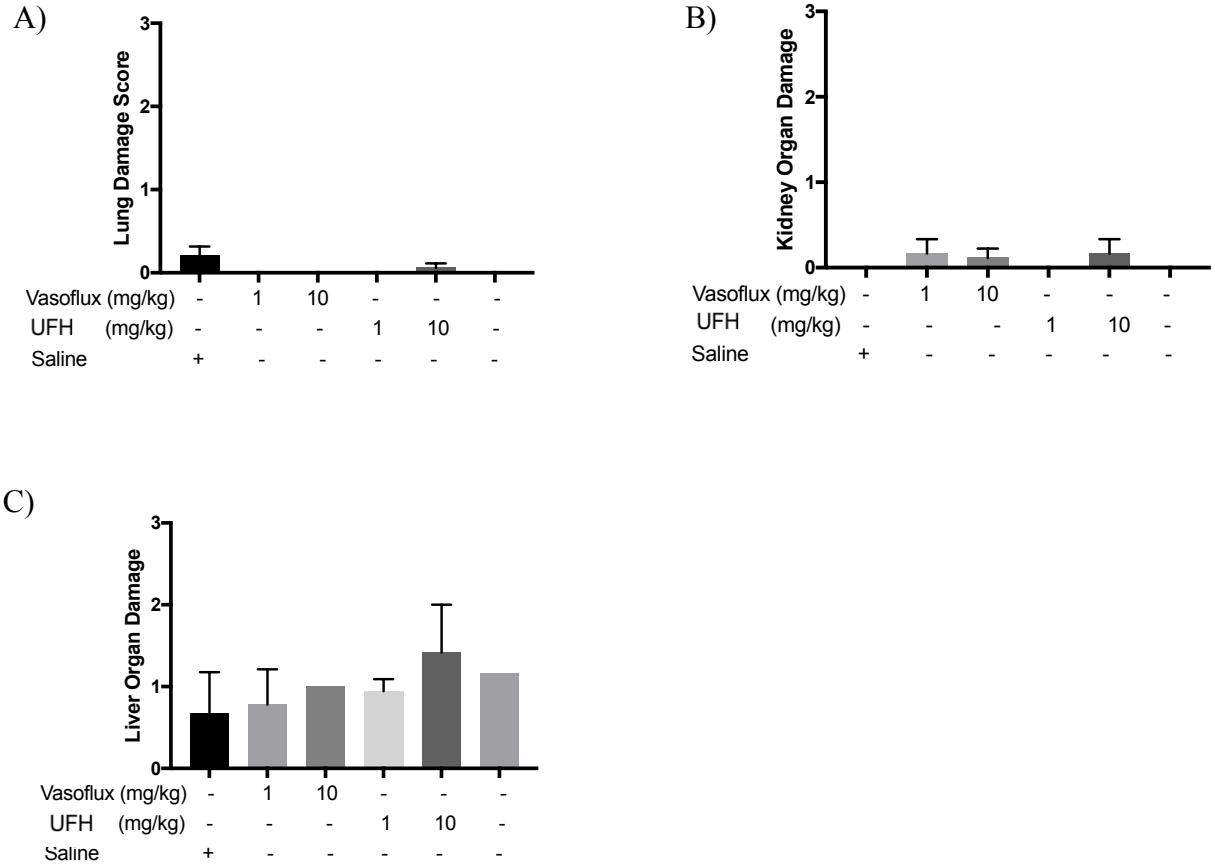

Figure 3.14: Histological photomicrographs of H&E stained lungs, livers, and kidneys from healthy mice injected via tail vein with saline, Vasoflux or UFH at 1 mg/kg or 10 mg/kg. Healthy mice were treated with either saline, Vasoflux, or UFH for 24 hours, after which organs were harvested in formalin and embedded in paraffin wax. The organs were sectioned 5 μm thick and stained with H&E for overall morphology. Photomicrographs of sections were visualized under 20X magnification. The length of the scale bar represents 25 μm.

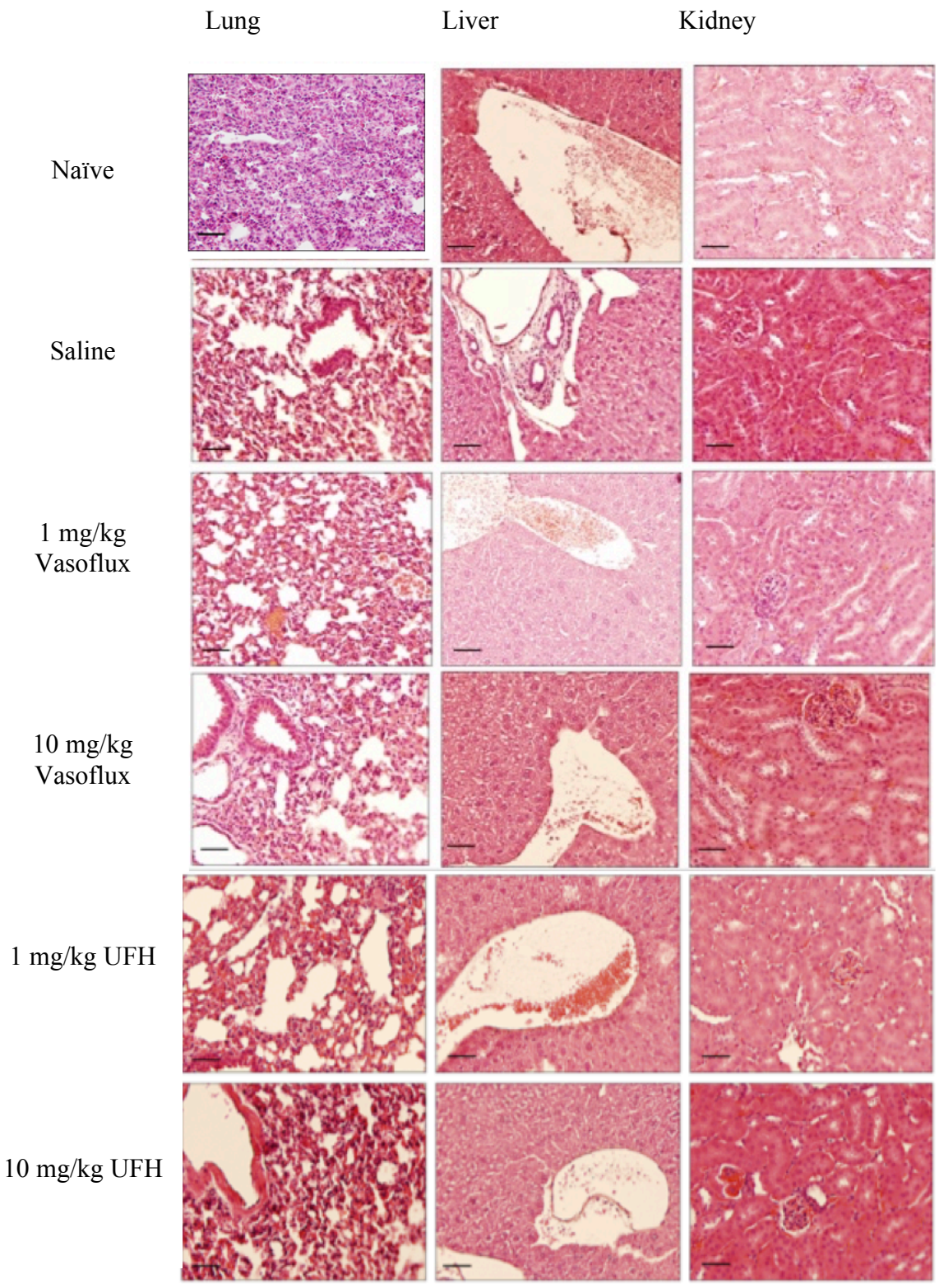
Lung
Liver
Kidney
Naïve
Saline
1 mg/kg Vasoflux
10 mg/kg Vasoflux
1 mg/kg UFH
10 mg/kg UFH

3.0.12 Effect of a tail vein injection of Vasoflux or UFH at 6 hours post-surgery in septic and sham mice

Given that a single tail vein injection at either 1 mg/kg and 10 mg/kg of Vasoflux or UFH into healthy mice did not show a harmful effect, this study was repeated in septic and sham mice. Briefly, 1 mg/kg or 10 mg/kg of either Vasoflux or UFH was injected into septic and sham C56Bl/6J mice via tail vein at 6 h post-surgery. During the 24 h study period, septic mice administered either 1 mg/kg of Vasoflux, 1 mg/kg of UFH or 10 mg/kg of Vasoflux showed 25% survival. This differed from the 75% percent survival observed at 24 hours in septic mice administered 10 mg/kg of UFH or saline and 100% percent survival in sham groups (Figure 3.15). There was no significant difference in temperature between septic mice administered Vasoflux, UFH, or saline (Figure 3.15).

There was no significant difference in MGS scores between mice administered 1 mg/kg of Vasoflux or 1 mg/kg or 10 mg/kg of heparin compared to mice administered saline. MGS scores were significantly higher at 18 h post-CLP in mice administered 10 mg/kg of Vasoflux compared to mice administered saline (Figure 3.16). There was a significant difference in MSS scores at 18 h and 21 h post-CLP in mice administered Vasoflux or 1 mg/kg of heparin, compared to mice administered saline, respectively. CLP treated mice exhibited significantly greater MGS and MSS scores compared to sham mice (Figure 3.16). This suggests that administration of Vasoflux in septic mice at later time points displayed worsened MGS and MSS compared to saline.

Figure 3.15: Kaplan-Meier survival curves (A and B) and temperature (C, D, E, and F) following CLP versus sham for mice administered a tail vein injection at 6 h post-surgery of either saline, Vasoflux, or UFH. Septic and sham mice were administered a tail vein injection of Vasoflux at either 1 mg/kg or 10 mg/kg, or UFH at either 1 mg/kg or 10 mg/kg. Data are presented as mean ± SEM from 2 independent experiments representing a total number of n=4.

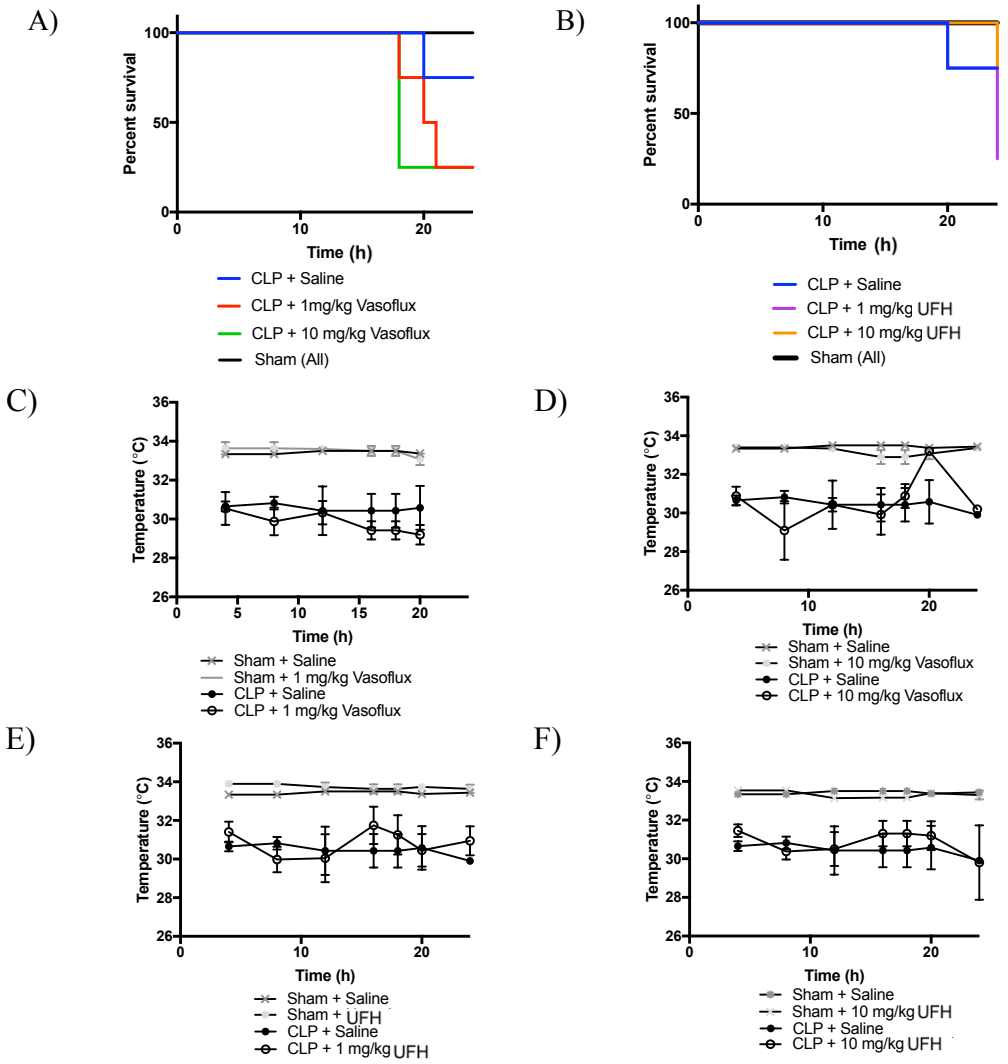

Figure 3.16: Mouse Grimace Scale (MGS) (A, B, C, D) and Murine Sepsis Score (MSS) (E, F, G, H) over time for septic and sham mice administered a tail vein injection 6 h post-surgery of Vasoflux or UFH at 1 mg/kg or 10 mg/kg. Mice were injected with Vasoflux at 1 mg/kg or 10 mg/kg, or UFH at 1 mg/kg or 10 mg/kg 6 hours post-CLP or sham surgery. Data are presented as mean ± SEM from 2 independent experiments representing a total number of n=4.

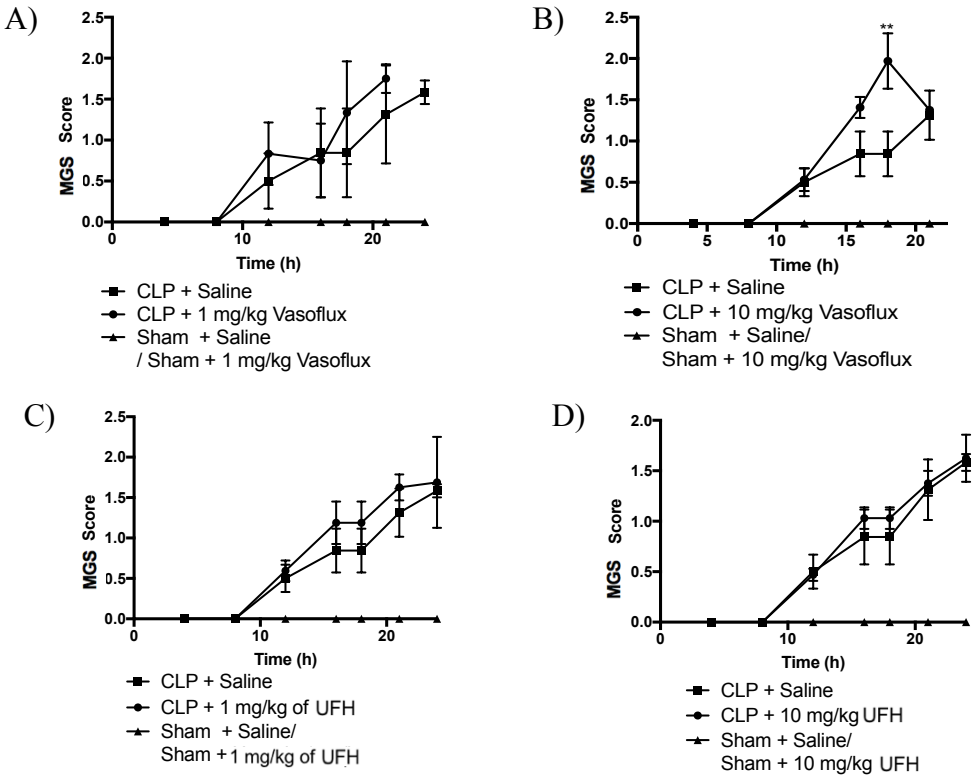

D)

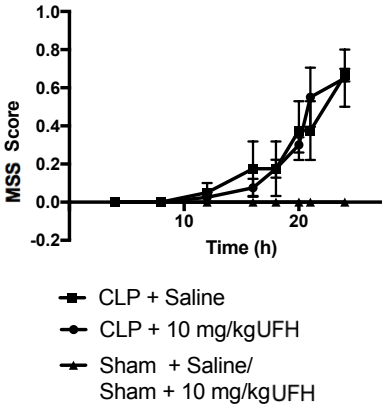
MSS Score
Time (h)
CLP + Saline
CLP + 10 mg/kgUFH
Sham + Saline/
Sham + 10 mg/kgUFH

E)

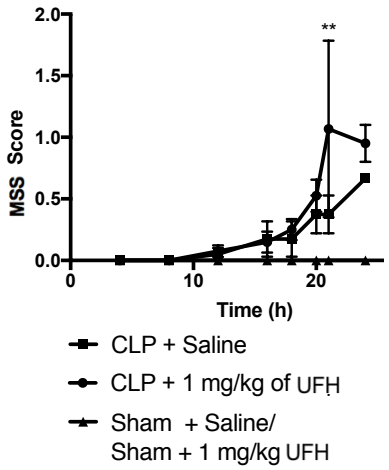
**
MSS Score
Time (h)
CLP + Saline
CLP + 1 mg/kg of UFH
Sham + Saline/
Sham + 1 mg/kg UFH

F)

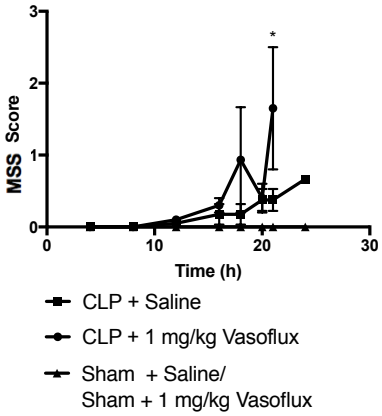
*
MSS Score
Time (h)
CLP + Saline
CLP + 1 mg/kg Vasoflux
Sham + Saline/
Sham + 1 mg/kg Vasoflux

G)

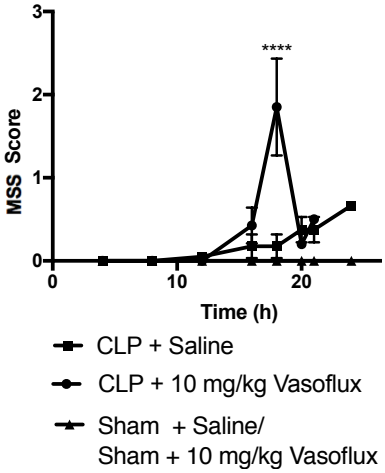
****
MSS Score
Time (h)
CLP + Saline
CLP + 10 mg/kg Vasoflux
Sham + Saline/
Sham + 10 mg/kg Vasoflux

3.0.13 Effect of a tail vein injection of Vasoflux or UFH at 6 hours post-surgery on organ histology in septic and sham mice

Organ histology from sham- and CLP-operated mice administered a tail vein injection 6 h post-CLP was examined to confirm the presence of organ damage. Septic mice administered 1 mg/kg Vasoflux or 1 mg/kg UFH exhibited significant lung and kidney damage compared to sham mice injected with Vasoflux (Figure 3.17 and 3.18). There was no significant difference in organ damage between septic mice administered 1 mg/kg or 10 mg/kg of Vasoflux or 1 mg/kg UFH.

Figure 3.17: Histology scores of sham-operated and CLP-operated mice administered saline or Vasoflux or heparin at 1 mg/kg or 10 mg/kg. Results are presented as mean organ damage scores for lung (A), liver (B), and kidney (C). One tail vein injection 6 hours post-CLP of Vasoflux or heparin was administered into sham and septic mice. Data are presented as mean ± SEM from 3 independent experiments representing a total number of n=3-4. * indicates P < 0.05, ** indicates P < 0.001, and *** indicates P<0.0001.

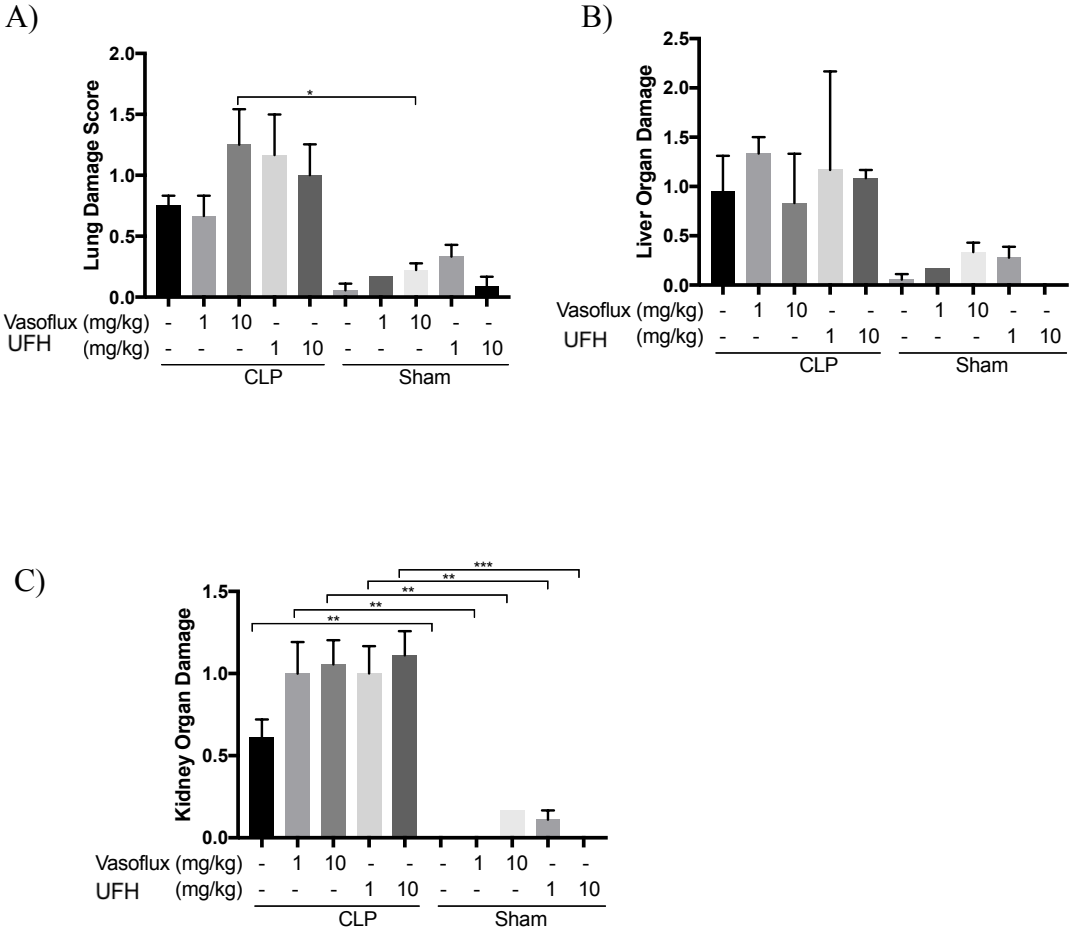

Figure 3.18: Histological photomicrographs of H&E stained lung, liver, and kidneys from sham-operated and CLP-operated mice administered saline, Vasoflux or UFH. Sections were stained with H&E and fibrin staining. A representative image is presented. Photomicrographs of sections were visualized under 20X magnification. The length of the scale bar represents 25 μm.

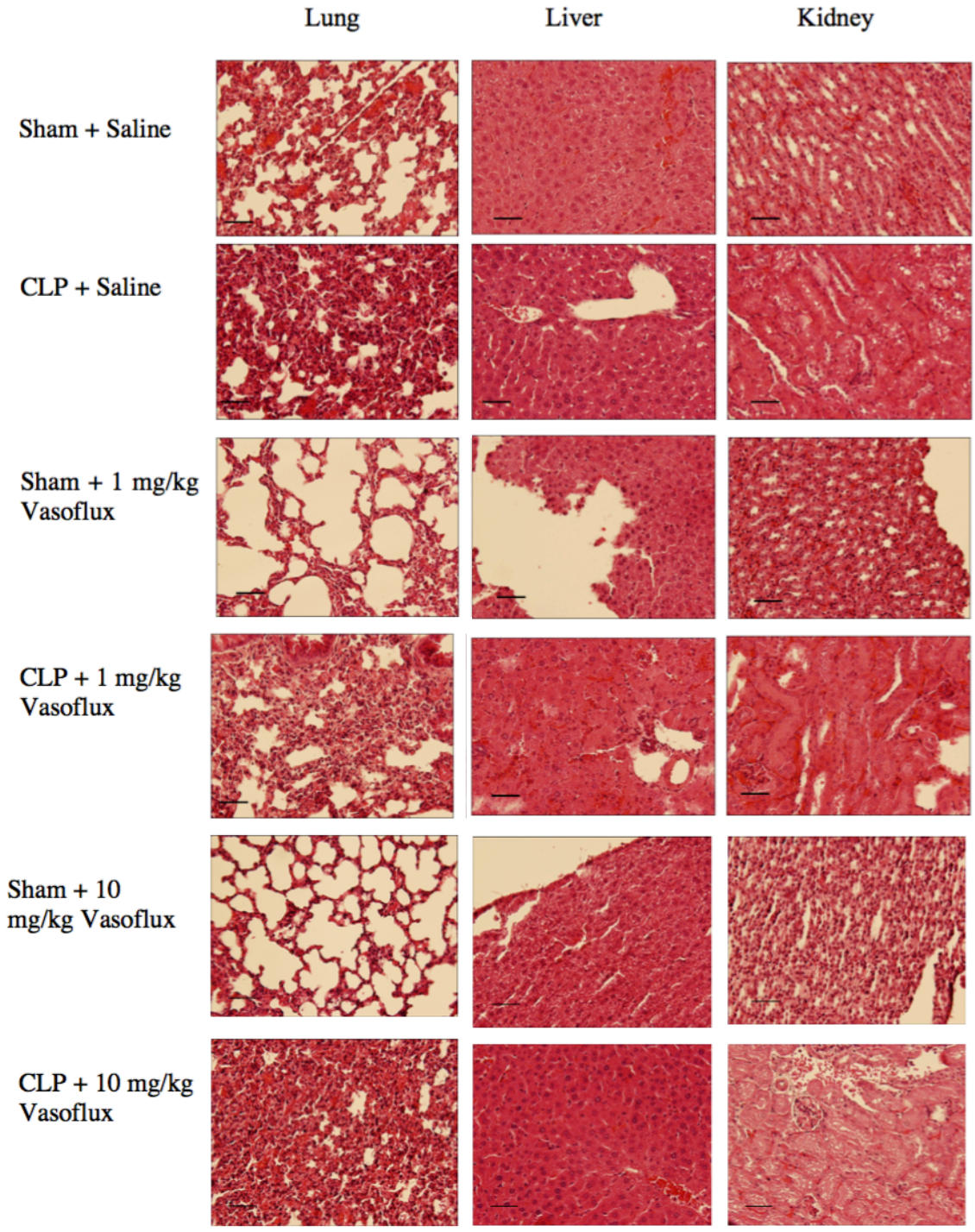
Lung
Liver
Kidney
Sham + Saline
CLP + Saline
Sham + 1 mg/kg Vasoflux
CLP + 1 mg/kg Vasoflux
Sham + 10 mg/kg Vasoflux
CLP + 10 mg/kg Vasoflux

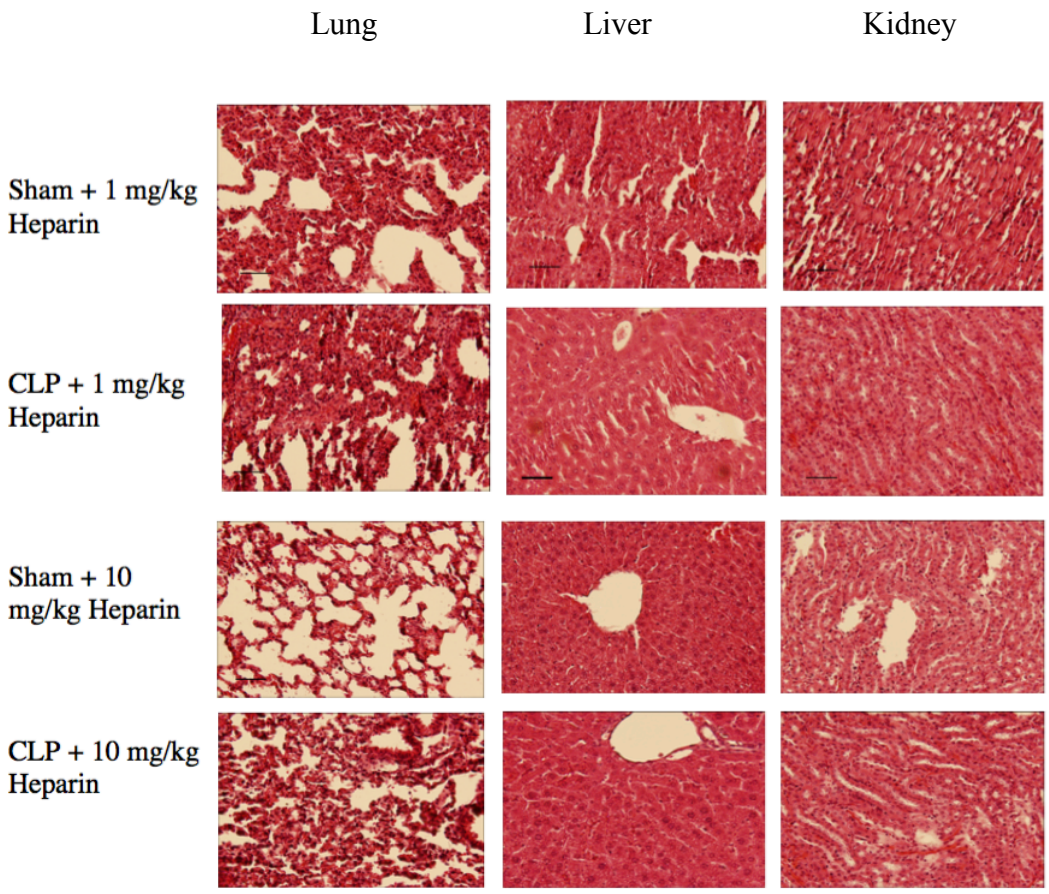
Lung
Liver
Kidney
Sham + 1 mg/kg Heparin
CLP + 1 mg/kg Heparin
Sham + 10 mg/kg Heparin
CLP + 10 mg/kg Heparin

3.0.14 Effect of Vasoflux on DNA-Histone complexes via gel electrophoresis

Contrary to our expectations, Vasoflux neutralized histone-mediated cytotoxicity in cell culture studies *in vitro*, but exhibited adverse effects in septic mice as shown by decreased survival, increased organ damage, and increased surrogate makers of death scores compared to saline-treated septic mice. We hypothesized that these unexpected results may reflect, in part, displacement of DNA from nucleosomes by the non-anticoagulant Vasoflux. Recent studies by Nouboussie et al., reported that while free DNA exerts procoagulant activity via the intrinsic pathway, nucleosomes are not procoagulant (Noubouossie et al., 2017). Furthermore, elevated levels of procoagulant cell-free DNA is a marker of poor outcome in septic patients (Dwivedi et al., 2012).

In order to assess the effect of Vasoflux or UFH on nucleosomes, Vasoflux or UFH was incubated with preformed DNA-histone complexes, followed by agarose gel electrophoresis. The addition of 300 μg/ml histones to 50 μg/ml of DNA reduced the mobility of the DNA as visualized by agarose gel electrophoresis, suggesting that the DNA is bound by the histones. Increasing concentrations of Vasoflux (> 1 μM) or heparin (≥ 3.3 μM) results in increased mobility of DNA through the gel (Figure 3.19). These results suggest that DNA-histone complexes can be disrupted by either Vasoflux or UFH, resulting in the release of free DNA.

Figure 3.19: Effect of UFH and Vasoflux on DNA-histone complex. Increasing concentrations of UFH (A) or Vasoflux (B) was incubated with preformed DNA-histone complexes, followed by agarose gel electrophoresis in a 1.5% agarose gel. Image is a representative n=3.

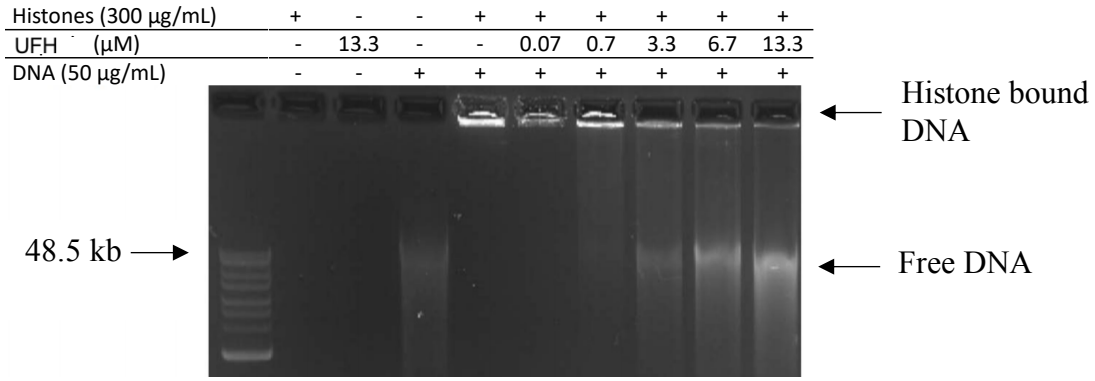

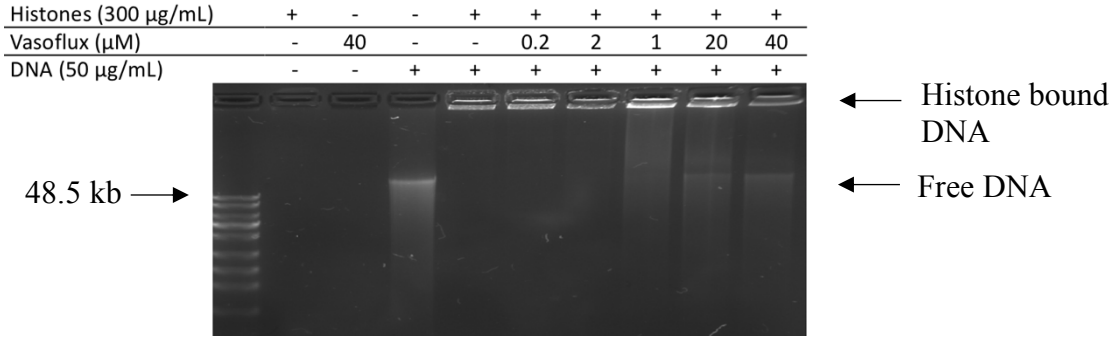

3.0.15 Effect of UFH-Histone complexes on thrombin generation via thrombin generation assay

In order to determine if UFH retains its anticoagulant activity when in complex with histones, TGAs were conducted. Coagulation was initiated with either TF (via the extrinsic pathways) or calf thymus DNA (via the intrinsic pathway). As shown in Fig 3.20, 200 μg/ml of histones has no effect on thrombin generation. UFH retained its anticoagulant activity in the presence of 1 to 200 μg/ml of histones, suggesting that UFH/histone complexes are anticoagulant.

Figure 3.20: Effects of UFH-histone complex on thrombin generation in platelet-poor plasma. Thrombin generation was initiated with either TF (panel A) or calf thymus DNA (panel B) in PPP in the presence of UFH-histone complexes. Thrombograms are expressed as mean ± SEM of 1 independent experiment with 2 technical replicates.

A)

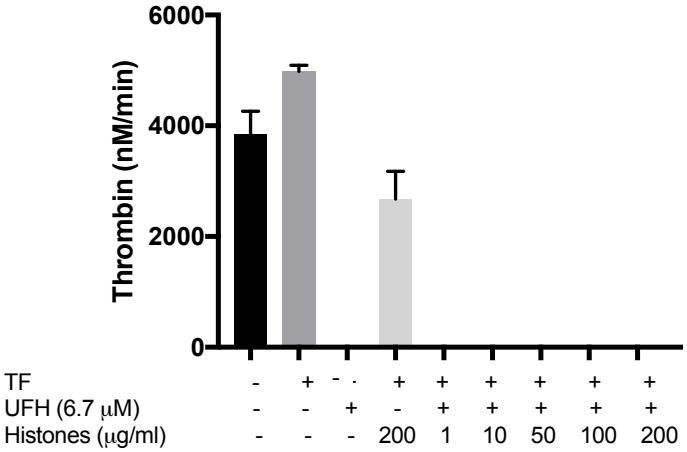

B)

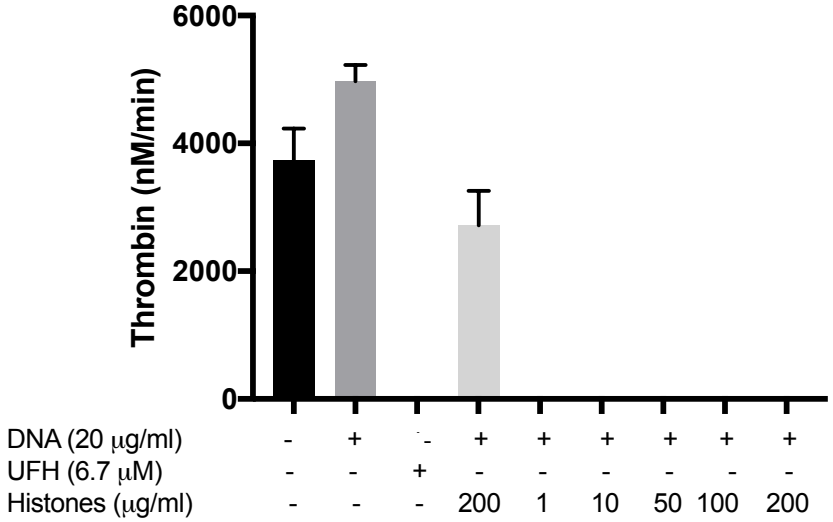

4.0 Discussion

In this study, our aim was to investigate the efficacy of Vasoflux as an anti-sepsis treatment. We first demonstrated that Vasoflux is a less potent anticoagulant compared to UFH and enoxaparin. Vasoflux is a LMWH with a reduced affinity of more than 1500-fold for AT, which reduces its anti-factor Xa activity from 100U/mg to <1U/mg (Peters et al., 2001; Weitz et al., 1999). In contrast, UFH and enoxaparin have their pentasaccharide sequence intact, allowing them to catalyze AT-mediated inactivation of thrombin and FXa (Hirsh, Anand, et al., 2001; Hirsh, Warkentin, et al., 2001). Thus, Vasoflux may improve outcome in sepsis without increasing the risk of bleeding in patients who are already at risk due to consumptive coagulopathy.

Previous studies have shown that injection of histones into healthy mice results in characteristic features of sepsis including neutrophil margination and accumulation in the lungs, microvascular thrombosis, and renal dysfunction (Fuchs et al., 2010; Xu et al., 2009). Co-administration of histones with APC (which cleaves histones) or with anti-histone antibodies rescues mice from the lethal effects of histones (Xu et al., 2009). Our results demonstrate that UFH, enoxaparin, and Vasoflux neutralize histone-mediated cytotoxicity in cell culture in a dose-dependent manner. Our findings are consistent with previous studies, which demonstrate that a 15 kDa nonanticoagulant heparin (termed AADH) as well as UFH dose-dependently inhibited the cytotoxic effect of histone H3 in cell culture (Wildhagen et al., 2014). We are the first to demonstrate that histones H2A, H3, and H4 bind to Vasoflux with K_D values of $3.6x10^2 \pm 149$ nM, $3.8x10^2 \pm 110$ nM, and $1.8\ x10^2 \pm 59$ nM, respectively. We further showed that UFH binds to histones H2A, H3, and H4 with

approximately 10-fold higher affinity compared to Vasoflux. Consistent with our findings, Wildhagen has shown high affinity binding between AADH and histone H3 with a K_D value of 86 nM (Wildhagen et al., 2014). In our cytotoxicity assays, a lower concentration of UFH (13 μM) was needed to completely neutralize the cytotoxic effects of histones, as compared to 40 μM of Vasoflux or enoxaparin. This suggests that the anti-histone effect of GAGs is chain-length dependent, but is independent of the AT-binding pentasaccharide. Furthermore, DNA exhibits dose dependent binding with H2A, H3 and H4 at concentrations lower than 5 μg/ml, 25 μg/ml, and 25 μg/ml, respectively. However, at higher concentrations, the data was not analyzable as DNA levels did not reach saturation. One way to overcome this limitation is to inject DNA for a longer period of time.

We next performed studies to determine the optimal dose, timing, and route of administration in a murine model of experimental sepsis (Refer to table 1 in methods section). In our first study, mice subjected to sham or CLP surgery were administered I.P. injections of either 0.9% saline, 8 mg/kg of enoxaparin, or 8 mg/kg of Vasoflux at 4 and 12 hours. Septic mice administered either saline, enoxaparin, or Vasoflux had survival rates of 80%, 75%, and 50%, respectively. In our second study, sham and CLP treated mice were intraperitoneally administered with either saline or 10 mg/kg, 30 mg/kg, or 50 mg/kg of Vasoflux at 6, 12, and 18 h post-surgery. During the 24 h study period, septic mice administered either 10 mg/kg, 30 mg/kg, or 50 mg/kg of Vasoflux showed 20%, 15%, and 9% percent survival respectively. In the group of septic mice treated with 10 mg/kg of Vasoflux, the MGS and MSS scoring system have modest predictive powers, with AUC values of 0.65 (95%CI, 0.18 to 1.12), 0.67 (95% CI, 0.34 to 0.99), respectively. This may

be due to the average of the range of scores for the individual components, as a mouse may have scored high on restlessness and responsiveness, but low on difficulty breathing. There was significant damage in the liver and kidney in Vasoflux-treated septic mice compared to saline-treated septic mice or Vasoflux-treated sham mice. A pink material (stained with H&E) was observed around the glomerulus, alveoli, and vessels in the kidney, lung and liver respectively (Figures 3.11-3.12). We hypothesize this may be due to unbound histones binding to and disrupting endothelial cells, leading to edema or proteinaceous exudate (Abrams et al., 2013). To determine if the components of this substance are rich in protein and polysaccharides such as glycogen, and mucosubstances like glycoproteins, we will conduct a periodic acid-schiff (PAS) stain. Thus, there was no survival benefit in septic mice injected intraperitoneally with Vasoflux. Our studies also suggest that administering higher doses of Vasoflux (at 10mg/kg to 50 mg/kg) into septic mice worsened outcome as compared to 8 mg/kg of Vasoflux.

To explore the possibility that the therapeutic efficacy of Vasoflux is dependent on the route of administration, sham- and CLP-treated mice were intravenously administered either saline, 1 mg/kg or 10 mg/kg of Vasoflux, or 1 mg/kg or 10 mg/kg of UFH 6 hours post-CLP. Septic mice treated with either 1 mg/kg or 10 mg/kg of Vasoflux had a lower percent survival compared to 10 mg/kg UFH or saline treated mice. The difference in survival between septic mice administered either UFH or Vasoflux may lie in the mechanism of action of these GAGs. Given the relationship between inflammation and blood clotting, anticoagulants such as heparin have been used to reduce inflammation as well the generation of clots (Allen et al., 2015). Compared to UFH, Vasoflux has a reduced

anticoagulant effect and this difference in activity may be responsible for the decreased survival in septic mice treated with Vasoflux. Furthermore, as shown by our SPR experiments UFH has a ~10-fold greater binding affinity for histones as compared to Vasoflux. This suggests that a lower concentration of UFH is needed to bind to and neutralize histones as compared to Vasoflux. As shown in our cytotoxicity assays, 13 μM of UFH is needed to completely neutralize histone-mediated cytotoxicity, whereas 40 μM of Vasoflux is required. As shown in Figure 3.20, UFH in complex with histones retains its anticoagulant activity. Table 3 summarizes the properties of AADH, Vasoflux, UFH, and enoxaparin.

It is interesting to note that AADH (a 15 kDa non-anticoagulant heparin) was effective in improving survival of septic mice, whereas Vasoflux (a 5.5 kDa non-anticoagulant heparin) led to a decrease in survival compared to saline-treated septic mice (Wildhagen et al., 2014). The difference in survival may be due to the difference in binding affinities for AADH and Vasoflux to histones. As shown in our cytotoxicity assays (section 3.0.5), we demonstrated that the anti-histone effect of GAGs is chain-length dependent, but is independent of the AT-binding pentasaccharide. As AADH has a molecular weight of 15 kDa, it binds to histones with a higher affinity (86 nM) as compared to Vasoflux (383 $\pm$ 110 nM), which has a molecular weight 5.5 kDa. Based on our gel electrophoresis experiments, increasing concentrations of either UFH or Vasoflux displaced DNA from the DNA-histone complex and resulted in free procoagulant DNA. It is possible that due to AADH's higher binding affinity to histones, it may be able to neutralize more histones as compared to Vasoflux. The release of procoagulant DNA may be degraded by endogenous

DNase1 in the body. Consequently, the decrease in survival observed in the septic mice administered Vasoflux may be due to more free histones, leading to a larger cytotoxic effect in the host. Therefore, the difference observed in survival of septic mice administered AADH or Vasoflux may be due to the binding affinities of these GAGs for histones.

Table 3: Comparison of the properties of AADH, Vasoflux, UFH, and enoxaparin.

Properties	AADH	Vasoflux	UFH	Enoxaparin
Molecular Weight (kDa)	15	5.5	15	5.5
Anti-histone effect	+++	+	+++	+
Anticoagulant Effect (anti-cfDNA)	+	+	+++	++
K_d of GAG to Histone H3	86 nM	300 $\pm$ 110 nM	19.4 $\pm$ 4.9 nM	?

Recently, a Wiggers-Bernard Conference was held to propose and develop standardized guidelines on how to improve the quality and efficiency of pre-clinical sepsis modelling (Osuchowski et al., 2018; Zingarelli et al., 2018). An international expert consensus initiative for improvement of animal modelling in sepsis was reached and referred to as the minimum quality threshold in pre-clinical sepsis studies (MQTiPSS) (Osuchowski et al., 2018; Zingarelli et al., 2018). The six working groups themes were: study design, humane modelling, infection types, organ failure/dysfunction, fluid resuscitation, and antimicrobial therapy endpoints (Osuchowski et al., 2018; Zingarelli et al., 2018). Our study has followed most of the recommendations that are proposed as good practices for animal models of sepsis. For example in our CLP model of sepsis, the therapeutic intervention was initiated after the septic insult (6 h post CLP), endpoint markers were utilized to monitor pain and distress, organ dysfunction was measured, and analgesics and fluid resuscitation were administered. Our future animal studies could take into consideration a randomization and blinding of treatments and the potential use of antimicrobial therapy in longer sepsis studies (Osuchowski et al., 2018).

Regarding clinical significance, anticoagulants such as UFH pose an increased risk of bleeding due to sepsis-associated consumption coagulopathy (Zarychanski et al., 2015). There have been numerous studies investigating the effects of heparin in animal models of sepsis (Li et al., 2011). Yan et al., showed that administration of heparin at 100, 500, or 2500 U/kg in mice challenged with *E.coil*, compared to saline treatment, was associated with dose-dependent increases in the hazard ratios of death, respectively (Li et al., 2011). Overall, heparin at 500 U/kg adversely effected survival and a dose of 2500 U/kg worsened

survival as it lead to excessive bleeding (Li et al., 2011). Based on a metaregression analysis of published preclinical studies, there was a considerable heterogeneity in the effects of heparins across the studies (Li et al., 2011). In 7 studies utilizing a monobacterial challenge, heparin (dose used in studies ranged from 400 U/kg to 10000 U/kg) did not improve survival significantly (Li et al., 2011). For the 23 studies employing LPS, there was low heterogeneity and heparin (dose used in studies ranged from 100 U/kg to 4000 U/kg) decreased the odds ratio of death (Li et al., 2011). Across the 15 studies using a CLP model of sepsis, heterogeneity was moderate to high and heparin showed a beneficial effect (dose used in studies ranged from 100 U/kg to 5000 U/kg) (Li et al., 2011). Overall, well designed and conducted clinical trials will be important to investigate if heparin is beneficial in patients with sepsis.

In a systematic review and metanalysis conducted by Zarychanski et al., patients with sepsis, septic shock, or DIC, had a 12% relative reduction when administered heparin as compared to placebo or usual care (Zarychanski et al., 2015). In one small trial of heparin compared with other anticoagulants, heparin was associated with an increased risk of major hemorrhage (Zarychanski et al., 2015). Van der Poll et al., has asserted that administration of anticoagulants increase the risk of bleeding (van der Poll et al., 2017). High dose of therapeutic levels of UFH are required to clear thrombi, however, they add an increased risk of bleeding. In large phase 3 trials investigating anticoagulant therapy for sepsis, serious bleeding was reported (Abraham et al., 2003; Bernard et al., 2001; Ranieri et al., 2012; Warren et al., 2001). For example, when high-dose AT was administered with either

UFH or LMWH, the number of bleeding events increased significantly (Warren et al., 2001).

Due to the bleeding risk that UFH poses, we investigated the use of non-anticoagulant heparin, Vasoflux, as an anti-sepsis agent. Our *in vitro* studies show that UFH, enoxaparin, and Vasoflux neutralize histone-mediated cytotoxicity by virtue of their ability to bind to and inhibit histones from exerting their cytotoxic effects on HEK 293 cells. Unexpectedly, administration of Vasoflux in mice subjected to CLP resulted in decreased survival and increased organ damage as compared to saline-treated or 10 mg/kg of UFH-treated septic mice. Thus, GAGs may function as a double-edged sword by neutralizing histones, while also releasing procoagulant DNA, as shown by our gels. Based on our results, future clinical practice should consider the antithrombin-dependent anticoagulant activity of UFH being used as a sepsis treatment.

5.0 Future Studies

To further investigate the effects of Vasoflux on the procoagulant potential of nucleosomes and NETs, the following *in vitro* studies will be performed: TGA, gel electrophoresis, and cytotoxicity assays.

Firstly, TGA will be conducted in CTI-inhibited platelet-rich-plasma (PRP) to prevent activation of FXII during plasma preparation. The following groups will be tested: DNA-histone complex, reconstituted nucleosomes, NETs with addition of increasing concentrations of Vasoflux. The ability of Vasoflux to displace DNA from nucleosomes or NETs and will be indirectly measured by analyzing the area under the curve to quantify

DNA-mediated thrombin generation. Nucleosomes will be isolated from HEK293 using the following method (Schnitzler, 2001). Nuclei will be released from cultured cells via homogenization and nonionic detergent (Schnitzler, 2001). Several washes with a lysis buffer containing detergent will be used to remove membranes and yield a pellet containing clean nuclei (Schnitzler, 2001). Subsequent extraction with 0.3 M KCl will remove loosely bound proteins from chromatin and will yield a nuclear pellet (Schnitzler, 2001). To generate NETs from activated neutrophils, blood will be collected from the veins of drug- and caffeine-free healthy volunteers into UFH (10 U/mL). Briefly, whole blood layered onto lympholyte poly cell separation media will be subjected to centrifugation for 40 min at 500 x g at 22°C.56 The neutrophil layer will be harvested and residual red blood cells will be lysed using the RBC lysis buffer. Neutrophils will be washed and resuspended in HBSS containing $CaCl_2MgCl_2$ and 2% human serum albumin. Neutrophils will be stimulated with phorbol myristate acetate and added to plasma to assess the effects of Vasoflux on the displacement of DNA from NETs. Secondly, agarose gel electrophoresis experiments will be repeated to investigate if the effects of Vasoflux and UFH are reproducible in the context of nucleosomes and NETs. Increasing concentrations of Vasoflux or UFH will be incubated with a fixed concentration of nucleosomes or NETs. DNA mobility will be visualized by agarose gel electrophoresis.

Cytotoxicity assays will be conducted to investigate the effects of Vasoflux and UFH on dissociating and releasing histones from nucleosomes and NETs. In brief, HEK 293 cells (50,000 cells/well) will be seeded in a tissue culture plate and grown to 50-60% confluency in medium. After an overnight incubation, cells will be treated with either

DNA-histone complex, nucleosomes, or NETs in the presence of Vasoflux or UFH (0-200 μg/ml) for 24 hours. Cell viability will be assessed using a trypan blue test.

To investigate if Vasoflux in combination with 20 mg/kg of DNase 1 will provide a protective effect in experimental sepsis a 24-hour survival surgery would be conducted. Theoretically, Vasoflux would neutralize histone-mediated cytotoxicity, whereas DNase would degrade any free DNA. CLP-treated mice and sham-treated mice will either receive 1 mg/kg of Vasoflux or 10 mg/kg of Vasoflux in combination with 20 mg/kg of DNase. Survival surgeries will begin in the morning and at the completion of surgeries, 24-hour continuous monitoring of the mice will begin and continue till the next day. Immediately after the experimental endpoint, 1 ml of blood will be collected via the inferior vena cava in one-tenth volume of 3.2% sodium citrate. Samples will be spun at 2000 × g and stored in aliquots at -80°C. The following experiments will be conducted for each animal: bacterial loads and organ sections will be stained with H&E visualize morphology and phosphotungstic acid hematoxylin to identify fibrin deposition will be performed using citrated samples. We expect the combination therapy will lead to decreased bacterial loads and less organ damage as compared to septic mice administered only Vasoflux.

6.0 References

A., Y., Dai, J., Xie, Z., Colman, R. W., Wu, Q., Birge, R. B., & Wu, Y. (2014). High Molecular Weight Kininogen Binds Phosphatidylserine and Opsonizes Urokinase Plasminogen Activator Receptor-Mediated Efferocytosis. *The Journal of Immunology*, *192*(9), 4398–4408.

Abraham, E., Reinhart, K., Opal, S., Demeyer, I., Doig, C., López Rodriguez, A., Beale, R., Svoboda, P., Laterre, P. F., Simon, S., Light, B., Spapen, H., Stone, J., Seibert, A., Peckelsen, C., De Deyne, C., Postier, R., Pettilä, V., Sprung, C. L., et al. (2003). Efficacy and Safety of Tifacogin (Recombinant Tissue Factor Pathway Inhibitor) in Severe Sepsis: A Randomized Controlled Trial. *Journal of the American Medical Association*, *290*(2), 238–247.

Abrams, S. T., Zhang, N., Manson, J., Liu, T., Dart, C., Baluwa, F., Wang, S. S., Brohi, K., Kipar, A., Yu, W., Wang, G., & Toh, C.-H. (2013). Circulating Histones Are Mediators of Trauma-associated Lung Injury. *American Journal of Respiratory and Critical Care Medicine*, *187*(2), 160–169.

Abu-Hijleh, M. F., Habbal, O. A., & Moqattash, S. T. (1995). The role of the diaphragm in lymphatic absorption from the peritoneal cavity. *Journal of Anatomy*, *186 (Pt 3*, 453–467.

Ahmad, S., Rawala-Sheikh, R., & Walsh, P. (1992). Components and Assembly of the Factor X Activating Complex. *Seminars in Thrombosis and Hemostasis*, *18*(03), 311–323.

Allen, K. S., Sawheny, E., & Kinasewitz, G. T. (2015). Anticoagulant modulation of inflammation in severe sepsis. *World Journal of Critical Care Medicine*, *4*(2), 105–115.

Alves-Filho, J. C., Freitas, A., Souto, F. O., Spiller, F., Paula-Neto, H., Silva, J. S., Gazzinelli, R. T., Teixeira, M. M., Ferreira, S. H., & Cunha, F. Q. (2009). Regulation of chemokine receptor by Toll-like receptor 2 is critical to neutrophil migration and resistance to polymicrobial sepsis. *Proceedings of the National Academy of Sciences*, *106*(10), 4018–4023.

Ammollo, C. T., Semeraro, F., Xu, J., Esmon, N. L., & Esmon, C. T. (2011). Extracellular histones increase plasma thrombin generation by impairing thrombomodulin-dependent protein C activation. *Journal of Thrombosis and Haemostasis*, *9*(9), 1795–1803.

Andrews, A. J., & Luger, K. (2011). Nucleosome Structure(s) and Stability: Variations on a Theme. *Annual Review of Biophysics*, *40*(1), 99–117.

Arango Duque, G., & Descoteaux, A. (2014). Macrophage cytokines: involvement in immunity and infectious diseases. *Frontiers in Immunology*, *5*, 491.

Ariëns, R. A. S., Lai, T. S., Weisel, J. W., Greenberg, C. S., & Grant, P. J. (2002, August 1). Role of factor XIII in fibrin clot formation and effects of genetic polymorphisms.

Blood.

Badimon, L., Suades, R., Fuentes, E., Palomo, I., & Padró, T. (2016). Role of Platelet-Derived Microvesicles As Crosstalk Mediators in Atherothrombosis and Future Pharmacology Targets: A Link between Inflammation, Atherosclerosis, and Thrombosis. *Frontiers in Pharmacology*, *7*, 293.

Bajzar, L. (2000, December). Thrombin activatable fibrinolysis inhibitor and an antifibrinolytic pathway. *Arteriosclerosis, Thrombosis, and Vascular Biology*.

Baldus, S., Rudolph, V., Roiss, M., Ito, W. D., Rudolph, T. K., Eiserich, J. P., Sydow, K., Lau, D., Szöcs, K., Klinke, A., Kubala, L., Berglund, L., Schrepfer, S., Deuse, T., Haddad, M., Risius, T., Klemm, H., Reichenspurner, H. C., Meinertz, T., et al. (2006). Heparins Increase Endothelial Nitric Oxide Bioavailability by Liberating Vessel-Immobilized Myeloperoxidase. *Circulation*, *113*(15), 1871–1878.

Bernard, G. R., Vincent, J.-L., Laterre, P.-F., LaRosa, S. P., Dhainaut, J.-F., Lopez-Rodriguez, A., Steingrub, J. S., Garber, G. E., Helterbrand, J. D., Ely, E. W., & Fisher, C. J. (2001a). Efficacy and Safety of Recombinant Human Activated Protein C for Severe Sepsis. *New England Journal of Medicine*, *344*(10), 699–709.

Bernard, G. R., Vincent, J.-L., Laterre, P.-F., LaRosa, S. P., Dhainaut, J.-F., Lopez-Rodriguez, A., Steingrub, J. S., Garber, G. E., Helterbrand, J. D., Ely, E. W., & Fisher, C. J. (2001b). Efficacy and Safety of Recombinant Human Activated Protein C for Severe Sepsis. *New England Journal of Medicine*, *344*(10), 699–709.

Beutler, B. A. (1999). The role of tumor necrosis factor in health and disease. *The Journal of Rheumatology. Supplement*, *57*, 16–21.

Brinkmann, V., Reichard, U., Goosmann, C., Fauler, B., Uhlemann, Y., Weiss, D. S., Weinrauch, Y., & Zychlinsky, A. (2004a). Neutrophil Extracellular Traps Kill Bacteria. *Science*, *303*(5663), 1532–1535.

Brinkmann, V., Reichard, U., Goosmann, C., Fauler, B., Uhlemann, Y., Weiss, D. S., Weinrauch, Y., & Zychlinsky, A. (2004b). Neutrophil Extracellular Traps Kill Bacteria. *Science*, *303*(5663), 1532–1535.

Broze, G. J., & Girard, T. J. (2012). Tissue factor pathway inhibitor: structure-function. *Frontiers in Bioscience (Landmark Edition)*, *17*, 262–280.

Broze, G. J., & Higuchi, D. a. (1996). Coagulation-dependent inhibition of fibrinolysis: role of carboxypeptidase-U and the premature lysis of clots from hemophilic plasma. *Blood*, *88*(10), 3815–3823.

Bu, G., Warshawsky, I., & Schwartz, A. L. (1994). Cellular receptors for the plasminogen activators. *Blood*, *83*(12), 3427–3436.

Buse, M. G. (2006). Hexosamines, insulin resistance, and the complications of diabetes: current status. *American Journal of Physiology. Endocrinology and Metabolism*, *290*(1), E1–E8.

Cavaillon, J.-M., & Adib-Conquy, M. (2005). Monocytes/macrophages and sepsis.

Critical Care Medicine, *33*(12 Suppl), S506-9.

Cesarman-Maus, G., & Hajjar, K. A. (2005). Molecular mechanisms of fibrinolysis. *British Journal of Haematology*, *129*(3), 307–321.

Clark, S. R., Ma, A. C., Tavener, S. A., McDonald, B., Goodarzi, Z., Kelly, M. M., Patel, K. D., Chakrabarti, S., McAvoy, E., Sinclair, G. D., Keys, E. M., Allen-Vercoe, E., DeVinney, R., Doig, C. J., Green, F. H. Y., & Kubes, P. (2007). Platelet TLR4 activates neutrophil extracellular traps to ensnare bacteria in septic blood. *Nature Medicine*, *13*(4), 463–469.

Colman, R. W., & Schmaier, A. H. (1997a). Contact system: a vascular biology modulator with anticoagulant, profibrinolytic, antiadhesive, and proinflammatory attributes. *Blood*, *90*(10), 3819–3843.

Colman, R. W., & Schmaier, A. H. (1997b). Contact system: a vascular biology modulator with anticoagulant, profibrinolytic, antiadhesive, and proinflammatory attributes. *Blood*, *90*(10), 3819–3843.

Comfurius, P., Senden, J. M., Tilly, R. H., Schroit, A. J., Bevers, E. M., & Zwaal, R. F. (1990). Loss of membrane phospholipid asymmetry in platelets and red cells may be associated with calcium-induced shedding of plasma membrane and inhibition of aminophospholipid translocase. *Biochimica et Biophysica Acta*, *1026*(2), 153–160.

Dahm, A., Van Hylckama Vlieg, A., Bendz, B., Rosendaal, F., Bertina, R. M., & Sandset, P. M. (2003). Low levels of tissue factor pathway inhibitor (TFPI) increase the risk of venous thrombosis. *Blood*, *101*(11), 4387–4392.

Davis, R. P., Miller-Dorey, S., & Jenne, C. N. (2016). Platelets and coagulation in infection. *Clinical & Translational Immunology*, *5*(7), e89.

de Boer, J. P., Creasy, A. A., Chang, A., Roem, D., Brouwer, M. C., Eerenberg, A. J., Hack, C. E., & Taylor, F. B. (1993). Activation patterns of coagulation and fibrinolysis in baboons following infusion with lethal or sublethal dose of Escherichia coli. *Circulatory Shock*, *39*(1), 59–67.

de Stoppelaar, S., van 't Veer, C., & Poll, T. van der. (2014). The role of platelets in sepsis. *Thrombosis and Haemostasis*, *112*(10), 666–677.

Derhaschnig, U., Pernerstorfer, T., Knechtelsdorfer, M., Hollenstein, U., Panzer, S., & Jilma, B. (2003). Evaluation of antiinflammatory and antiadhesive effects of heparins in human endotoxemia. *Critical Care Medicine*, *31*(4), 1108–1112.

Dewitte, A., Lepreux, S., Villeneuve, J., Rigothier, C., Combe, C., Ouattara, A., & Ripoche, J. (2017). Blood platelets and sepsis pathophysiology: A new therapeutic prospect in critical ill patients? *Annals of Intensive Care*, *7*(1), 115.

Drake, T. A., Morrissey, J. H., & Edgington, T. S. (1989). Selective cellular expression of tissue factor in human tissues. Implications for disorders of hemostasis and thrombosis. *The American Journal of Pathology*, *134*(5), 1087–1097.

Dwivedi, D. J., Toltl, L. J., Swystun, L. L., Pogue, J., Liaw, K.-L., Weitz, J. I., Cook, D.

J., Fox-Robichaud, A. E., Liaw, P. C., & Canadian Critical Care Translational Biology Group. (2012). Prognostic utility and characterization of cell-free DNA in patients with severe sepsis. *Critical Care*, *16*(4), R151.

Egorina, E. M., Sovershaev, M. A., & Hansen, J.-B. (2011). The role of tissue factor in systemic inflammatory response syndrome. *Blood Coagulation & Fibrinolysis*, *22*(6), 451–456.

Engelmann, B., Luther, T., & Müller, I. (2003). Intravascular tissue factor pathway – a model for rapid initiation of coagulation within the blood vessel. *Thrombosis and Haemostasis*, *89*(01), 3–8.

Engelmann, B., & Massberg, S. (2013). Thrombosis as an intravascular effector of innate immunity. *Nature Reviews Immunology*, *13*(1), 34–45.

Esmon, C. T. (2003). The protein C pathway. *Chest*, *124*(3 Suppl), 26S–32S.

Fuchs, T. A., Brill, A., Duerschmied, D., Schatzberg, D., Monestier, M., Myers, D. D., Wrobleski, S. K., Wakefield, T. W., Hartwig, J. H., & Wagner, D. D. (2010). Extracellular DNA traps promote thrombosis. *Proceedings of the National Academy of Sciences*, *107*(36), 15880–15885.

Fukudome, K., & Esmon, C. T. (1994). Identification, cloning, and regulation of a novel endothelial cell protein C/activated protein C receptor. *The Journal of Biological Chemistry*, *269*(42), 26486–26491. http://www.ncbi.nlm.nih.gov/pubmed/7929370

Fukudome, K., & Esmon, C. T. (1995). Molecular cloning and expression of murine and bovine endothelial cell protein C/activated protein C receptor (EPCR). The structural and functional conservation in human, bovine, and murine EPCR. *The Journal of Biological Chemistry*, *270*(10), 5571–5577.

Gawaz, M., Dickfeld, T., Bogner, C., Fateh-Moghadam, S., & Neumann, F. J. (1997). Platelet function in septic multiple organ dysfunction syndrome. *Intensive Care Medicine*, *23*(4), 379–385.

GE Healthcare Biacore T200 Getting Started. (2012).

Girard, T. J., Warren, L. A., Novotny, W. F., Likert, K. M., Brown, S. G., Miletich, J. P., & Broze, G. J. (1989). Functional significance of the Kunitz-type inhibitory domains of lipoprotein-associated coagulation inhibitor. *Nature*, *338*(6215), 518–520.

Gould, T. J., Vu, T. T., Stafford, A. R., Dwivedi, D. J., Kim, P. Y., Fox-Robichaud, A. E., Weitz, J. I., & Liaw, P. C. (2015). Cell-Free DNA Modulates Clot Structure and Impairs Fibrinolysis in SepsisSignificance. *Arteriosclerosis, Thrombosis, and Vascular Biology*, *35*(12), 2544–2553.

Gould, T. J., Vu, T. T., Swystun, L. L., Dwivedi, D. J., Mai, S. H. C., Weitz, J. I., & Liaw, P. C. (2014). Neutrophil Extracellular Traps Promote Thrombin Generation Through Platelet-Dependent and Platelet-Independent Mechanisms. *Arteriosclerosis, Thrombosis, and Vascular Biology*, *34*(9), 1977–1984.

Gruber, A., & Griffin, J. H. (1992). Direct detection of activated protein C in blood from

human subjects. *Blood*, *79*(9), 2340–2348.

Haselmayer, P., Grosse-Hovest, L., von Landenberg, P., Schild, H., & Radsak, M. P. (2007). TREM-1 ligand expression on platelets enhances neutrophil activation. *Blood*, *110*(3), 1029–1035.

Hawkins, D. (2004). Limitations of traditional anticoagulants. *Pharmacotherapy*, *24*(7 Pt 2), 62S–65S.

Heit, J. A. (2013). Thrombophilia: Clinical and Laboratory Assessment and Management. *Consultative Hemostasis and Thrombosis*, 205–239.

Heparin Anticoagulation in Septic Shock - Full Text View - ClinicalTrials.gov. (2018).

Hirsh, J. (1998). Low-molecular-weight heparin : A review of the results of recent studies of the treatment of venous thromboembolism and unstable angina. *Circulation*, *98*(15), 1575–1582.

Hirsh, J., Anand, S. S., Halperin, J. L., & Fuster, V. (2001). Mechanism of action and pharmacology of unfractionated heparin. *Arteriosclerosis, Thrombosis, and Vascular Biology*, *21*(7), 1094–1096.

Hirsh, J., Warkentin, T. E., Shaughnessy, S. G., Anand, S. S., Halperin, J. L., Raschke, R., Granger, C., Ohman, E. M., & Dalen, J. E. (2001). Heparin and low-molecular-weight heparin: mechanisms of action, pharmacokinetics, dosing, monitoring, efficacy, and safety. *Chest*, *119*(1 Suppl), 64S–94S.

Hoffman, M., & Monroe, D. M. (2001). A cell-based model of hemostasis. *Thrombosis and Haemostasis*, *85*(6), 958–965. Retrieved from http://www.ncbi.nlm.nih.gov/pubmed/11434702

Hou, Y., Carrim, N., Wang, Y., Gallant, R. C., Marshall, A., & Ni, H. (2015). Platelets in hemostasis and thrombosis: Novel mechanisms of fibrinogen-independent platelet aggregation and fibronectin-mediated protein wave of hemostasis. *Journal of Biomedical Research*, *29*(6), 437.

Houston, B. L., Dwivedi, D. J., Grin, P., Kwong, M., Rullo, E., Khan, M. A., Asma, S., Pare, G., Liaw, P. C., Zarychanski, R., & Fox-Robichaud, A. E. (2015). Biological Rational for the Use of Heparin in Septic Shock: Translational Data from the Halo Pilot RCT. *Blood*, *126*(23).

Hoylaerts, M., Rijken, D. C., Lijnen, H. R., & Collen, D. (1982). Kinetics of the activation of plasminogen by human tissue plasminogen activator. Role of fibrin. *The Journal of Biological Chemistry*, *257*(6), 2912–2919.

Husak, L., Marcuzzi, A., Herring, J., Wen, E., Yin, L., Capan, D. D., & Cernat, G. (2010). National analysis of sepsis hospitalizations and factors contributing to sepsis in-hospital mortality in Canada. *Healthcare Quarterly (Toronto, Ont.)*, *13 Spec No*, 35–41.

Jaimes, F., De La Rosa, G., Morales, C., Fortich, F., Arango, C., Aguirre, D., & Muñoz, Á. (2009). Unfractioned heparin for treatment of sepsis: A randomized clinical trial

(The HETRASE Study)*. *Critical Care Medicine*, *37*(4), 1185–1196.

Jiménez-Alcázar, M., Rangaswamy, C., Panda, R., Bitterling, J., Simsek, Y. J., Long, A. T., Bilyy, R., Krenn, V., Renné, C., Renné, T., Kluge, S., Panzer, U., Mizuta, R., Mannherz, H. G., Kitamura, D., Herrmann, M., Napirei, M., & Fuchs, T. A. (2017). Host DNases prevent vascular occlusion by neutrophil extracellular traps. *Science*, *358*(6367), 1202–1206.

Jordan, R. E., Oosta, G. M., Gardner, W. T., & Rosenberg, R. D. (1980). The kinetics of hemostatic enzyme-antithrombin interactions in the presence of low molecular weight heparin. *The Journal of Biological Chemistry*, *255*(21), 10081–10090.

Kalil, A. C., & Florescu, D. F. (2013). Severe sepsis: are PROWESS and PROWESS-SHOCK trials comparable? A clinical and statistical heterogeneity analysis. *Critical Care*, *17*(4), 167.

Kaplan, M. J., & Radic, M. (2012). Neutrophil Extracellular Traps: Double-Edged Swords of Innate Immunity. *The Journal of Immunology*, *189*(6), 2689–2695.

Kisiel, W. (1979). Human plasma protein C: isolation, characterization, and mechanism of activation by alpha-thrombin. *The Journal of Clinical Investigation*, *64*(3), 761–769.

Kleinjan, A., Böing, A. N., Sturk, A., & Nieuwland, R. (2012). Microparticles in vascular disorders: how tissue factor-exposing vesicles contribute to pathology and physiology. *Thrombosis Research*, *130 Suppl 1*, S71-3.

Kolaczkowska, E., Jenne, C. N., Surewaard, B. G. J., Thanabalasuriar, A., Lee, W.-Y., Sanz, M.-J., Mowen, K., Opdenakker, G., & Kubes, P. (2015). Molecular mechanisms of NET formation and degradation revealed by intravital imaging in the liver vasculature. *Nature Communications*, *6*(1), 6673.

Komissarov, A. A., Florova, G., & Idell, S. (2011). Effects of Extracellular DNA on Plasminogen Activation and Fibrinolysis. *Journal of Biological Chemistry*, *286*(49), 41949–41962.

Kovach, M. A., & Standiford, T. J. (2012). The function of neutrophils in sepsis. *Current Opinion in Infectious Diseases*, *25*(3), 321–327.

Kubier, A., & O'Brien, M. (2012). Endogenous Anticoagulants. *Topics in Companion Animal Medicine*, *27*(2), 81–87.

Kufel, W. D., Seabury, R. W., Darko, W., Probst, L. A., & Miller, C. D. (2017). Clinical Feasibility of Monitoring Enoxaparin Anti-Xa Concentrations: Are We Getting It Right? *Hospital Pharmacy*, *52*(3), 214–220.

Le, D. T., Rapaport, S. I., & Rao, L. V. (1992). Relations between factor VIIa binding and expression of factor VIIa/tissue factor catalytic activity on cell surfaces. *The Journal of Biological Chemistry*, *267*(22), 15447–15454. Retrieved from http://www.ncbi.nlm.nih.gov/pubmed/1639786

Levi, M. (2008). The Coagulant Response in Sepsis. *Clinics in Chest Medicine*, *29*(4),

627–642.

Levi, M., Keller, T. T., van Gorp, E., & ten Cate, H. (2003). Infection and inflammation and the coagulation system. *Cardiovascular Research*, *60*(1), 26–39. Retrieved from http://www.ncbi.nlm.nih.gov/pubmed/14522404

Levi, M., Schultz, M., & van der Poll, T. (2010). Disseminated Intravascular Coagulation in Infectious Disease. *Seminars in Thrombosis and Hemostasis*, *36*(04), 367–377.

Levi, M., & ten Cate, H. (1999). Disseminated Intravascular Coagulation. *New England Journal of Medicine*, *341*(8), 586–592.

Li, P., Li, M., Lindberg, M. R., Kennett, M. J., Xiong, N., & Wang, Y. (2010). PAD4 is essential for antibacterial innate immunity mediated by neutrophil extracellular traps. *The Journal of Experimental Medicine*, *207*(9), 1853–1862.

Li, X., Li, Z., Zheng, Z., Liu, Y., & Ma, X. (2013). Unfractionated Heparin Ameliorates Lipopolysaccharide-Induced Lung Inflammation by Downregulating Nuclear Factor-κB Signaling Pathway. *Inflammation*, *36*(6), 1201–1208.

Li, X., & Ma, X. (2017). The role of heparin in sepsis: much more than just an anticoagulant. *British Journal of Haematology*, *179*(3), 389–398.

Li, Y., Sun, J.-F., Cui, X., Mani, H., Danner, R. L., Li, X., Su, J.-W., Fitz, Y., & Eichacker, P. Q. (2011). The effect of heparin administration in animal models of sepsis: a prospective study in Escherichia coli-challenged mice and a systematic review and metaregression analysis of published studies. *Critical Care Medicine*, *39*(5), 1104–1112.

Liu, F.-C., Chuang, Y.-H., Tsai, Y.-F., & Yu, H.-P. (2014). Role of Neutrophil Extracellular Traps Following Injury. *Shock*, *41*(6), 491–498.

Liu, X., Yuan, L., Li, D., Tang, Z., Wang, Y., Chen, G., Chen, H., & Brash, J. L. (2014). Blood compatible materials: state of the art. *J. Mater. Chem. B*, *2*(35), 5718–5738.

Longstaff, C., Hogwood, J., Gray, E., Komorowicz, E., Varjú, I., Varga, Z., & Kolev, K. (2016). Neutralisation of the anti-coagulant effects of heparin by histones in blood plasma and purified systems. *Thrombosis and Haemostasis*, *115*(3), 591–599.

Longstaff, C., Varjú, I., Sótonyi, P., Szabó, L., Krumrey, M., Hoell, A., Bóta, A., Varga, Z., Komorowicz, E., & Kolev, K. (2013). Mechanical stability and fibrinolytic resistance of clots containing fibrin, DNA, and histones. *The Journal of Biological Chemistry*, *288*(10), 6946–6956.

Ludwig, R. J. (2009). Therapeutic use of heparin beyond anticoagulation. *Current Drug Discovery Technologies*, *6*(4), 281–289.

Lukas, G., Brindle, S. D., & Greengard, P. (1971). The route of absorption of intraperitoneally administered compounds. *The Journal of Pharmacology and Experimental Therapeutics*, *178*(3), 562–564.

Lwaleed, B. A., & Bass, P. S. (2006). Tissue factor pathway inhibitor: structure, biology and involvement in disease. *The Journal of Pathology*, *208*(3), 327–339.

Mai, S. H. C., Khan, M., Dwivedi, D. J., Ross, C. A., Zhou, J., Gould, T. J., Gross, P. L., Weitz, J. I., Fox-Robichaud, A. E., Liaw, P. C., & Canadian Critical Care Translational Biology Group. (2015). Delayed but not Early Treatment with DNase Reduces Organ Damage and Improves Outcome in a Murine Model of Sepsis. *Shock*, *44*(2), 166–172.

Maroney, S. A., & Mast, A. E. (2008). Expression of tissue factor pathway inhibitor by endothelial cells and platelets. *Transfusion and Apheresis Science : Official Journal of the World Apheresis Association : Official Journal of the European Society for Haemapheresis*, *38*(1), 9–14.

Martin, C. M., Priestap, F., Fisher, H., Fowler, R. A., Heyland, D. K., Keenan, S. P., Longo, C. J., Morrison, T., Bentley, D., Antman, N., & STAR Registry Investigators. (2009). A prospective, observational registry of patients with severe sepsis: The Canadian Sepsis Treatment and Response Registry*. *Critical Care Medicine*, *37*(1), 81–88.

Matzner, Y., Bar-Ner, M., Yahalom, J., Ishai-Michaeli, R., Fuks, Z., & Vlodavsky, I. (1985). Degradation of heparan sulfate in the subendothelial extracellular matrix by a readily released heparanase from human neutrophils. Possible role in invasion through basement membranes. *Journal of Clinical Investigation*, *76*(4), 1306–1313.

Maynard, J. R., Heckman, C. A., Pitlick, F. A., & Nemerson, Y. (1975). Association of tissue factor activity with the surface of cultured cells. *Journal of Clinical Investigation*, *55*(4), 814–824.

McDonald, B., Urrutia, R., Yipp, B. G., Jenne, C. N., & Kubes, P. (2012). Intravascular Neutrophil Extracellular Traps Capture Bacteria from the Bloodstream during Sepsis. *Cell Host & Microbe*, *12*(3), 324–333.

Meng, W., Paunel-Görgülü, A., Flohé, S., Witte, I., Schädel-Höpfner, M., Windolf, J., & Lögters, T. T. (2012). Deoxyribonuclease Is a Potential Counter Regulator of Aberrant Neutrophil Extracellular Traps Formation after Major Trauma. *Mediators of Inflammation*, *2012*, 1–8.

Monroe, D. M., & Hoffman, M. (2006). What Does It Take to Make the Perfect Clot? *Arteriosclerosis, Thrombosis, and Vascular Biology*, *26*(1), 41–48.

Mossie, A. (2013). PATHOPHYSIOLOGY OF SEPSIS. *World Journal of Medicine and Medical ScienceOnline) World Journal of Medicine and Medical Science*, *1*(8), 159–168.

Naldini, L., Tamagnone, L., Vigna, E., Sachs, M., Hartmann, G., Birchmeier, W., Daikuhara, Y., Tsubouchi, H., Blasi, F., & Comoglio, P. M. (1992). Extracellular proteolytic cleavage by urokinase is required for activation of hepatocyte growth factor/scatter factor. *The EMBO Journal*, *11*(13), 4825–4833. Retrieved from http://www.ncbi.nlm.nih.gov/pubmed/1334458

Napirei, M., Ludwig, S., Mezrhab, J., Klöckl, T., & Mannherz, H. G. (2009). Murine serum nucleases - contrasting effects of plasmin and heparin on the activities of

DNase1 and DNase1-like 3 (DNase1l3). *FEBS Journal*, *276*(4), 1059–1073.

Nawroth, P. P., & Stern, D. M. (1986). Modulation of endothelial cell hemostatic properties by tumor necrosis factor. *The Journal of Experimental Medicine*, *163*(3), 740–745.

Nelson, R. M., Cecconi, O., Roberts, W. G., Aruffo, A., Linhardt, R. J., & Bevilacqua, M. P. (1993). Heparin oligosaccharides bind L- and P-selectin and inhibit acute inflammation. *Blood*, *82*(11), 3253–3258.

Nemerson, Y. (1968). The phospholipid requirement of tissue factor in blood coagulation. *The Journal of Clinical Investigation*, *47*(1), 72–80.

Neuenschwander, P. F., Fiore, M. M., & Morrissey, J. H. (1993). Factor VII autoactivation proceeds via interaction of distinct protease-cofactor and zymogen-cofactor complexes. Implications of a two-dimensional enzyme kinetic mechanism. *The Journal of Biological Chemistry*, *268*(29), 21489–21492.

Noubouossie, D. F., Whelihan, M. F., Yu, Y.-B., Sparkenbaugh, E., Pawlinski, R., Monroe, D. M., & Key, N. S. (2017). In vitro activation of coagulation by human neutrophil DNA and histone proteins but not neutrophil extracellular traps. *Blood*, *129*(8), 1021–1029.

Okajima, K., Koga, S., Kaji, M., Inoue, M., Nakagaki, T., Funatsu, A., Okabe, H., Takatsuki, K., & Aoki, N. (1990). Effect of protein C and activated protein C on coagulation and fibrinolysis in normal human subjects. *Thrombosis and Haemostasis*, *63*(1), 48–53. Retrieved from http://www.ncbi.nlm.nih.gov/pubmed/2140205

Opal, S. M., Kessler, C. M., Roemisch, J., & Knaub, S. (2002). Antithrombin, heparin, and heparan sulfate. *Critical Care Medicine*, *30*(5 Suppl), S325-31. Retrieved from http://www.ncbi.nlm.nih.gov/pubmed/12004255

Osuchowski, M. F., Ayala, A., Bahrami, S., Bauer, M., Boros, M., Cavaillon, J.-M., Chaudry, I. H., Coopersmith, C. M., Deutschman, C., Drechsler, S., Efron, P., Frostell, C., Fritsch, G., Gozdzik, W., Hellman, J., Huber-Lang, M., Inoue, S., Knapp, S., Kozlov, A. V., et al. (2018). Minimum quality threshold in pre-clinical sepsis studies (MQTiPSS): an international expert consensus initiative for improvement of animal modeling in sepsis. *Intensive Care Medicine Experimental*, *6*(1), 26.

Owens, A. P., & Mackman, N. (2010). Tissue factor and thrombosis: The clot starts here. *Thrombosis and Haemostasis*, *104*(09), 432–439.

Palta, S., Saroa, R., & Palta, A. (2014). Overview of the coagulation system. *Indian Journal of Anaesthesia*, *58*(5), 515–523.

Papayannopoulos, V. (2017). Neutrophil extracellular traps in immunity and disease. *Nature Reviews Immunology*, *18*(2), 134–147.

Peters, R. J. G., Spickler, W., Théroux, P., White, H., Gibson, M., Molhoek, P. G.,

Anderson, H. V., Weitz, J. I., Hirsh, J., & Weaver, W. D. (2001). Randomized comparison of a novel anticoagulant, vasoflux, and heparin as adjunctive therapy to streptokinase for acute myocardial infarction: Results of the VITAL study (Vasoflux International Trial for Acute Myocardial Infarction Lysis). *American Heart Journal*, *142*(2), 237–243.

Prince, W. S., Baker, D. L., Dodge, A. H., Ahmed, A. E., Chestnut, R. W., & Sinicropi, D. V. (1998). Pharmacodynamics of recombinant human DNase I in serum. *Clinical and Experimental Immunology*, *113*(2), 289–296.

Qu, D., Wang, Y., Esmon, N. L., & Esmon, C. T. (2007). Regulated endothelial protein C receptor shedding is mediated by tumor necrosis factor-α converting enzyme/ADAM17. *Journal of Thrombosis and Haemostasis*, *5*(2), 395–402.

Ranieri, V. M., Thompson, B. T., Barie, P. S., Dhainaut, J.-F., Douglas, I. S., Finfer, S., Gårdlund, B., Marshall, J. C., Rhodes, A., Artigas, A., Payen, D., Tenhunen, J., Al-Khalidi, H. R., Thompson, V., Janes, J., Macias, W. L., Vangerow, B., & Williams, M. D. (2012a). Drotrecogin Alfa (Activated) in Adults with Septic Shock. *New England Journal of Medicine*, *366*(22), 2055–2064.

Ranieri, V. M., Thompson, B. T., Barie, P. S., Dhainaut, J.-F., Douglas, I. S., Finfer, S., Gårdlund, B., Marshall, J. C., Rhodes, A., Artigas, A., Payen, D., Tenhunen, J., Al-Khalidi, H. R., Thompson, V., Janes, J., Macias, W. L., Vangerow, B., & Williams, M. D. (2012b). Drotrecogin Alfa (Activated) in Adults with Septic Shock. *New England Journal of Medicine*, *366*(22), 2055–2064.

Rao, L. V. M., Kothari, H., & Pendurthi, U. R. (2012). Tissue factor: mechanisms of decryption. *Frontiers in Bioscience (Elite Edition)*, *4*, 1513–1527. Retrieved from http://www.ncbi.nlm.nih.gov/pubmed/22201972

Rauch, U., Bonderman, D., Bohrmann, B., Badimon, J. J., Himber, J., Riederer, M. A., & Nemerson, Y. (2000). Transfer of tissue factor from leukocytes to platelets is mediated by CD15 and tissue factor. *Blood*, *96*(1), 170–175. Retrieved from http://www.ncbi.nlm.nih.gov/pubmed/10891447

Research, C. for D. E. and. (n.d.). Drug Safety and Availability - FDA Drug Safety Communication: Voluntary market withdrawal of Xigris [drotrecogin alfa (activated)] due to failure to show a survival benefit. Retrieved from https://www.fda.gov/Drugs/DrugSafety/ucm277114.htm

Rios-Santos, F., Alves-Filho, J. C., Souto, F. O., Spiller, F., Freitas, A., Lotufo, C. M. C., Soares, M. B. P., dos Santos, R. R., Teixeira, M. M., & de Queiroz Cunha, F. (2007). Down-regulation of CXCR2 on Neutrophils in Severe Sepsis Is Mediated by Inducible Nitric Oxide Synthase–derived Nitric Oxide. *American Journal of Respiratory and Critical Care Medicine*, *175*(5), 490–497.

Rittirsch, D., Flierl, M. A., & Ward, P. A. (2008). Harmful molecular mechanisms in sepsis. *Nature Reviews Immunology*, *8*(10), 776–787.

Rittirsch, D., Huber-Lang, M. S., Flierl, M. A., & Ward, P. A. (2009). Immunodesign of

experimental sepsis by cecal ligation and puncture. *Nature Protocols*, *4*(1), 31–36.

Roemisch, J., Gray, E., Hoffmann, J. N., & Wiedermann, C. J. (2002). Antithrombin: a new look at the actions of a serine protease inhibitor. *Blood Coagulation & Fibrinolysis : An International Journal in Haemostasis and Thrombosis*, *13*(8), 657–670. Retrieved from http://www.ncbi.nlm.nih.gov/pubmed/12441904

Rosing, J., Hoekema, L., Nicolaes, G. A. F., Christella, M., Thomassen, L. G. D., Coenraad Hemker, H., Varadi, K., Schwarz, H. P., & Tans, G. (1995). *Effects of Protein S and Factor Xa on Peptide Bond Cleavages during Inactivation of Factor Va and Factor Va R506Q by Activated Protein C**. Retrieved from http://www.jbc.org/

Rossaint, J., & Zarbock, A. (2015). Pathogenesis of Multiple Organ Failure in Sepsis. *Critical Reviews in Immunology*, *35*(4), 277–291. Retrieved from http://www.ncbi.nlm.nih.gov/pubmed/26757392

Russwurm, S., Vickers, J., Meier-Hellmann, A., Spangenberg, P., Bredle, D., Reinhart, K., & Lösche, W. (2002). Platelet and leukocyte activation correlate with the severity of septic organ dysfunction. *Shock (Augusta, Ga.)*, *17*(4), 263–268. Retrieved from http://www.ncbi.nlm.nih.gov/pubmed/11954824

Schneider, M., & Nesheim, M. (2004). A Study of the Protection of Plasmin from Antiplasmin Inhibition within an Intact Fibrin Clot during the Course of Clot Lysis. *Journal of Biological Chemistry*, *279*(14), 13333–13339.

Schnitzler, G. R. (2001). Isolation of Histones and Nucleosome Cores from Mammalian Cells. In *Current Protocols in Molecular Biology* (Vol. Chapter 21, p. Unit 21.5). Hoboken, NJ, USA: John Wiley & Sons, Inc.

Seitz, R., Wolf, M., Egbring, R., & Havemann, K. (1989). The disturbance of hemostasis in septic shock: role of neutrophil elastase and thrombin, effects of antithrombin III and plasma substitution. *European Journal of Haematology*, *43*(1), 22–28.

Semeraro, F., Ammollo, C. T., Esmon, N. L., & Esmon, C. T. (2014). Histones induce phosphatidylserine exposure and a procoagulant phenotype in human red blood cells. *Journal of Thrombosis and Haemostasis*, *12*(10), 1697–1702.

Semeraro, F., Ammollo, C. T., Morrissey, J. H., Dale, G. L., Friese, P., Esmon, N. L., & Esmon, C. T. (2011). Extracellular histones promote thrombin generation through platelet-dependent mechanisms: involvement of platelet TLR2 and TLR4. *Blood*, *118*(7), 1952–1961.

Semeraro, N., Ammollo, C. T., Semeraro, F., & Colucci, M. (2010). Sepsis-associated disseminated intravascular coagulation and thromboembolic disease. *Mediterranean Journal of Hematology and Infectious Diseases*, *2*(3), e2010024.

Semple, J. W., Italiano, J. E., & Freedman, J. (2011). Platelets and the immune continuum. *Nature Reviews Immunology*, *11*(4), 264–274.

Shaikh, S. A., & Regal, R. E. (2017). Dosing of Enoxaparin in Renal Impairment. *P & T :*

A Peer-Reviewed Journal for Formulary Management, *42*(4), 245–249. Retrieved from http://www.ncbi.nlm.nih.gov/pubmed/28381917

Shaw, A. W., Pureza, V. S., Sligar, S. G., & Morrissey, J. H. (2007). The Local Phospholipid Environment Modulates the Activation of Blood Clotting. *Journal of Biological Chemistry*, *282*(9), 6556–6563.

Silk, E., Zhao, H., Weng, H., & Ma, D. (2017). The role of extracellular histone in organ injury. *Cell Death and Disease*, *8*(5), e2812.

Singer, M., Deutschman, C. S., Seymour, C. W., Shankar-Hari, M., Annane, D., Bauer, M., Bellomo, R., Bernard, G. R., Chiche, J.-D., Coopersmith, C. M., Hotchkiss, R. S., Levy, M. M., Marshall, J. C., Martin, G. S., Opal, S. M., Rubenfeld, G. D., van der Poll, T., Vincent, J.-L., & Angus, D. C. (2016). The Third International Consensus Definitions for Sepsis and Septic Shock (Sepsis-3). *JAMA*, *315*(8), 801.

Sira, J., & Eyre, L. (2016). Physiology of haemostasis. *Anaesthesia & Intensive Care Medicine*, *17*(2), 79–82.

Smith, S. A., Travers, R. J., & Morrissey, J. H. (2015). How it all starts: Initiation of the clotting cascade. *Critical Reviews in Biochemistry and Molecular Biology*, *50*(4), 326–336.

Sneddon, L. U., Halsey, L. G., & Bury, N. R. (2017). Considering aspects of the 3Rs principles within experimental animal biology. *The Journal of Experimental Biology*, *220*(Pt 17), 3007–3016.

Sônego, F., Alves-Filho, J. C., & Cunha, F. Q. (2014). Targeting neutrophils in sepsis. *Expert Review of Clinical Immunology*, *10*(8), 1019–1028.

Sônego, F., Castanheira, F. V. E. S., Ferreira, R. G., Kanashiro, A., Leite, C. A. V. G., Nascimento, D. C., Colón, D. F., Borges, V. de F., Alves-Filho, J. C., & Cunha, F. Q. (2016). Paradoxical Roles of the Neutrophil in Sepsis: Protective and Deleterious. *Frontiers in Immunology*, *7*, 155.

Stalker, T. J., Traxler, E. A., Wu, J., Wannemacher, K. M., Cermignano, S. L., Voronov, R., Diamond, S. L., & Brass, L. F. (2013). Hierarchical organization in the hemostatic response and its relationship to the platelet-signaling network. *Blood*, *121*(10), 1875–1885.

Statistics Canada. (n.d.). *Health at a glance*. Statistics Canada.

Stearns-Kurosawa, D. J., Osuchowski, M. F., Valentine, C., Kurosawa, S., & Remick, D. G. (2011). The pathogenesis of sepsis. *Annual Review of Pathology*, *6*, 19–48.

Suffredini, A. F., Harpel, P. C., & Parrillo, J. E. (1989). Promotion and Subsequent Inhibition of Plasminogen Activation after Administration of Intravenous Endotoxin to Normal Subjects. *New England Journal of Medicine*, *320*(18), 1165–1172.

Summers, C., Rankin, S. M., Condliffe, A. M., Singh, N., Peters, A. M., & Chilvers, E. R. (2010). Neutrophil kinetics in health and disease. *Trends in Immunology*, *31*(8), 318–324.

Szerlong, H. J., Herman, J. A., Krause, C. M., DeLuca, J. G., Skoultchi, A., Winger, Q. A., Prenni, J. E., & Hansen, J. C. (2015). Proteomic characterization of the nucleolar linker histone H1 interaction network. *Journal of Molecular Biology*, *427*(11), 2056–2071.

Takeuchi, O., & Akira, S. (2010). Pattern Recognition Receptors and Inflammation. *Cell*, *140*(6), 805–820.

Thomas, P., & Smart, T. G. (2005). HEK293 cell line: A vehicle for the expression of recombinant proteins. *Journal of Pharmacological and Toxicological Methods*, *51*(3), 187–200.

Tollefsen, D. M., Pestka, C. A., & Monafo, W. J. (1983). Activation of heparin cofactor II by dermatan sulfate. *The Journal of Biological Chemistry*, *258*(11), 6713–6716.

Triplett, D. A. (2000). Coagulation and bleeding disorders: review and update. *Clinical Chemistry*, *46*(8 Pt 2), 1260–1269.

Urban, C. F., Ermert, D., Schmid, M., Abu-Abed, U., Goosmann, C., Nacken, W., Brinkmann, V., Jungblut, P. R., & Zychlinsky, A. (2009). Neutrophil Extracellular Traps Contain Calprotectin, a Cytosolic Protein Complex Involved in Host Defense against Candida albicans. *PLoS Pathogens*, *5*(10), e1000639.

van der Poll, T., & Opal, S. M. (2008). Host–pathogen interactions in sepsis. *The Lancet Infectious Diseases*, *8*(1), 32–43.

van der Poll, T., & Opal, S. M. (2017). Should all septic patients be given systemic anticoagulation? No. *Intensive Care Medicine*, *43*(3), 455–457.

Varjú, I., Longstaff, C., Szabó, L., Farkas, Á. Z., Varga-Szabó, V. J., Tanka-Salamon, A., Machovich, R., & Kolev, K. (2015). DNA, histones and neutrophil extracellular traps exert anti-fibrinolytic effects in a plasma environment. *Thrombosis and Haemostasis*, *113*(06), 1289–1298.

Versteeg, H. H., Heemskerk, J. W. M., Levi, M., & Reitsma, P. H. (2013). New Fundamentals in Hemostasis. *Physiological Reviews*, *93*(1), 327–358.

von Brühl, M.-L., Stark, K., Steinhart, A., Chandraratne, S., Konrad, I., Lorenz, M., Khandoga, A., Tirniceriu, A., Coletti, R., Köllnberger, M., Byrne, R. A., Laitinen, I., Walch, A., Brill, A., Pfeiler, S., Manukyan, D., Braun, S., Lange, P., Riegger, J., et al. (2012). Monocytes, neutrophils, and platelets cooperate to initiate and propagate venous thrombosis in mice in vivo. *The Journal of Experimental Medicine*, *209*(4), 819–835.

von Hundelshausen, P., & Weber, C. (2007). Platelets as Immune Cells: Bridging Inflammation and Cardiovascular Disease. *Circulation Research*, *100*(1), 27–40.

Walenga, J. M., Jeske, W. P., Prechel, M. M., Bacher, P., & Bakhos, M. (2004). Decreased Prevalence of Heparin-Induced Thrombocytopenia with Low-Molecular-Weight Heparin and Related Drugs. *Seminars in Thrombosis and Hemostasis*, *30*(S 1), 69–80.

Wang, L., Brown, J. R., Varki, A., & Esko, J. D. (2002). Heparin's anti-inflammatory effects require glucosamine 6-O-sulfation and are mediated by blockade of L- and P-selectins. *The Journal of Clinical Investigation*, *110*(1), 127–136.

Wang, X., Qin, W., & Sun, B. (2014). New strategy for sepsis: Targeting a key role of platelet-neutrophil interaction. *Burns & Trauma*, *2*(3), 114–120.

Warren, B. L., Eid, A., Singer, P., Pillay, S. S., Carl, P., Novak, I., Chalupa, P., Atherstone, A., Pénzes, I., Kübler, A., Knaub, S., Keinecke, H. O., Heinrichs, H., Schindel, F., Juers, M., Bone, R. C., Opal, S. M., & KyberSept Trial Study Group. (2001). Caring for the critically ill patient. High-dose antithrombin III in severe sepsis: a randomized controlled trial. *JAMA*, *286*(15), 1869–1878. Retrieved from http://www.ncbi.nlm.nih.gov/pubmed/11597289

Washington, A. V., Gibot, S., Acevedo, I., Gattis, J., Quigley, L., Feltz, R., De La Mota, A., Schubert, R. L., Gomez-Rodriguez, J., Cheng, J., Dutra, A., Pak, E., Chertov, O., Rivera, L., Morales, J., Lubkowski, J., Hunter, R., Schwartzberg, P. L., & McVicar, D. W. (2009). TREM-like transcript-1 protects against inflammation-associated hemorrhage by facilitating platelet aggregation in mice and humans. *Journal of Clinical Investigation*, *119*(6), 1489–1501.

Weitz, J. I., Young, E., Johnston, M., Stafford, A. R., Fredenburgh, J. C., & Hirsh, J. (1999). Vasoflux, a new anticoagulant with a novel mechanism of action. *Circulation*, *99*(5), 682–689. Retrieved from http://www.ncbi.nlm.nih.gov/pubmed/9950667

Wilcox, J. N., Smith, K. M., Schwartz, S. M., & Gordon, D. (1989). Localization of tissue factor in the normal vessel wall and in the atherosclerotic plaque. *Proceedings of the National Academy of Sciences of the United States of America*, *86*(8), 2839–2843. Retrieved from http://www.ncbi.nlm.nih.gov/pubmed/2704749

Wildhagen, K. C. A. A., García de Frutos, P., Reutelingsperger, C. P., Schrijver, R., Aresté, C., Ortega-Gómez, A., Deckers, N. M., Hemker, H. C., Soehnlein, O., & Nicolaes, G. A. F. (2014). Nonanticoagulant heparin prevents histone-mediated cytotoxicity in vitro and improves survival in sepsis. *Blood*, *123*(7), 1098–1101.

Wolberg, A. S., & Campbell, R. A. (2008). Thrombin generation, fibrin clot formation and hemostasis. *Transfusion and Apheresis Science : Official Journal of the World Apheresis Association : Official Journal of the European Society for Haemapheresis*, *38*(1), 15–23.

Wolberg, A. S., Monroe, D. M., Roberts, H. R., & Hoffman, M. R. (1999). Tissue factor de-encryption: ionophore treatment induces changes in tissue factor activity by phosphatidylserine-dependent and -independent mechanisms. *Blood Coagulation & Fibrinolysis : An International Journal in Haemostasis and Thrombosis*, *10*(4), 201–210. Retrieved from http://www.ncbi.nlm.nih.gov/pubmed/10390120

Wood, J. P., Bunce, M. W., Maroney, S. A., Tracy, P. B., Camire, R. M., & Mast, A. E. (2013). Tissue factor pathway inhibitor-alpha inhibits prothrombinase during the

initiation of blood coagulation. *Proceedings of the National Academy of Sciences*, *110*(44), 17838–17843.

Wu, Y. (2015). Contact pathway of coagulation and inflammation. *Thrombosis Journal*. BioMed Central.

Xu, J., Zhang, X., Monestier, M., Esmon, N. L., & Esmon, C. T. (2011). Extracellular Histones Are Mediators of Death through TLR2 and TLR4 in Mouse Fatal Liver Injury. *The Journal of Immunology*, *187*(5), 2626–2631.

Xu, J., Zhang, X., Pelayo, R., Monestier, M., Ammollo, C. T., Semeraro, F., Taylor, F. B., Esmon, N. L., Lupu, F., & Esmon, C. T. (2009). Extracellular histones are major mediators of death in sepsis. *Nature Medicine*, *15*(11), 1318–1321.

Yang, H., Biermann, M. H., Brauner, J. M., Liu, Y., Zhao, Y., & Herrmann, M. (2016). New Insights into Neutrophil Extracellular Traps: Mechanisms of Formation and Role in Inflammation. *Frontiers in Immunology*, *7*, 302.

Yau, J. W., Teoh, H., & Verma, S. (2015). Endothelial cell control of thrombosis. *BMC Cardiovascular Disorders*, *15*, 130.

Yipp, B. G., & Kubes, P. (2013). NETosis: how vital is it? *Blood*, *122*(16), 2784–2794.

Zarychanski, R., Abou-Setta, A. M., Kanji, S., Turgeon, A. F., Kumar, A., Houston, D. S., Rimmer, E., Houston, B. L., McIntyre, L., Fox-Robichaud, A. E., Hébert, P., Cook, D. J., Fergusson, D. A., & Canadian Critical Care Trials Group. (2015). The Efficacy and Safety of Heparin in Patients With Sepsis. *Critical Care Medicine*, *43*(3), 511–518.

Zarychanski, R., Doucette, S., Fergusson, D., Roberts, D., Houston, D. S., Sharma, S., Gulati, H., & Kumar, A. (2008). Early intravenous unfractionated heparin and mortality in septic shock*. *Critical Care Medicine*, *36*(11), 2973–2979.

Zingarelli, B., Coopersmith, C. M., Drechsler, S., Efron, P., Marshall, J. C., Moldawer, L., Wiersinga, W. J., Xiao, X., Osuchowski, M. F., & Thiemermann, C. (2018). Part I. *SHOCK*, 1.

7.0 Appendix

Mai et al. Intensive Care Medicine Experimental (2018) 6:20
https://doi.org/10.1186/s40635-018-0184-3

Intensive Care Medicine Experimental

RESEARCH Open Access

Body temperature and mouse scoring systems as surrogate markers of death in cecal ligation and puncture sepsis

Safiah H. C. Mai[1†], Neha Sharma[1†], Andrew C. Kwong[1], Dhruva J. Dwivedi[1,2], Momina Khan[1], Peter M. Grin[1,2], Alison E. Fox-Robichaud[1,2] and Patricia C. Liaw[1,2*]

* Correspondence: patricia.liaw@taari.ca
†Safiah H. C. Mai and Neha Sharma contributed equally to this work.
[1]Thrombosis and Atherosclerosis Research Institute (TaARI), McMaster University, 237 Barton St. E., DBRI Room C5-107, Hamilton, ON L8L 2X2, Canada
[2]Department of Medicine, McMaster University, 1280 Main St. W, Hamilton, ON L8S 4K1, Canada

Abstract

Background: Despite increasing ethical standards for conducting animal research, death is still often used as an endpoint in mouse sepsis studies. Recently, the Murine Sepsis Score (MSS), Mouse Clinical Assessment Score for Sepsis (M-CASS), and Mouse Grimace Scale (MGS) were developed as surrogate endpoint scoring systems for assessing pain and disease severity in mice. The objective of our study was to compare the effectiveness of these scoring systems and monitoring of body temperature for predicting disease progression and death in the cecal ligation and puncture (CLP) sepsis model, in order to better inform selection of surrogate endpoints for death in experimental sepsis.

Methods: C57Bl/6J mice were subjected to control sham surgery, or moderate or severe CLP sepsis. All mice were monitored every 4 h for surrogate markers of death using modified versions of the MSS, M-CASS, and MGS scoring systems until 24 h post-operatively, or until endpoint (inability to ambulate) and consequent euthanasia.

Results: Thirty percent of mice subjected to moderate severity CLP reached endpoint by 24 h post-CLP, whereas 100% undergoing severe CLP reached endpoint within 20 h. Modified MSS, M-CASS, and MGS scores all increased, while body temperature decreased, in a time-dependent and sepsis severity-dependent manner, although modified M-CASS scores showed substantial variability. Receiver operating characteristic curves demonstrate that the last recorded body temperature (AUC = 0.88; 95% CI 0.77–0.99), change in body temperature (AUC = 0.89; 95% CI 0.78–0.99), modified M-CASS (AUC = 0.93; 95% CI 0.85–1.00), and modified MSS (AUC = 0.95; 95% CI 0.88–1.01) scores are all robust for predicting death in CLP sepsis, whereas modified MGS (AUC = 0.78; 95% CI 0.63–0.92) is less robust.

Conclusions: The modified MSS and body temperature are effective markers for assessing disease severity and predicting death in the CLP model, and should thus be considered as valid surrogate markers to replace death as an endpoint in mouse CLP sepsis studies.

Keywords: Mouse model, Surrogate endpoints, Murine sepsis score, Mouse grimace scale, Mouse clinical assessment score for sepsis, Animal ethics, Humane research, 3Rs, ARRIVE guidelines

Background

Experimental animal models have been created and refined for over 80 years to investigate the development, management, and treatment of sepsis [1], and have contributed to many important advances in our understanding of sepsis pathophysiology [2]. Recognizing the ethical implications of using animals in research, the "3Rs"—Replacement, Refinement, and Reduction—form the guiding principles for ethical standards when conducting animal research [3]. These guidelines exclude death as an endpoint, and suggest the use of surrogate markers of death to establish humane endpoints where possible. Surrogate markers of death involve using criteria related to pain, suffering, and/or illness, such as clinically relevant scoring systems that semi-quantitatively assess the physical appearance and/or behavior of an animal [4–6], in order to gauge the time at which animals should be humanely euthanized [7]. These decisions must be carefully balanced with minimizing premature termination of animal studies, which may lead to incomplete observations and may necessitate use of even more animals [7, 8]. Improvements are necessary to achieve more ethical and humane treatment of animals in research related to critical care medicine [7, 9, 10], and specifically for experimental sepsis research [10], where clear endpoint markers have not been established for the gold standard sepsis model of cecal ligation and puncture (CLP).

Treatment of septic patients relies heavily on the monitoring of vital signs and patients at higher risk of death can be identified through early warning scores, which document changes in body temperature, respiratory rate, heart rate, blood pressure, and level of consciousness of the patient [11–13]. A recent pilot study by our group also suggests that applying the Hamilton Early Warning Score at triage in the emergency department may facilitate earlier identification of patients with sepsis [14]. In experimental sepsis, researchers have designed scoring systems similar to the clinical Early Warning Scores as tools to ethically assess the progression of sepsis in mice: the Murine Sepsis Score (MSS) was developed by Shrum et al. in 2014 using the intraperitoneal fecal slurry injection model of septic shock [4]; the Mouse Clinical Assessment Score for Sepsis (M-CASS) was developed in a pneumonia model of septic shock by Huet et al. in 2013 [5]; and the Mouse Grimace Scale (MGS) was developed by Langford et al. in 2010 for the purposes of assessing pain [6], including post-surgical pain [15], which may be applicable to the CLP model due to its surgical nature of sepsis induction.

Despite the development of these validated scoring systems, there is a paucity of animal sepsis research utilizing these tools. Furthermore, these scoring systems have not been previously compared in the widely utilized and clinically relevant CLP sepsis model, and in contrast to clinical scoring systems [13, 14], none of these experimental scoring systems evaluate body temperature in mice. Therefore, the objective of our study was to compare the MSS, M-CASS, and MGS scoring systems, and investigate the utility of body temperature monitoring, to determine which of these markers are most informative for predicting death in the mouse CLP model of sepsis.

Methods

Experimental sepsis: cecal ligation and puncture model

C57Bl/6J mice (*Helicobacter hepaticus*-free) were purchased from Charles River Laboratories (Sherbrooke, Quebec, Canada) and bred at the Thrombosis and Atherosclerosis Research Institute at McMaster University (Hamilton, ON, Canada). Mice were housed in

a Helicobacter/Murine Norovirus-negative clean room in individually ventilated cages (Tecniplast Sealsafe Plus system) under 12 h dark/light cycles. Air was filtered through HEPA filters using Touch Slimline air handling units, which guarantee 75 air changes per hour in each cage. The mice were provided with enrichment, and sterilized water and food (Harlan Teklad Rodent Diet #2018) ad libitum. Mice received humane care in accordance with Canadian Council on Animal Care (CCAC) guidelines and all studies were approved by the Animal Research Ethics Board at McMaster University (Hamilton, ON, Canada).

Healthy male C57Bl/6J mice, 8–12 weeks of age and weighing 20–25 g, were randomized to either CLP surgery to induce sepsis ($n = 23$ for moderate severity CLP, $n = 17$ for severe CLP; $n = 3$–4 per group per experiment) or sham surgery as a non-septic control ($n = 18$ total, 3 per experiment). These sample sizes were calculated to detect a 30% or greater difference in survival between CLP groups with 80% power and $\alpha = 0.05$. Since the majority of CLP studies are conducted using male mice, female mice were not used to reduce the total number of mice needed in this study and to control for the potential effects of estrogen on modulating sepsis severity [16]. In accordance with Rittirsch et al. (Nature Protocols, [17]), we used the C57Bl/6 mouse strain which is most commonly used in CLP sepsis because most genetically manipulated (knockout or transgenic) mice are on this genetic background. Methods for randomization and experimenter blinding were used to reduce allocation, selection, and experimenter biases according to Animal Research: Reporting of In Vivo Experiments (ARRIVE) guidelines [18]. The CLP model used in these studies was adapted from protocols by others [17, 19, 20], and has been extensively utilized by our group [21–23]. Briefly, under isofluorane anesthesia, the abdominal area of the mouse was shaved and sterilized with iodine and 70% ethanol. All mice underwent laparotomy prior to exteriorization of the cecum onto the sterilized abdominal surface. In CLP mice, 1 cm of the cecum was ligated and punctured through-and-through using a sterile 18-gauge needle. For the moderate severity of CLP, 0.5 cm of fecal matter was extruded from each puncture hole to ensure patency, whereas 1 cm of fecal matter was extruded from each puncture hole for the severe CLP model, after which the cecum was returned and both layers of the incision were closed with suture. In sham-operated mice, the cecum was exteriorized and returned to the peritoneal cavity without ligation or puncture. Buprenorphine (0.1 mg/kg, Temgesic) and Ringer's lactate (1 mL) were administered subcutaneously pre-operatively and every 4 h post-operatively for pain relief and fluid resuscitation, respectively. Following surgery, mice were kept 3/cage together with mice of the same treatment group. Since previous reports show that correction of hypothermia post-CLP surgery affects mortality [24], external heat was provided for all mice through heating blankets placed below half of each cage to allow mice to regulate their own body temperature. Mice were monitored every 4 h until 24 h post-surgery, or until reaching endpoint as characterized by complete inability to ambulate (since death is not acceptable as an endpoint in accordance with CCAC ethics standards). Mice were placed under brief isofluorane anesthesia for body temperature measurements, carried out using a rectal probe thermometer (Harvard Apparatus Homeothermic Monitor, Harvard Apparatus Canada, Saint-Laurent, QC) with a consistent insertion depth of 2 cm.

Modified Murine Sepsis Score

The Murine Sepsis Score (MSS) system involves observing seven components: appearance, level of consciousness, activity, response to stimulus, eyes, respiratory rate, and respiratory

quality [4]. The established MSS score is the average of these seven components. Changes in respiratory rate were not quantifiable by visual inspection in the CLP model over a 24-h study period, and were therefore excluded from the modified MSS (Table 1).

Modified Mouse Clinical Assessment Score for Sepsis

The Mouse Clinical Assessment Score for Sepsis (M-CASS) system involves observation of eight markers: fur aspect, activity, posture, behavior, chest movements, chest sounds, eyelids, and weight loss [5]. The established M-CASS score is an average of these eight components. Weight loss was excluded in the modified M-CASS system in our sepsis studies as changes in body weight are not observable over a 24-h study period. Since the M-CASS score was developed in a pneumonia model where chest sounds are informative for disease progression [5], and chest sounds were not audible in our CLP studies, this component was also excluded from the modified M-CASS (Table 2).

Modified Mouse Grimace Scale

The Mouse Grimace Scale (MGS) scoring system involves the scoring of five components: orbital tightening, nose bulge, cheek bulge, ear positioning, and whisker change [6, 15]. The established MGS score is the average of these five components. In contrast to the CD-1 mouse strain (which has white cheeks with pink nose) used to develop the MGS [6], our study used the C57Bl/6J mouse strain (which has black cheeks and black nose) as is standard for the CLP model [17]; nose bulge and cheek bulge were indistinguishable from one another in these mice due to lack of color contrast, and were thus grouped as a single component score (Table 3).

Scoring

For the purpose of our comparisons, the modified MSS, M-CASS, and MGS component scores were standardized to a four-point scale ranging from 0 to 3 to make relevant comparisons between these modified scoring systems (Tables 1, 2, and 3). Scoring was

Table 1 Modified MSS scoring system for monitoring of surrogate endpoints and assessment of disease severity in mouse CLP sepsis, adapted from Shrum et al. [4]

Murine Sepsis Score (MSS)				
Score	0	1	2	3
Appearance	Smooth coat	Slightly ruffled fur	Majority of fur on back is ruffled	Piloerection, puffy appearance
Level of consciousness	Active	Active, avoids standing upright	Active only when provoked	Non-responsive, even when provoked
Activity	Normal	Suppressed eating, drinking, or running	Stationary	Stationary, even when provoked
Response to stimulus	Normal	Slowed response to auditory or touch stimuli	No response to auditory, slowed response to touch	No response to touch stimuli
Eyes	Open	Not fully open, potentially secretions	Half closed, potential secretions	Mostly or completely closed
Respiration quality	Normal	Periods of labored breathing	Consistently labored breathing	Labored breathing with gasps

Table 2 Modified M-CASS scoring system for monitoring of surrogate endpoints and assessment of disease severity in mouse CLP sepsis, adapted from Huet et al. [5]

Mouse Clinical Assessment Score for Sepsis (M-CASS)				
Score	0	1	2	3
Fur aspect	Normal coat	Slightly ruffled fur	Ruffled fur	Ruffled fur and piloerection
Activity	Normal	Reduced	Only when provoked	Little or none with provocation
Posture	Normal	Hunched, moving freely	Hunched, strained or stiff movement	Hunched, little or no movement
Behavior	Normal	Slow	Abnormal when disturbed or provoked	Abnormal, no relocation
Chest movements	Normal	Mild dyspnea	Moderate dyspnea	Severe dyspnea
Eyelids	Normal, open	Opened when disturbed	Partially closed, even when disturbed	Mostly or completely closed, even when provoked

performed independently by two blinded observers, and the mean of these scores was recorded at each time-point for each component in each animal.

Statistical analyses

Data are represented as mean ± standard error of the mean (SEM) and were statistically analyzed using Student's unpaired t test, two-way analysis of variance (ANOVA) with Bonferroni post-hoc tests, or Mantel-Cox log-rank test for survival curve analyses. Receiver operating characteristic (ROC) curves were computed using the last documented value for each parameter, or change from baseline to final value for temperature, to compare the predictive value for mice that survived the duration of the study vs. those that were sacrificed due to reaching endpoint. All analyses were performed using GraphPad Prism 5.0 software (La Jolla, CA, USA), and differences between groups were considered significant at $p < 0.05$.

Results

Body temperature can assess disease progression and predict death in CLP sepsis

To determine whether body temperature could be utilized to monitor disease progression in sepsis, mice were subjected to sham surgery, moderate CLP or severe CLP procedures, and body temperature was monitored through a rectal probe every 4 h. During the 24-h

Table 3 Modified MGS scoring system for monitoring of surrogate endpoints and assessment of disease severity in mouse CLP sepsis, adapted from Langford et al. [6]

Mouse Grimace Scale (MGS)				
Score	0	1	2	3
Orbital tightening	Eyes open	Eyes slightly closed	Eyes half closed	Eyes closed
Nose and cheek bulge	Normal, flat	Slightly rounded extension of skin around nose bridge	Wrinkled nose or cheeks, slight bulge in cheeks	Obvious, rigid appearing nose and cheek bulge
Ear positioning	Ears flat, back against body	Ears alert, slightly angled from back	Ears partially positioned forward or apart	Ears completely erect, far apart
Whisker change	Normal	Some whiskers erect	Whiskers mostly erect or clumping	All whiskers standing on end

study period, severe CLP resulted in 100% mortality by 20 h, which differed significantly from the 30% mortality observed at 24 h in moderate CLP and 0% in sham groups (Fig. 1a). Furthermore, mice subjected to severe CLP had significantly lower body temperature compared to mice undergoing moderate CLP (Fig. 1b), which demonstrates that body temperature can be used as a marker to monitor disease progression in CLP sepsis. Interestingly, body temperature decreased in trends that were parallel to survival, and preceded sharp decreases in survival by approximately 4 h for both CLP groups (compare Fig. 1a, b). These observations led us to compare body temperature over time in CLP mice that survived the full study duration and in non-survivors, the latter exhibiting significantly lower body temperature (< 30 °C) at 12, 16, and 18 h post-CLP (Fig. 1c) and significantly greater changes in body temperature (Fig. 1d). To investigate whether temperature could be used as a predictor of death in the CLP model of sepsis, we conducted ROC analyses using the last recorded body temperature, and using change from baseline to final temperature of survivors and non-survivors. The area under the

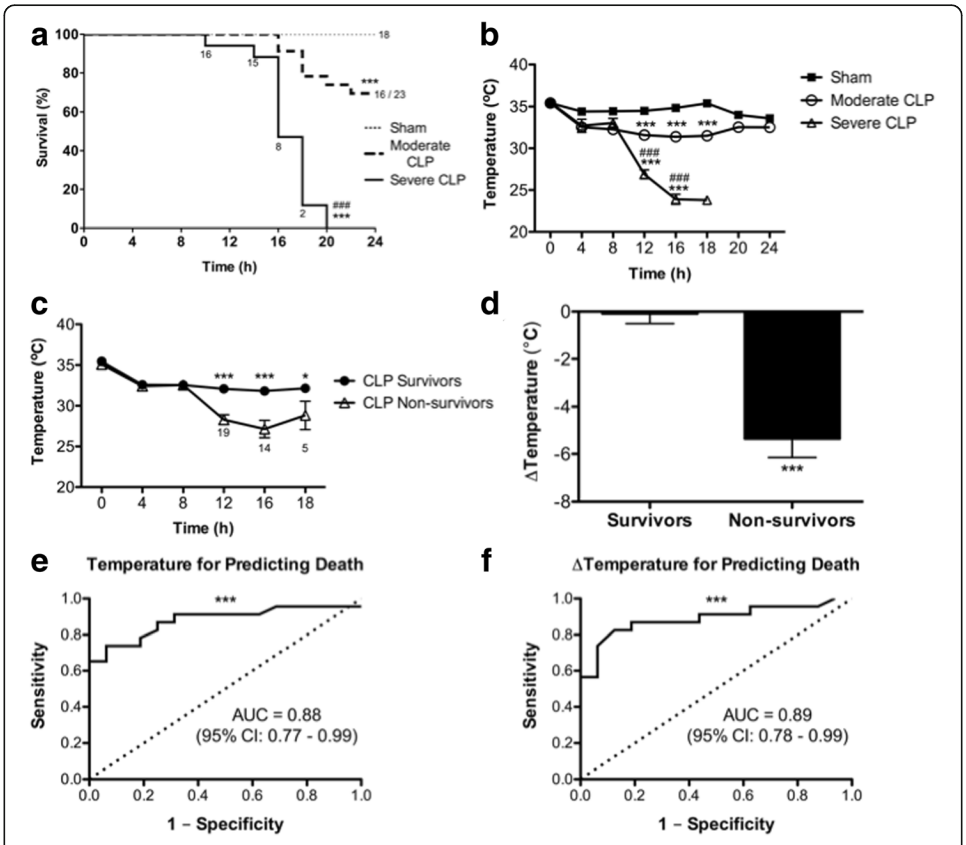

Fig. 1 Kaplan-Meier survival curves (**a**) and body temperature over time in sham, moderate, or severe CLP mice (**b**), temperature (**c**), and change in temperature (**d**) over time in survivors vs. non-survivors, and ROC analyses of last body temperature (**e**) and change in body temperature (**f**) as predictors of death in septic mice. Data are presented as mean ± SEM from six independent experiments representing a total number of $n = 18$ sham, $n = 23$ moderate CLP, and $n = 17$ severe CLP mice; $^{*}p < 0.05$, $^{**}p < 0.01$, $^{***}p < 0.001$ (vs. sham in (**a**, **b**)), $^{\#}p < 0.05$, $^{\#\#}p < 0.01$, $^{\#\#\#}p < 0.001$ vs. moderate CLP, by two-way ANOVA (or by Mantel-Cox log-rank test in (**a**) or *t* test in (**d**)). Note: Only two mice undergoing severe CLP survived past 18 h, therefore statistical analyses were not performed at this time-point in (**b**); similarly in (**c**), time-points past 18 h lacked sufficient *n* in the CLP non-survivors group to perform comparisons, and therefore are not included. Dotted line in (**e**, **f**) represents the line of identity for statistical comparison in ROC analyses. *AUC* area under the curve, *95% CI* 95% confidence interval

curve (AUC) of 0.88 (95% confidence interval 0.77–0.99) for last recorded temperature indicates that body temperature < 30 °C (Fig. 1e) is a robust marker for animals that reached endpoint in our study, as is reduction in body temperature (> 5 °C) over time (AUC 0.89, 95% confidence interval 0.78–0.99) in each animal (Fig. 1f). Therefore, body temperature can be used as a surrogate marker for death in CLP sepsis studies.

Modified Mouse Grimace Scale can assess disease progression, but cannot predict death, in CLP sepsis

To assess the utility of the modified MGS for monitoring disease progression, we computed mean modified MGS scores as well as individual MGS component scores over time for each mouse undergoing moderate or severe CLP, or sham surgery, and further examined the ability of modified MGS scores to predict death using ROC analyses. Modified MGS scores were significantly higher as early as 8 h post-CLP in mice undergoing severe CLP sepsis compared to moderate CLP, whereas the latter group had significantly greater scores than sham mice starting 16 h post-surgery (Fig. 2a), which together indicates that modified MGS scores are useful for assessing disease progression over time in the CLP model of sepsis. However, modified MGS scores were not as robust (AUC = 0.78, 95% confidence interval 0.63–0.92) as temperature for predicting endpoint in the CLP model of sepsis (Fig. 2b). Each component score of the modified MGS—orbital tightening, nose and cheek bulge, ear position, and whisker change—demonstrated the same trends and differences between moderate and severe CLP groups as the overall modified MGS score (Fig. 2c–f), suggesting that each of these scores are equally useful for measuring disease progression. Collectively, these observations demonstrate that the modified MGS and its component scores may be useful for monitoring disease progression during CLP, but modified MGS is not sensitive and specific enough to predict death in murine CLP sepsis.

Modified Murine Sepsis Score can assess disease progression and predict death in CLP sepsis

To determine whether the modified MSS is useful for monitoring progression of disease and predicting death in CLP sepsis, we evaluated the overall modified MSS along with its individual component scores over time and computed an ROC curve to measure the predictive ability of the overall score. Similarly to the modified MGS scores, modified MSS was useful in distinguishing the progression of disease between severe and moderate CLP sepsis as early as 8 h post-CLP; however, the differences in modified MSS between moderate CLP and sham mice was significantly different from 12 h onward (Fig. 3a; vs. 16 h for modified MGS, Fig. 2a), suggesting that the modified MSS is more sensitive than modified MGS for assessing disease progression in CLP sepsis. Furthermore, the modified MSS was more robust (AUC = 0.95; 95% confidence interval 0.88–1.01) than temperature (Fig. 1d) for predicting death in the CLP model of sepsis utilized in this study (Fig. 3b). Interestingly, the individual score components of modified MSS appeared to have variable ability to differentiate between sham, moderate, and severe CLP sepsis groups over time. For instance, while "Appearance" was able to differentiate between sham and both CLP groups as early as 8 h post-surgery, it was not able to distinguish moderate CLP from severe CLP until 16 h (Fig. 3c)—at which time only 8 of 17 severe CLP mice remained alive (Fig. 1a). On the other hand, "Level of Consciousness, Activity, and Responsiveness" and "Respiratory Quality" were not able to

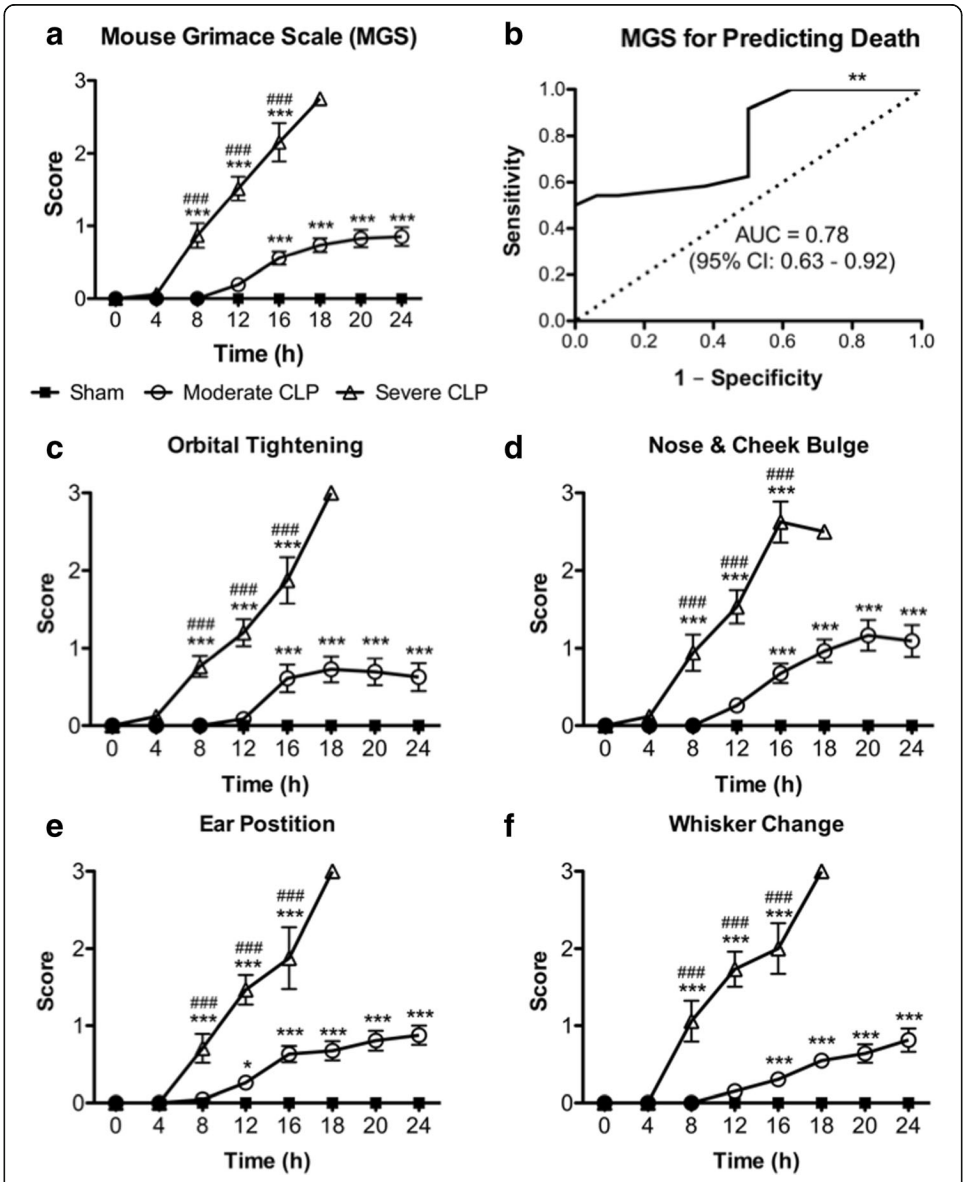

Fig. 2 Modified Mouse Grimace Scale (MGS) score over time (**a**), MGS score as a predictor of death in septic mice (**b**), and MGS individual component scores (**c**–**f**) over time in mice undergoing moderate or severe CLP. Data are presented as mean ± SEM from six independent experiments representing a total number of $n = 18$ sham, $n = 23$ moderate CLP, and $n = 17$ severe CLP mice; $^{*}p < 0.05$, $^{**}p < 0.01$ (vs. line of identity in (**b**)), $^{***}p < 0.001$ vs. sham; $^{\#\#\#}p < 0.001$ vs. moderate CLP, by two-way ANOVA. Note: Only two mice undergoing severe CLP survived past 18 h, therefore statistical comparisons were not performed at this time-point (**a**, **c**–**f**). Dotted line in (**b**) represents the line of identity for statistical comparison in ROC analyses. *AUC* area under the curve, *95% CI* 95% confidence interval

consistently differentiate between sham and moderate CLP mice, but were useful for monitoring disease progression in severe CLP mice starting at 12 and 8 h post-CLP, respectively (Fig. 3d, f). The most useful component of the modified MSS for assessing disease progression in CLP sepsis appears to be the "Eye Aspect" score, which varied significantly between moderate and severe CLP groups from 8 h post-surgery onward, and between moderate CLP and sham groups from 16 h onward (Fig. 3e). Taken together, these data demonstrate

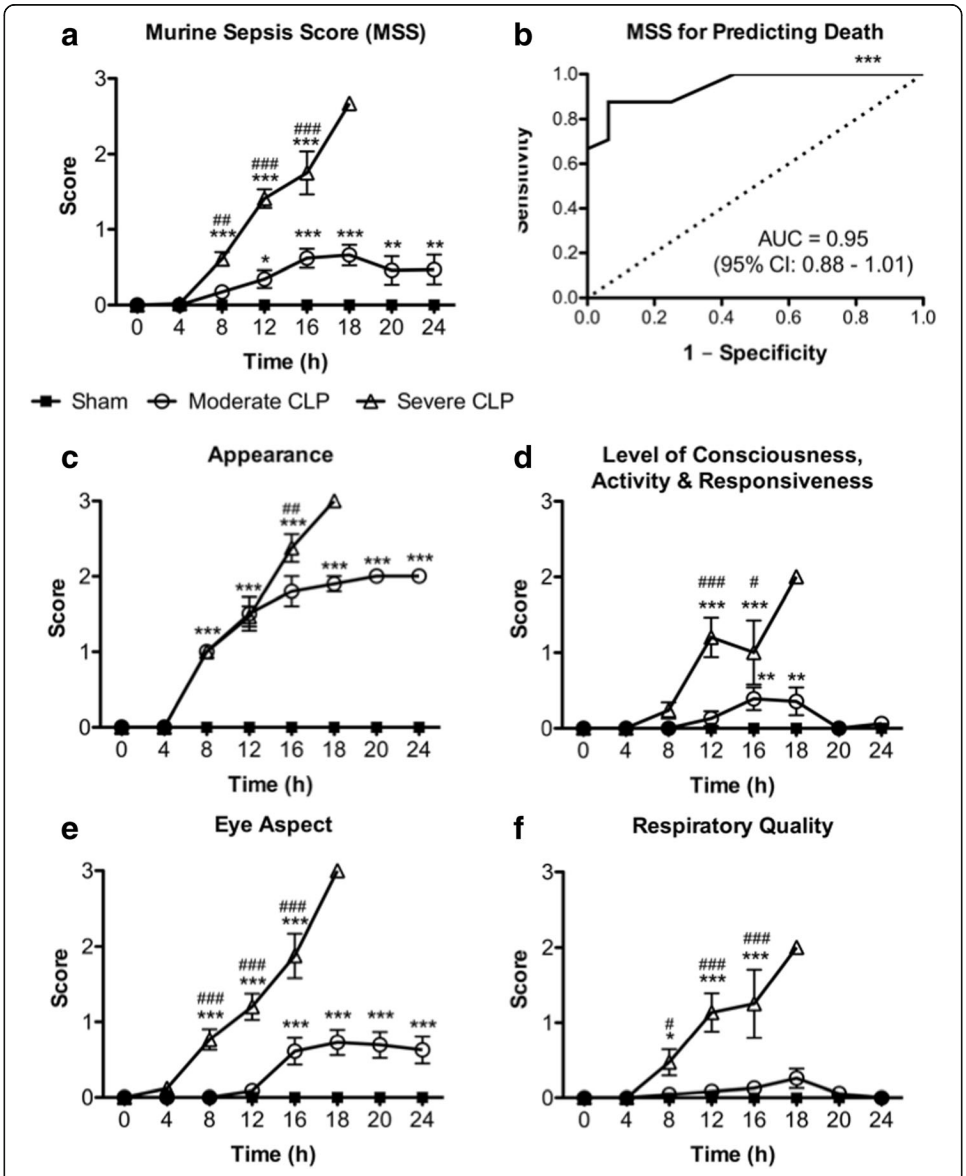

Fig. 3 Modified Murine Sepsis Score (MSS) over time (**a**), MSS score as a predictor of death (**b**), and MSS individual component scores (**c**–**f**) over time in mice subjected to moderate or severe CLP. Data are presented as mean ± SEM from six independent experiments representing a total number of $n = 18$ sham, $n = 23$ moderate CLP, and $n = 17$ severe CLP mice; $^{*}p < 0.05$, $^{**}p < 0.01$, $^{***}p < 0.001$ vs. sham (or vs. line of identity in (**b**)); $^{\#}p < 0.05$, $^{\#\#}p < 0.01$, $^{\#\#\#}p < 0.001$ vs. moderate CLP, by two-way ANOVA. Note: Only two mice undergoing severe CLP survived past 18 h, therefore statistical comparisons were not performed at this time-point (**a**, **c**–**f**). Dotted line in (**b**) represents the line of identity for statistical comparison in ROC analyses. Level of consciousness, activity, and response to stimuli scores were the same for each mouse, and therefore are displayed together in (**d**). *AUC* area under the curve, *95% CI* 95% confidence interval

that the modified MSS is effective for monitoring disease progression and for predicting death in our CLP model of sepsis.

Modified Mouse Clinical Assessment Score for Sepsis can predict death in CLP sepsis

In order to determine if the modified M-CASS system is useful for monitoring sepsis progression, we evaluated each component score as well as modified M-CASS scores

over time in mice following sham surgery, moderate CLP, or severe CLP, and further assessed the ability of modified M-CASS scores to predict endpoint by conducting ROC analysis. As shown in Fig. 4a, modified M-CASS scores were able to differentiate disease progression between sham, moderate CLP, and severe CLP groups at 12 h post-surgery, albeit with notable variability in the scores of severe CLP mice. Overall, modified M-CASS scores had similar sensitivity and specificity (AUC = 0.93, 95% confidence interval 0.85–1.00) as modified MSS scores (Fig. 3b) for predicting death in mice subjected to moderate or severe CLP sepsis (Fig. 4b). The modified M-CASS and MSS systems share three similar component scores: (1) "Fur Aspect" and "Appearance" (respectively), (2) "Activity," and (3) "Eye Aspect" and "Eyelids" (respectively), which resulted in identical scores for these components in both systems based on our standardization of each scoring system to a four-point grading scale (data shown in Fig. 3c–e). The remaining M-CASS component scores of "Posture," "Chest Movements," and "Behavior" demonstrated relatively poor ability to differentiate between sham and moderate CLP groups, and only "Posture" and "Chest Movements" were useful in discriminating between moderate and severe CLP sepsis (Fig. 4c–e). Therefore, while modified M-CASS appears to be useful for predicting death in CLP sepsis, these scores have greater variability than modified MSS for monitoring disease progression in our models of moderate and severe CLP sepsis.

Discussion

In this study, we compared modified versions of the MSS [4], M-CASS [5], and MGS [6, 15] scoring systems that were standardized to a four-point grading scale, in order to determine which system would best serve as a surrogate endpoint for mortality in the gold standard CLP sepsis model. Our findings demonstrate that the modified MSS—a composite score monitoring Appearance, Level of Consciousness, Activity, Response to Stimuli, Eye Aspect, and Respiratory Quality [4]—is the most useful of these scoring systems for distinguishing between moderate and severe CLP models, and for predicting death in mouse CLP sepsis. In contrast, modified MGS was effective for tracking the severity of disease in our CLP model, but was not as robust as modified MSS for predicting death. On the other hand, modified M-CASS was effective at predicting death in our CLP sepsis model, but was more variable than the other two scores for differentiating disease severity in septic mice. Due to the semi-quantitative and subjective nature of all three scoring systems, we monitored body temperature as an objective vital sign: our data show that temperature decreases over time in a sepsis severity-dependent manner and that reduced body temperature is a robust predictor of death in the CLP mouse model of sepsis—a novel and important finding. Recent studies by Lewis et al. have shown that body temperature tracking with an implanted wireless biotelemetry device is useful for monitoring the physiologic response to antibiotic treatment and fluid resuscitation in murine sepsis [25], which is consistent with our findings that body temperature can be used to monitor disease severity in CLP sepsis.

Based on our observations, we recommend that these surrogate markers be used in murine sepsis studies for several reasons. First, these tools offer a general non-invasive assessment of disease progression and are amenable to high monitoring frequency, unlike repetitive blood sampling which has been shown to reduce red blood cell count and hemoglobin concentrations after 5 days of sampling only 35 μL daily [26]. Second, evaluation of symptoms provides easily accessible information regarding the change in an animal's health status, facilitating macroscopic monitoring of the physiologic response when

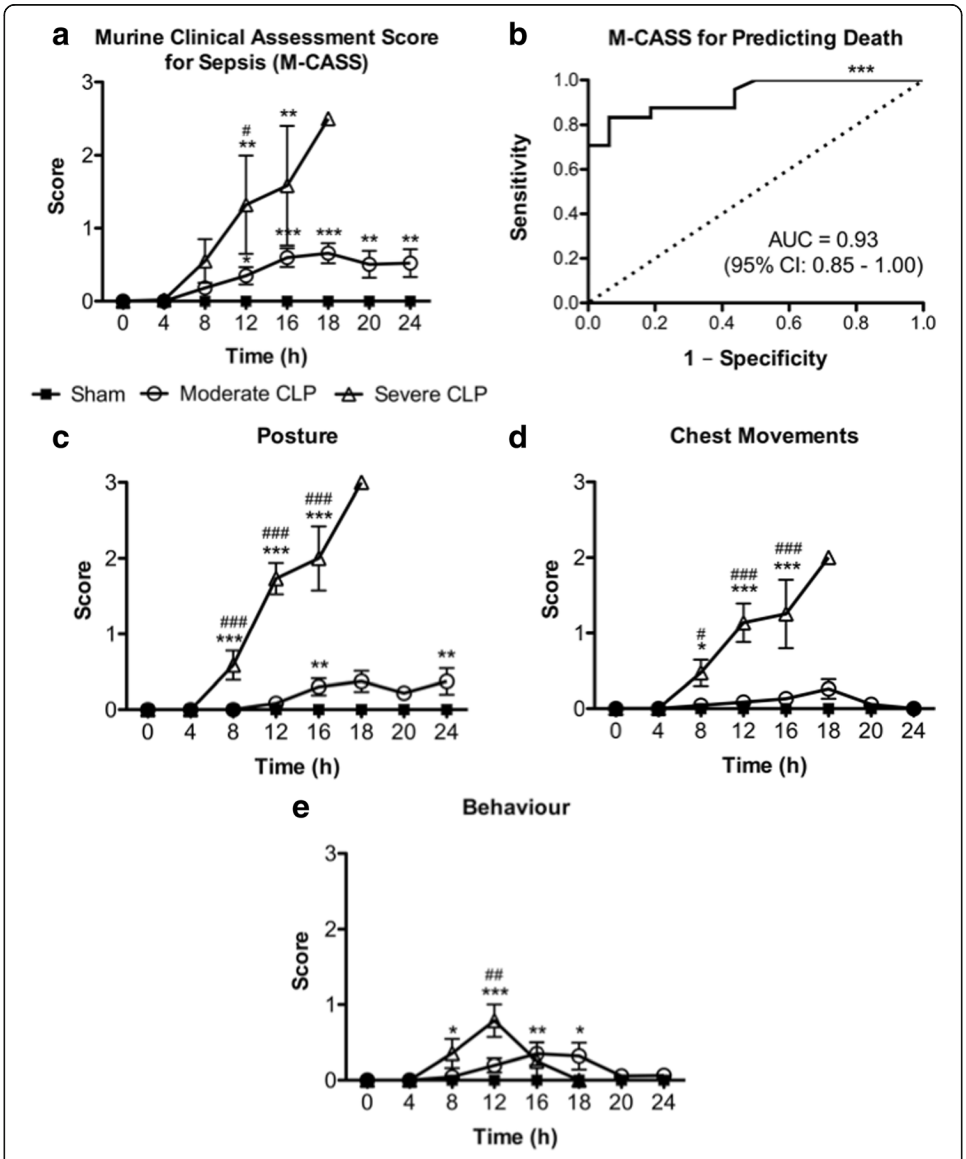

Fig. 4 Modified Mouse Clinical Assessment Score for Sepsis (M-CASS) over time (**a**), M-CASS score as a predictor of death in septic mice (**b**), and individual M-CASS component scores (**c**–**f**) over time in mice undergoing moderate or severe CLP. Data are presented as mean ± SEM from six independent experiments representing a total number of $n = 18$ sham, $n = 23$ moderate CLP, and $n = 17$ severe CLP mice; $^{*}p < 0.05$, $^{**}p < 0.01$, $^{***}p < 0.001$ vs. sham (or vs. line of identity in (**b**)); $^{\#\#\#}p < 0.001$ vs. moderate CLP, by two-way ANOVA. Note: Only two mice undergoing severe CLP survived past 18 h, therefore statistical comparisons were not performed at this time-point (**a**, **c**–**e**). Dotted line in (**b**) represents the line of identity for statistical comparison in ROC analyses. Fur Aspect, Activity, and Eyelid component scores are identical to scores in Fig. 3c–e, respectively, thus are not shown again here, but are included as part of the overall M-CASS score. *AUC* area under the curve, *95% CI* 95% confidence interval

testing novel therapeutic interventions or effects of comorbidities. Lastly, monitoring of vital signs improves the clinical relevance of experimental sepsis studies, and our study shows that core body temperature measured using a rectal thermometer is an objective marker of sepsis progression and death. Therefore, we recommend that body temperature be routinely monitored in CLP studies and, based on our data, body temperature below 30 °C or a

reduction in body temperature of > 5 °C could be utilized as thresholds to replace death as an endpoint in mouse CLP studies involving male C57Bl/6J mice.

To maximize the relevance of this study, we took several factors into consideration when selecting which variation of the CLP model to utilize. For instance, the severe model of CLP implemented in this study resulted in 100% mortality (i.e., sacrifice at endpoint) within 24 h, a finding consistent with mortality rates reported during initial development of the CLP procedure [19]. Furthermore, our moderate severity CLP model resulted in 30% mortality, which is consistent with typical mortality rates observed in septic patients with multiple organ dysfunction [27, 28]. In both CLP models, early and aggressive fluid resuscitation was given to prevent shock and rapid death due to circulatory collapse [29]. Additionally, buprenorphine analgesic at the upper range of the recommended dose was given every 4 h, in order to minimize pain and the potential confounder of facial grimacing as a pain response rather than a reflection of disease progression. Previous studies have demonstrated that buprenorphine analgesia alone has minimal effects on the MGS scores in mice [30], which is consistent with our observations of normal MGS scores in sham mice throughout the study period, and taken together with our sham MSS and M-CASS data, suggests that these observations likely extend to the MSS and M-CASS scoring systems also.

There are some limitations to our CLP model, which should be considered when interpreting the results of our study in the context of other variations to the CLP model. For instance, antibiotics were not administered in order to allow for the natural course of sepsis pathophysiology to progress over a manageable study period of 24 h, since mice had to be monitored every 4 h (including overnight) over the entire study duration in accordance with ethics approval by our Animal Research Ethics Board and CCAC standards. Furthermore, in order to induce varying degrees of sepsis severity in our CLP model in a 24-h study period, we extruded varying amounts of fecal matter into the peritoneal cavity in our 18-gauge double-puncture model, rather than other commonly utilized variables such as cecal ligation length [17]. The shorter study duration may have also impacted the utility of the modified M-CASS for monitoring disease progression, as we excluded "Weight Loss" and "Chest Sounds" components from the modified composite M-CASS score due to undetectable changes in these components over the 24-h study period. In other CLP models where sepsis develops over 3–10 days [17], weight loss and chest sounds may be effective components of the M-CASS scoring system. Therefore, the utility of M-CASS and MSS should be validated over longer study periods that employ more mild CLP models, and with administration of antibiotics, in order to determine the widespread applicability of these scoring systems as surrogate markers of death in CLP studies. Finally, similar studies should be conducted in rat models of CLP sepsis to determine which surrogate markers are appropriate to replace death in other widely applicable animal sepsis models.

Conclusions

In summary, the modified MSS and body temperature measurements are effective, clinically relevant methods for monitoring endpoint, assessing sepsis progression, and predicting death in our mouse model of acute CLP sepsis. Further efforts to use techniques such as these scoring systems, rather than death as an endpoint, should be made to meet the increasing standards for conducting ethical and humane research using murine models to study sepsis. Finally, based on our observations, body temperature monitoring should be considered to replace death as an endpoint in future mouse CLP studies.

Abbreviations
ANOVA: Analysis of variance; ARRIVE: Animal Research: Reporting of In Vivo Experiments; AUC: Area under the curve; CCAC: Canadian Council on Animal Care; CLP: Cecal ligation and puncture; M-CASS: Mouse clinical assessment score for sepsis; MGS: Mouse grimace scale; MSS: Murine sepsis score; ROC: Receiver operating characteristic; SEM: Standard error of the mean

Acknowledgements
This research was supported by grants-in-aid from the Canadian Institutes for Health Research (MOP-136878).

Funding
This research was funded by grants-in-aid from the Canadian Institutes of Health Research (MOP-136878) and by an Ontario Graduate Scholarship, and these funding bodies did not influence the study design or data analysis/interpretation.

Availability of data and materials
All data generated or analyzed during this study are included in this published article (and its supplementary information files).

Authors' contributions
SHM and NS designed and conducted experiments, and analyzed data, with significant contributions from ACK. DJD, MK, and PMG contributed to data acquisition and analysis. SHM and PMG wrote and revised the manuscript. PCL and AEF conceived of the study design, secured funding, provided supervision, and critically revised the manuscript. All authors read and approved the final manuscript.

Ethics approval
All animal studies were approved by the Animal Research Ethics Board at McMaster University (Hamilton, ON, Canada) and are in accordance with CCAC standards. No human tissues were obtained during or utilized for these experiments.

Consent for publication
Not applicable.

Competing interests
The authors declare that they have no competing interests.

Publisher's Note

Received: 12 April 2018 Accepted: 9 July 2018
Published online: 27 July 2018

References
1. Clowes GH Jr, Zuschneid W, Turner M, Blackburn G, Rubin J, Toala P, Green G (1968) Observations on the pathogenesis of the pneumonitis associated with severe infections in other parts of the body. Ann Surg 167:630–650
2. Osuchowski MF, Remick DG, Lederer JA, Lang CH, Aasen AO, Aibiki M, Azevedo LC, Bahrami S, Boros M, Cooney R, Cuzzocrea S, Jiang Y, Junger WG, Hirasawa H, Hotchkiss RS, Li XA, Radermacher P, Redl H, Salomao R, Soebandrio A, Thiemermann C, Vincent JL, Ward P, Yao YM, Yu HP, Zingarelli B, Chaudry IH (2014) Abandon the mouse research ship? Not just yet! Shock 41:463–475
3. Sneddon LU, Halsey LG, Bury NR (2017) Considering aspects of the 3Rs principles within experimental animal biology. J Exp Biol 220:3007–3016
4. Shrum B, Anantha RV, Xu SX, Donnelly M, Haeryfar SM, McCormick JK, Mele T (2014) A robust scoring system to evaluate sepsis severity in an animal model. BMC Res Notes 7:233
5. Huet O, Ramsey D, Miljavec S, Jenney A, Aubron C, Aprico A, Stefanovic N, Balkau B, Head GA, de Haan JB, Chin-Dusting JP (2013) Ensuring animal welfare while meeting scientific aims using a murine pneumonia model of septic shock. Shock 39:488–494
6. Langford DJ, Bailey AL, Chanda ML, Clarke SE, Drummond TE, Echols S, Glick S, Ingrao J, Klassen-Ross T, Lacroix-Fralish ML, Matsumiya L, Sorge RE, Sotocinal SG, Tabaka JM, Wong D, van den Maagdenberg AM, Ferrari MD, Craig KD, Mogil JS (2010) Coding of facial expressions of pain in the laboratory mouse. Nat Methods 7:447–449
7. Nemzek JA, Xiao HY, Minard AE, Bolgos GL, Remick DG (2004) Humane endpoints in shock research. Shock 21:17–25
8. Drechsler S, Weixelbaumer KM, Weidinger A, Raeven P, Khadem A, Redl H, van Griensven M, Bahrami S, Remick D, Kozlov A, Osuchowski MF (2015) Why do they die? Comparison of selected aspects of organ injury and dysfunction in mice surviving and dying in acute abdominal sepsis. Intensive Care Med Exp 3:48
9. Bara M, Joffe AR (2014) The ethical dimension in published animal research in critical care: the public face of science. Crit Care 18:R15
10. Lilley E, Armstrong R, Clark N, Gray P, Hawkins P, Mason K, Lopez-Salesansky N, Stark AK, Jackson SK, Thiemermann C, Nandi M (2015) Refinement of animal models of sepsis and septic shock. Shock 43:304–316
11. Reini K, Fredrikson M, Oscarsson A (2012) The prognostic value of the modified early warning score in critically ill patients: a prospective, observational study. Eur J Anaesthesiol 29:152–157
12. Corfield AR, Lees F, Zealley I, Houston G, Dickie S, Ward K, McGuffie C, Scottish Trauma Audit Group Sepsis Steering G (2014) Utility of a single early warning score in patients with sepsis in the emergency department. Emerg Med J 31:482–487

13. Subbe CP, Kruger M, Rutherford P, Gemmel L (2001) Validation of a modified early warning score in medical admissions. QJM 94:521–526
14. Skitch S, Tam B, Xu M, McInnis L, Vu A, Fox-Robichaud A (2018) Examining the utility of the Hamilton early warning scores (HEWS) at triage: Retrospective pilot study in a Canadian emergency department. CJEM 20(2):266–274
15. Matsumiya LC, Sorge RE, Sotocinal SG, Tabaka JM, Wieskopf JS, Zaloum A, King OD, Mogil JS (2012) Using the mouse grimace scale to reevaluate the efficacy of postoperative analgesics in laboratory mice. J Am Assoc Lab Anim Sci 51:42–49
16. Zellweger R, Wichmann MW, Ayala A, Stein S, DeMaso CM, Chaudry IH (1997) Females in proestrus state maintain splenic immune functions and tolerate sepsis better than males. Crit Care Med 25:106–110
17. Rittirsch D, Huber-Lang MS, Flierl MA, Ward PA (2009) Immunodesign of experimental sepsis by cecal ligation and puncture. Nat Protoc 4:31–36
18. Kilkenny C, Browne WJ, Cuthill IC, Emerson M, Altman DG (2010) Improving bioscience research reporting: the ARRIVE guidelines for reporting animal research. PLoS Biol 8:e1000412
19. Baker CC, Chaudry IH, Gaines HO, Baue AE (1983) Evaluation of factors affecting mortality rate after sepsis in a murine cecal ligation and puncture model. Surg 94:331–335
20. Hubbard WJ, Choudhry M, Schwacha MG, Kerby JD, Rue LW 3rd, Bland KI, Chaudry IH (2005) Cecal ligation and puncture. Shock 24(Suppl 1):52–57
21. Mai SH, Khan M, Dwivedi DJ, Ross CA, Zhou J, Gould TJ, Gross PL, Weitz JI, Fox-Robichaud AE, Liaw PC, Canadian Critical Care Translational Biology G (2015) Delayed but not early treatment with DNase reduces organ damage and improves outcome in a murine model of Sepsis. Shock 44:166–172
22. Dwivedi DJ, Grin PM, Khan M, Prat A, Zhou J, Fox-Robichaud AE, Seidah NG, Liaw PC (2016) Differential expression of PCSK9 modulates infection, inflammation, and coagulation in a murine model of Sepsis. Shock 46:672–680
23. Patrick AL, Grin PM, Kraus N, Gold M, Berardocco M, Liaw PC, Fox-Robichaud AE, Canadian Critical Care Translational Biology G (2017) Resuscitation fluid composition affects hepatic inflammation in a murine model of early sepsis. Intensive Care Med Exp 5:5
24. Xiao H, Remick DG (2005) Correction of perioperative hypothermia decreases experimental sepsis mortality by modulating the inflammatory response. Crit Care Med 33:161–167
25. Lewis AJ, Griepentrog JE, Zhang X, Angus DC, Seymour CW, Rosengart MR (2018) Prompt administration of antibiotics and fluids in the treatment of sepsis: a murine trial. Crit Care Med 46:e426–e434
26. Weixelbaumer KM, Raeven P, Redl H, van Griensven M, Bahrami S, Osuchowski MF (2010) Repetitive low-volume blood sampling method as a feasible monitoring tool in a mouse model of sepsis. Shock 34:420–426
27. Stoller J, Halpin L, Weis M, Aplin B, Qu W, Georgescu C, Nazzal M (2016) Epidemiology of severe sepsis: 2008-2012. J Crit Care 31:58–62
28. Fleischmann C, Scherag A, Adhikari NK, Hartog CS, Tsaganos T, Schlattmann P, Angus DC, Reinhart K, International Forum of Acute Care T (2016) Assessment of global incidence and mortality of hospital-treated Sepsis. Current estimates and limitations. Am J Respir Crit Care Med 193:259–272
29. Zanotti-Cavazzoni SL, Guglielmi M, Parrillo JE, Walker T, Dellinger RP, Hollenberg SM (2009) Fluid resuscitation influences cardiovascular performance and mortality in a murine model of sepsis. Intensive Care Med 35:748–754
30. Miller A, Kitson G, Skalkoyannis B, Leach M (2015) The effect of isoflurane anaesthesia and buprenorphine on the mouse grimace scale and behaviour in CBA and DBA/2 mice. Appl Anim Behav Sci 172:58–62